Environmental
Studies
Revolving
Funds

045 Iceberg Detection by Airborne Radar: Technology Review and Proposed Field Program

Canada

September 1986

The Environmental Studies Revolving Funds are financed from special levies on the oil and gas industry and administered by the Canada Oil and Gas Lands Administration for the Minister of Energy, Mines and Resources, and by the Northern Affairs Program for the Minister of Indian Affairs and Northern Development.

Environmental Studies Revolving Funds

Report No. 045

September 1986

ICEBERG DETECTION BY AIRBORNE RADAR: TECHNOLOGY REVIEW AND PROPOSED FIELD PROGRAM

Prepared by

CANPOLAR Consultants Ltd.
421 Eglinton Ave. West
Suite 4
Toronto, Ontario
M5N 1A4

Scientific Adviser: D. Strong

The correct citation for this report is:

CANPOLAR Consultants Ltd., 1986, "Iceberg Detection by Airborne Radar: Technology Review and Proposed Field Program", Environmental Studies Revolving Funds Report No. 045, Ottawa, 135 p.

Published under the auspices
of the Environmental Studies
Revolving Funds
ISBN-0-920783-44-9

TABLE OF CONTENTS

LIST OF TABLES

TABLE

LIST OF FIGURES

FIGURE

SUMMARY

1. Airborne radar appears to be the single, most promising sensor for reliable, all-weather detection of icebergs over wide areas. However, current knowledge is inadequate to determine conclusively the optimum system or systems, configuration, and operating precedures. The field program proposed in this report is designed to collect the data that would be required to address this issue.

2. High-resolution radars offer the greatest potential for detection of small icebergs, bergy bits and growlers. Although surveillance radars appear well suited to the problem, there is little experience with them for iceberg detection, their data output format is not ideal, and their capability for mapping pack ice is uncertain. Therefore, the experimental use of a surveillance radar is recommended to assess these limitations.

3. New synthetic aperture radars (SAR) show significant promise for both detection and mapping. Recent work suggests that earlier limitations may be overcome with data enhancement techniques. Simultaneous SAR data should be collected and the Canada Centre for Remote Sensing should be encouraged to support this effort, because it would be directly relevant to the RADARSAT project.

4. Real aperture side-looking airborne radars (SLAR) are being used operationally for iceberg detection, although they are theoretically non-ideal for this application. Both the Atmospheric Environment Service and the International Ice Patrol have agreed informally to make their aircraft available for an experimental program. These data would be useful for comparative purposes and to assist in quantifying the performance of these radars; however, their availability is not essential in the design of the field program.

5. The full cost of a nominal, six-week field program using a surveillance radar and including adequate surface data and interpretation is estimated to be $737,000. Costs for four- and two-week programs are estimated to be $549,500 and $440,500. Although these reduced programs would include collection of some surface information, they might not include an adequate range of environmental conditions, nor allow for adequate calibration of the radars.

6. The experiment design builds upon **BERGSEARCH '84**, which was successful in acquiring semi-quantitative results for several SARs and SLARs over limited environmental conditions. The optimum time and place appear to be March to May, operating out of Gander, Newfoundland. Surface data would be essential to the success of the experiment, including aerial photography, ship observations, and waverider buoy information.

7. Several of the radars most appropriate to this study -- Litton APS-504-V5, Eaton APS-128PC (search radars); Intera Star-2, MDA C-IRIS (SAR); and AES CAL SLAR-100 (SLAR), are unlikely to be available in spring 1986. All are expected to be available for spring 1987. On this basis, spring 1987 would offer some advantages. However, this option would mean few new data would be available for 1987 operational support services. Therefore , it is suggested that a reduced experiment using aircraft-of-opportunity be conducted in spring 1986, to collect a limited, quantitative data set.

8. The major uncertainties in quantitative assessment of radar performance are in knowledge of iceberg and ocean backscatter characteristics. Therefore, wide-bandwidth tape recording of data is strongly recommended.

9. Computer modelling of radar performance is a very cost-effective means of comparing performance and extrapolating to configurations and conditions not measured. It is recommended that modelling effort be an integral part of the data analysis effort.

10. Electronic support measures (ESM) appear to offer the capability of discriminating between ships and icebergs by listening for ships' marine radar signals. Although very expensive military systems are available, a relatively low-cost system could probably be designed. Further feasibility studies are recommended to investigate this possibility.

11. Useful information could be obtained by analysing data already available from **BERGSEARCH '84** and other programs. Suggested topics include: further understanding of SAR returns, particularly azimuth smear; examination of radiometric echo-strength data collected during **BERGSEARCH '84**; further improvements to existing computer models.

RESUME

1. Les radars aéroportés semblent constitutuer le moyen unique le plus prometteur de détection fiable des icebergs dans n'importe quelle condition atmosphérique et sur de vastes zones. Cependant, les connaissances actuelles sont insuffisantes pour déterminer avec certitude quels seraient les meilleurs systèmes, configurations et processus de fonctionnement. Le programme sur terraine, proposé dans ce rapport, a été conçu pour recueillir les données nécessaires pour traiter cette question de façon scientifique.

2. Les radars à résolution élevée offrent le meilleur potential de détection des icebergs de petite taille. Même si les radars de surveillance semblent convenir à cette fin, on ne possède pas assez d'expérience de leur application dans la détection des icebergs, leur présentation des données n'est pas parfait et leur utilité pour dresser des cartes des packs est peu connue. Ce programme recommande donc l'utilisation expérimentale d'un radar de surveillance afin de mieux connaître ces restrictions.

3. Les nouveaux radars à ouverture synthétique (SAR) s'avèrent très prometteurs pour la détection comme pour l'établissement de cartes. Des études récentes suggèrent que les restrictions pourraient être surmontées grâce à des techniques de mise en valeur des données. On devrait recueillir les données simultanées SAR et inciter le Centre canadien de télédétection à soutenir cet effort directement lié au projet RADARSAT.

4. Les radars aéroportés d'ouverture synthétique à balayage latéral (SLAR) sont, en fait, utilisés pour la détection d'icebergs, bien qu'en théorie, ils ne conviennent pas à cette application. Le Service de l'environnement atmosphérique (SEA) et la Patrouille internationale sur glace (IIP) ont officieusement accepté de mettre leurs appareils au service d'un programme expérimental. Ces données peuvent avoir une valeur comparative et servir à quantifier le rendement des radars; toutefois, elles ne sont pas absolument essentielles à la conception de l'expérience.

5. Le coût total d'un programme nominal de six semaines sur le terrain en utilisant un radar de surveillance de même que les données et l'interprétation adéquates en surface est estimé à 737 000 $. Le coût respectif des programmes de quatre et de deux semaines est estimé à

549 000 $ et à 440 500 $. Bien que ces programmes réduits comprennent la collecte de certaines informations en surface, ils risquent de ne pas inclure une gamme suffisante de conditions environnementales, ni de permettre un calibrage adéquat des radars.

6. La conception de l'expérience se fonde sur celle de **BERGSEARCH '84**, au cours de laquelle on a réussi à obtenir des résultats semi-quantitifs sur plusieurs SAR et SLAR dans des conditions environnementales limitées. Mais l'époque idéale et le meilleur endroit semblent être de mars à mai, à partir de Gander (Terre-Neuve). Les données de surface seront essentielles au succès de l'expérience, y compris les photos aériennes, l'observation à partir de bateaux et l'information provenant de bouées.

7. Parmi les radars convenant le mieux à cette étude -- Litton APS-504-V5, Eaton APS-128PC (radars de balayage), Intera Star-2, MDA C-IRIS (SAR), et CAL SLAR-100 (SLAR) -- certains ne seront probablement pas disponibles d'ici le printemps 1986, mais on s'attend à ce qu'ils le soient tous au printemps 1987. C'est pourquoi le printemps 1987 peut présenter certains avantages. Cependant, cette option risque d'avoir pour conséquence que très peu de renseignements nouveaux soient à la disposition des services de soutien operationnel en 1987. Par conséquent, on suggère de mener une petite expérience de reconnaissance aérienne au printemps 1986, afin de recueillir un ensemble de données quantitatives limitées.

8. La plus grande incertitude quant à l'évaluation quantitative du rendement d'un radar est la connaissance des caractéristiques de rétrodiffusion des icebergs et de l'océan. Par conséquent, on recommande l'enregistrement des données sur bande magnétique large.

9. Les modèles informatiques du rendement des radars constituent une façon très économique de comparer leur performance et de trouver des extrapolations pour les configurations et les conditions non encore mesurées. On recommande donc d'effectuer des modèles dans le cadre de l'analyse des données.

10. Il semble que les mesures de support électronique (ESM) permettront de départager les bateaux des icebergs en captant les signaux des radars de bateaux. Bien que des systèmes militaires très onéreux soient disponibles, on pourrait probablement mettre au point un système relativement économique. On recommande d'effectuer des études de faisabilité plus poussées afin d'étudier cette possibilité.

11. On pourrait obtenir de précieuses informations en analysant les données d'ores et déjà disponibles de **BERGSEARCH '84** et d'autres programmes. Les thèmes recommandés comprennent une connaissance plus approfondie des retours de SAR, surtout la déformation sur l'axe d'azimut, l'examen des données concernant l'intensité de l'écho radiométrique collectées au cours de **BERGSEARCH '84**, et le perfectionnement des modèles informatiques qui existent déjà.

1.0 INTRODUCTION

The Environmental Studies Revolving Funds (ESRF) contracted a team led by CANPOLAR Consultants Ltd. to design and cost a field program that would evaluate the ability of airborne radars to detect small icebergs and, especially, growlers and bergy bits, in open water. Before preparing the field program design, the team was asked to review and assess the state-of-the-art in airborne radars for iceberg detection.

1.1 TEAM INVOLVEMENT

Other team members were Communications Research Laboratory of McMaster University, Hamilton; INTERA Technologies Ltd., Calgary; and NORDCO Limited, St. John's. Background review papers were prepared on the following topics: Side-Looking Airborne Radar (CANPOLAR), Synthetic Aperture Radar (INTERA), Surveillance Radar (McMaster), Computer Modelling (NORDCO), Electronic Support Measures (INTERA), and Surveillance Radar Aircraft (INTERA). These reviews are given in Appendices A through F, respectively.

A planning meeting was held in September 1985 at McMaster University with the following attendees:

Mr. Brian Currie, McMaster
Mr. Byron Dawe, NORDCO
Dr. Simon Haykin, McMaster
Dr. Ray Lowry, INTERA
Mr. Jeff Proctor, CANPOLAR
Dr. Jamie Rossiter, CANPOLAR
Mr. Derek Strong, COGLA (Scientific Adviser).

Out of this meeting emerged a Draft Field Program Design which was circulated widely for comment (see Appendix G). This report incorporates comments received and discussions held up to the end of October 1985.

1.2 AIM OF THE FIELD PROGRAM

The aim of this field program would be to provide operators and regulatory groups with a clear idea of capability of airborne radars to provide ice hazard information under different environmental conditions, particularly those of high winds, high sea state, and poor visibility.

The field program should be a controlled scientific experiment to determine the best airborne radar(s) and system configuration for the detection of icebergs in open water. At the conclusion of the experiment it should be possible to recommend suitable operational radar system(s) and to estimate quantitatively their performance.

Upon examination of the results of **BERGSEARCH '84** (Rossiter et al. 1985) we concluded that the following three specific areas are most important to examine:

- probabilities of detection of various sizes of icebergs in high wind and wave conditions;
- capabilities of surveillance radars to detect iceberg targets and pack ice; and
- optimum operational procedures for iceberg detection, including areal coverage rate.

2.0 METHODOLOGY

2.1 RADAR SYSTEMS

It appears that the physical mechanisms for detection of icebergs are different for real and synthetic aperture radars. However, knowledge of the first- and second-order statistics of sea clutter is essential to the performance of both systems. Therefore, experiments with both real and synthetic aperature radar systems are recommended, with priority on use of surveillance radars to assess their performance quantitatively.

It is recommended that a primary radar be used over a one- to two-month interval. During such time it is likely that a variety of environmental conditions would be encountered, and that aerial photography and waverider information could be collected simultaneously. Additional surface information would become available on an opportunity basis, including a specific period of about ten days during which intensive surface data would be collected from a dedicated ship. During this time additional aircraft, which might be available only for limited period, would be invited to participate.

2.1.1 Real Aperture Radar

Because of the theoretical attractiveness of surveillance radars and the relative inexperience with these radars for iceberg operations, it is recommended that the prime radar used be a surveillance radar. As described in Appendix C, there are three main choices of radar: the TI APS-134, Litton APS-504-V5, and Eaton APS-128PC. All three of these radars have pulse compression and scan-to-scan integration capability. It is recommended that both video-tape and full-bandwidth recording be used for the prime radar.

Although a number of search radars are in current use, it is not clear at time of writing which radar or radars would be available, particularly for spring 1986. It is possible that older versions of the TI radar might be available from the Canadian Department of National Defence, on the Aurora and Tracker aircraft, or from the U.S. Office of Naval Research. Litton V3 radars are available, but do not have pulse compression. The V5, pulse compression, unit will not be available until summer 1986. The only possibility might be use of a prototype that is currently being used in Florida. The Eaton APS-128PC test system, which was used last spring in a preliminary study (Currie and Haykin 1985), is not expected to be available for spring

1986. Non-pulse compression Eaton units are being used around the world, and one might be available for a limited period.

It is likely that much of the data and experience that are required from this program could be achieved with a non-pulse compression unit, by use of proper data recording and post-experiment analysis. However, it is expected that the large advantage of surveillance radars will come through pulse compression systems with their greater range resolution.

It is recognized that there are currently several real aperture SLARs which have been and will continue to be used for iceberg surveillance (see Appendix A). It is recommended that one or more of these be used for comparative purposes on an opportunity basis during the field program. They could include the Atmospheric Environment Service (AES) APS-94E, the International Ice Patrol (IIP) APS-135, or the Intradam MAPR. The new AES CAL SLAR-100 is not likely to be ready for operation until late spring or early summer 1986. The APS-94E and MAPR both have digital-recording capability, which is considered essential for quantitative analysis.

2.1.2 Synthetic Aperture Radar

A complementary experiment with SAR is recommended. Experience during **BERGSEARCH '84** indicated the importance of high resolution, particularly in reducing false targets from sea spikes. In addition, synthetic aperature radar will be used from satellite platforms, such as RADARSAT.

The Canada Centre for Remote Sensing (CCRS) has indicated a willingness to fly the new IRIS C-band radar (MDA C-IRIS) for this experiment. It is expected to be commissioned in early 1986. Alternatively, INTERA STAR-1 radar, which was used during **BERGSEARCH '84**, could be used, or the new STAR-2 radar, which will not be available until late 1986. Of particular importance in use of synthetic aperture radar will be examination of the effects and causes of azimuth smear and sea spikes. New procedures for data enhancement may reduce the effects of azimuth smear significantly (see Appendix B).

2.1.3 Electronic Support Measures

Electronic Support Measures (ESM) appear to offer a feasible technique for descriminating between ships and icebergs by detecting the radar emissions of ships' marine radars (see Appendix E). However, the cost and complexity of implementing ESM are substantial. Therefore, it is recommended that a more detailed feasibility study be

undertaken to examine specific equipment that might be tested experimentally.

2.1.4 Radar Calibration

Calibration of the primary radar radiometrically against known radar reflectors is highly recommended. This calibration would enable absolute estimates of the strength of ocean returns under various conditions and of echoes from targets such as ships, icebergs and buoys. This information would be important in comparing radars that would not be used in the field program through numerical modelling, and would be required for prediction of iceberg detectability.

Calibration could be carried out by mounting several known radar reflectors on or near the runway at Gander. The aircraft could fly at a known altitude and range from these before or after each flight or both. Several sizes (i.e., reflectivities) of radar reflector should be used from about .1-1 m^2 cross-sections..

In addition, the primary radar should be internally callibrated in the aircraft with known test signals, to ascertain the system losses and the output level for given input signals.

2.2 DATA RECORDING

Recording of radar data on magnetic tape is considered essential to the success of this experiment. In general, surveillance radars do not have tape-recording capability. Therefore, it is recommended that wide-bandwidth (full-waveform) recording be used for specific portions of each flight. Full-waveform recording would enable detailed study of sea clutter statistics.

In addition, it is recommended that videotape recordings be collected for the entire period over the target area. For SLARs, it is recommended that tape-recording be employed, which is possible with several of the radars that may be involved. The SARs that might be used all have tape-recording capability.

Original imagery, flight logs, photographs, and notes should be available to the data interpretation group. These could be reproduced as required for detailed analysis. It is important that Greenwich Mean Time (GMT) be used throughout by all the groups so that there might be no confusion as to the time of collection of any particular piece of data.

2.3 DATA VOLUME

Based on exerience with **BERGSEARCH '84**, an estimate of the number of aircraft flights is given in Table 1. This estimate gives 40 aircraft flights over the data collection period, which compares with 23 flights during **BERGSEARCH '84**. (For the purposes of this discussion, one aircraft mission per day is considered one flight, although in fact smaller aircraft may refuel during the day.) During **BERGSEARCH '84** each aircraft averaged about 12 passes over the survey area per flying day. The coverage would depend to some extent on the details of the flight patterns required and on the distance of icebergs from Gander. This volume would be somewhat more than that collected during **BERGSEARCH '84**, and would put commensurate requirements on the data analysis and interpretation portions of the project.

TABLE 1

Estimated number of flights

Purpose and period	Number of flights
Prime radar, non-intensive period 5 weeks, 4 flights/week	20
Prime radar, intensive period	5
SLARs (2 aircraft, intensive period)	10
SAR (1 aircraft, intensive period)	5
Total flights	40

Note: During **BERGSEARCH '84**, aircraft averaged 12 passes per flying day.

2.4 DATA COLLECTION

The collection of the data has been divided into two types of operation: an intensive period of about seven to ten days, during which the ship would be on site in the iceberg target area, and a less-intensive period of about five to six weeks, during which the prime radar and aerial photography would be used together. This less-intensive period would be used to familiarize the operations crew with the use of the radar, to calibrate the radar, to optimize

operational procedures, and to collect data during environmental conditions that might not be encountered during the intensive period. The intensive period would be used to coordinate as many radars-of-opportunity as available. Its timing would depend on the availability of alternative aircraft and the ship, but it should be about one-half to two-thirds of the way through the less-intensive period.

2.4.1 Less-Intensive Data Collection

During this experimental period, the initial goals would be to calibrate the radar, to become thoroughly familiar with its operation, and to optimize its use. Reconnaissance surveys should be made to determine an area in which there are a number of iceberg targets of a variety of sizes. Experiments should be conducted to determine the optimum altitude of operation, flight orientation with respect to wind and waves, and maximum range of detectability using search radar.

Only a few flights per week would be planned to allow the ground crew time to analyse the results in a preliminary fashion on site. This would involve detailed comparison with aerial photography, which should be taken as close to simultaneously with the radar aircraft as is physically possible. Without photographic information it would be impossible to determine objectively the performance of the radar in any particular configuration.

Additional experiments should be run to examine the repeatability of detection of icebergs of various sizes by running the same line up to ten times in rapid succession. Information on possible flight patterns could be obtained from similar experiments assessing the performance of search radars for other types of targets, such as search and rescue operations and anti-submarine warfare.

2.4.2 Intensive Data Collection

During some portion of the data collection there should be an intensive period during which the ship would be positioned in an area of icebergs. Previous missions could be used to determine the most effective location for the ship. This period would also be the best time for aircraft-of-opportunity to join the experiment. The operations manual and daily briefing/de-briefing sessions in Gander were very effective in co-ordinating various aircraft during **BERGSEARCH '84**, and it is recommended that this approach be used again.

Data collection was also most effective when specific flight patterns were assigned to each of the aircraft. These might take the form as shown in Figure 1 for side looking

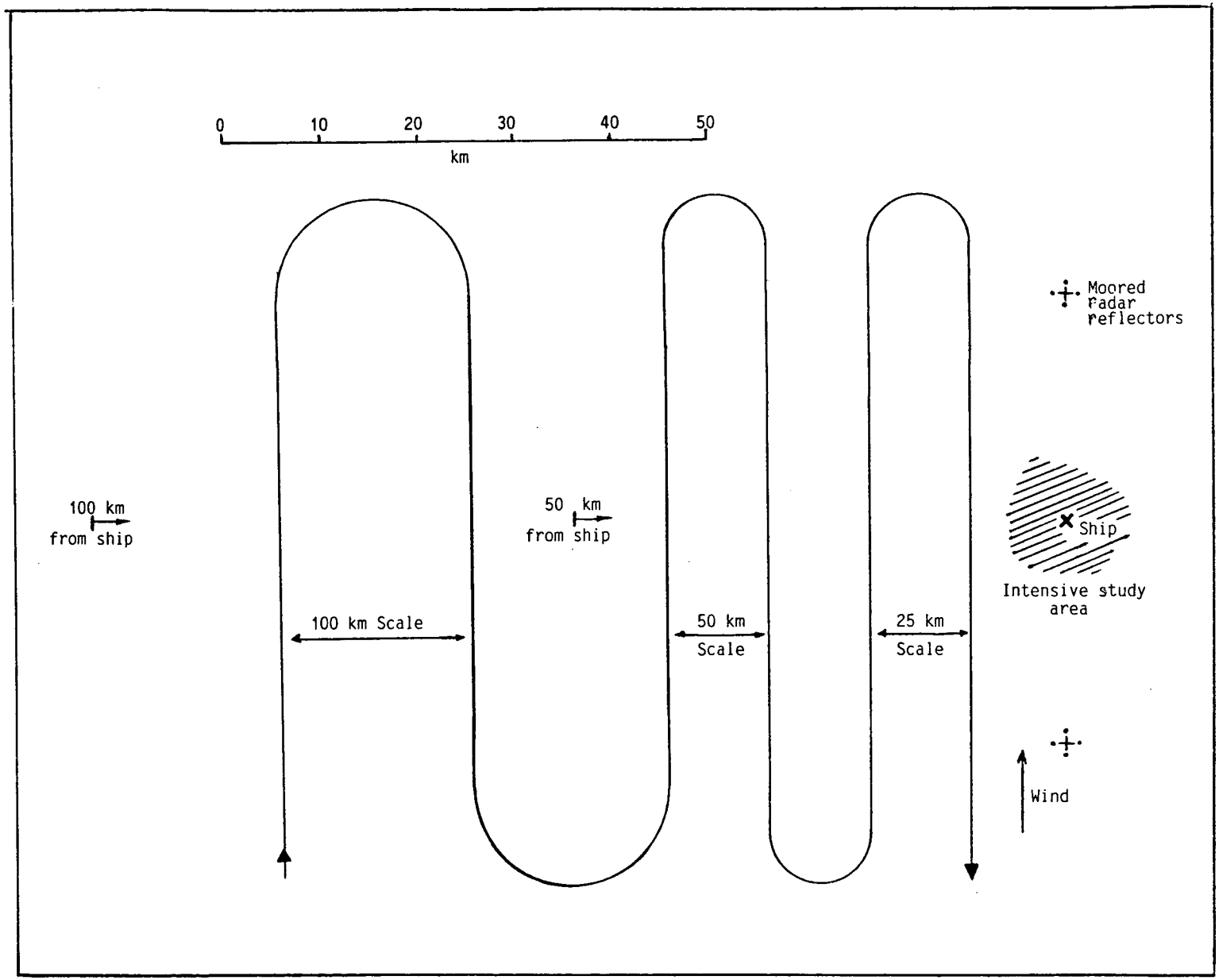

Figure 1. Possible SLAR flight pattern; repeat pattern at second altitude and parallel to waves.

airborne raders. Because it was determined during **BERGSEARCH '84** that the cross-wind or cross-wave direction was most effective, it would not be necessary to fly upwind and downwind looking directions. However, it is still not clear whether looking cross-wind or cross-wave is most effective; it is likely that this depends on the relative intensity of the wind and sea state -- i.e., building, fully developed, or dying sea.

Careful coordination would be required with the ship to ensure that the ship observers could record information on as many small icebergs as possible without the ship actually interfering with the data collection, i.e., becoming an ambiguous target in its own right. It is suggested that the ship moor a distinctive pattern of reflectors in a spot that could be used as a fixed reference by all the aircraft.

It would also be important to assess the relative aerial coverage of the main types of radar. As shown in Figure 2, side-looking radars collect one or two swaths of data off to the side of the aircraft. These swaths can be as much as 50 or 100 km wide, although it is not clear how effective the far edges would be for detection of the smallest targets, particularly with real aperture systems. Because sensing is not effective directly below the aircraft, there is always a gap in systems that look both right and left, which must be filled in by overlapping coverage.

Search radars, on the other hand, cover a moving "donut" of area (see Figure 2) so that infilling is not required. However, this coverage also implies that some portions of the area are surveyed in a less advantageous, upwind direction. Also, the width of the coverage area cannot be as large with a search radar flown at low altitudes.

The period of intensive data collection should allow direct, scientific comparisons to be made between various radars by collecting data as close to simultaneously as possible under controlled conditions. These comparisons would be important in calibrating the numerical modelling algorithms, which would be used to compare performance for conditions other than those encountered during the intensive period.

2.5 DATA ANALYSIS

The objective of data analysis would be to assess quantitatively the performance of the radars in their detection of growlers, bergy bits, and small icebergs under varying conditions. This procedure will involve not only assessment of targets present or absent, as performed during

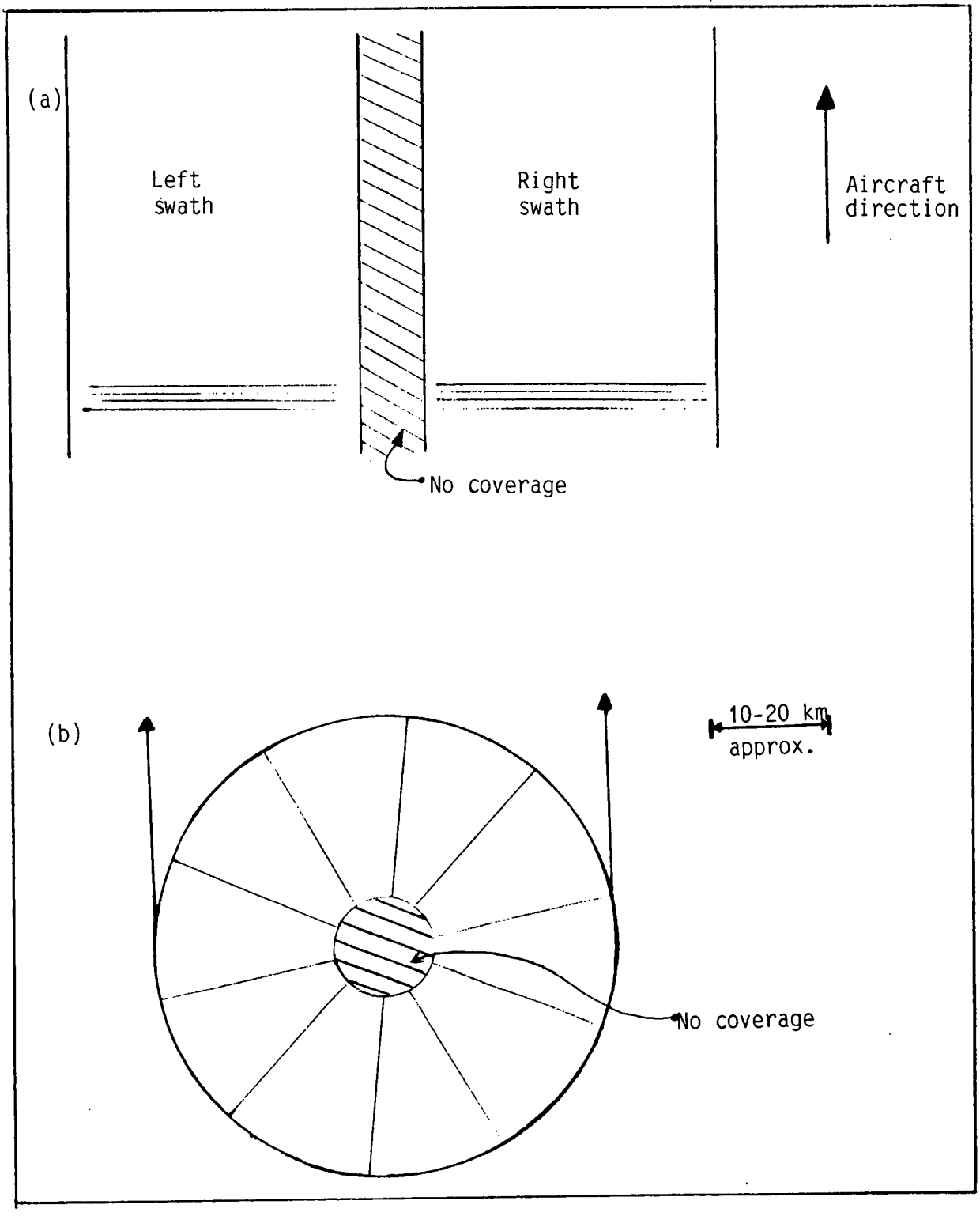

Figure 2. Comparison of (a) side-looking radar coverage area, in which image is built up line by line as aircraft moves; and (b) search radar coverage area, in which entire coverage area moves with aircraft.

BERGSEARCH '84, but also some estimate of the false alarm rate. To do this, the settings of the radars must be carefully controlled.

2.5.1 In-field Data Analysis

Analysis of data should commence as soon as they are available in the field. They should be annotated with a uniform system for logging pass numbers over the target area, along with ancillary information, such as time (GMT), position, altitude, heading, and ground speed. Data tapes and imagery should be cross-indexed with the flight logs. Data interpreters should be closely involved with the aircraft missions, and should participate in some of the flights.

A comparison of real-time imagery and aerial photography should proceed as soon as possible after flight, implying that aerial photographic film should be processed near the flight centre and that video tapes should be played back for detailed examination. In this way, it would be possible to determine optimum settings for the radar as the experiment progresses.

2.5.2 Post-Experiment Analysis

Detailed analysis of the majority of the data would likely have to take place after the data collection. Although it is possible that significant amounts of semi-quantitative comparison between radar data and aerial photography would be possible in the field, detailed processing of full-bandwidth recording, comparisons between different radars and incorporation of ships' data would not be available until after the experiment.

Tabulations should be made of the number of targets of different sizes that are seen in each pass as a function of the various operational and environmental conditions. This number should be included with an estimate of the false alarm rate -- i.e., the number of targets that appear in the radar image but that are not attributable to an actual iceberg target.

Although this work is relatively straightforward, it was the experience with **BERGSEARCH '84** that accurate registration of data, i.e., being certain that the radar scene corresponds with aerial photographic or surface information, is exceedingly time consuming. Misregistration invalidates the entire data set that is being examined. Such work would be ideal for one or more undergraduate students working during the summer or work term under the supervision of a more senior scientist.

2.5.3 Full-Bandwidth Recording

It has been recommended that some data be collected during the majority of environmental conditions, using full-bandwidth recording, so that the actual radar waveforms could be examined. If this recording were carried out it would be possible to estimate quantitatively significant information about the first- and second-order statistics (mean and deviation) of the sea clutter for a variety of conditions and operating parameters. Again, playback, registration, and plotting of this data set would be likely to take several months after the experiment. It would require a fairly senior scientist or engineer to analyse the data for the required statistics. The data set would also contain new information on the nature of the reflectivity of icebergs in open water as a function of depression angle. These two sets of information would be essential to quantitative modelling of the detection process.

2.5.4 Computer Modelling

One way that the data collected in this experiment could be made very effective is to incorporate them with computer modelling of the radar detection process (see Appendix D). Once a model were verified, it could be used to predict the performance of many classes of radars under differing operational conditions without the need to conduct extensive field programs. Although the radar equation is well understood and most of the input parameters are well known, the major limitations appear to be in the knowledge of the reflectivity of icebergs, particularly under bobbing conditions, and in the knowledge of backscatter from differing wind/wave conditions. Because these two types of information are likely to come out of the experiment, accurate computer models of radar detection of icebergs are within reach. In this way, the contribution of airborne radar to the process of detecting ice hazards, particularly in conjunction with other types of data such as marine radar, could be made.

It is important to recognize that radars involving doppler processing (SAR) use different detection techniques from real aperture systems. These differences could effect the detection probabilities. It is likely that significant assistance with this work could come from the CCRS, who are faced with similar problems for the RADARSAT program. For example, subsequent to **BERGSEARCH '84**, RADARSAT sponsored a follow-on study specifically to examine synthetic aperture radar and azimuth smear (CANPOLAR Consultants Ltd. and INTERA Technologies Ltd. 1985).

3.0 FIELD PROGRAM LOGISTICS

3.1 LOCATION AND TIME OF YEAR

Based on airport weather conditions (Table 2), Gander appears the best choice as a centre of operations. Although somewhat less accessible than St. John's, it has excellent airport facilities.

Icebergs are most likely encountered about 100-200 naut mi to the east and northeast of Gander between March and May (see Table 3 and Figure 3). Although the probability of encountering icebergs free of pack ice increases later in this period, the incidence of high winds decreases.

3.2 SURFACE DATA VERIFICATION

3.2.1 Aerial Photography

Aerial photographs were the single, most useful source of comparative data during **BERGSEARCH '84**, and, therefore, explicit provision for aerial photography is included in the budget. Helicoptor-mounted photography is considered be inappropriate because use of helicoptors in high winds and sea states is not possible. Oblique photographs should be taken from the radar aircraft whenever visibility permits.

3.2.2 Ship Observations

Ship observations are essential to a quantitative experimental program, even if budget limitations were to prevent the use of a ship during all the flying days in the program. Observer personnel on the ship should include two, trained ice observers, one of whom would act as waverider buoy technician. Abundant Polaroid and 35-mm photographs should be taken, and all cameras should have automatic time/date (GMT) annotation. Photographers should keep an accurate bearing log for photographs. Weather and descriptive information about icebergs and sea conditions should be noted on waterproof logs similar to those used for **BERGSEARCH '84**.

Effective communication links between the ship, ground, and aircraft are essential. HF and VHF radios should be carried on the ship. Redundant ship navigation systems are essential; for example, Loran-C and satellite systems. The ship's marine radar can be used to assist the observation crew in locating and annotating targets. Automatic logging of time, ship's heading and position, and marine radar data could be accomplished relatively easily.

TABLE 2.

Average time that selected airports have been below specified flying units, 30 years history.

Flying Units:	St. John's	Sydney	Gander	Goose Bay	Dear Lake
Percentage of hours below Category I limits	32.4%	8.8%	8.3%	1.6%	1.1%
Percentage of year when weather is below Category I limits for six hours or longer duration	17.2%	5.1%	4.9%	0.5%	.27%
Percentage of hours below Category I limits but above Category II limits	21.8%				
Percentage of hours below Category II limits	10.6%				
Percentage of year below Category I limits but above Catagory II limits for six hours or longer duration	10.5%				
Percentage of year below Category II limits for six hours or longer duration	6.7%				

TABLE 3
Monthly average fluxes of icebergs across each degree of latitude

Area	Flux across	Jan	Feb	Mar	Apr	May	June	July	Aug	Sept	Oct	Nov	Dec	Total
Saglek	61°N	106	95	134	135	145	138	122	86	60	49	49	87	1206
Bay	60°N	103	95	128	131	144	142	124	87	51	40	40	74	1159
	59°N	97	94	122	130	142	141	129	90	53	26	36	59	1119
	58°N	87	92	115	129	139	140	135	95	62	21	26	43	1084
	57°N	73	88	112	128	132	137	127	99	56	20	16	31	1019
	56°N	49	77	112	112	133	134	122	106	68	28	10	19	966
Hamilton	55°N	31	59	99	105	126	130	120	118	75	35	11	10	909
Bay	54°N	17	39	82	98	116	118	91	81	49	32	15	6	744
	53°N	12	30	73	93	111	107	64	54	33	23	11	2	613
	52°N	9	23	62	89	106	102	42	34	22	14	9	0	512
	51°N	4	14	40	76	86	67	37	11	2	5	5	0	347
	50°N	3	8	35	66	75	32	22	5	1	2	3	0	263
	49°N	2	5	25	67	29	15	1	0	0	0	0	0	197
	48°N	0	5	18	46	57	23	8	0	0	0	0	0	157
Hibernia	47°N													

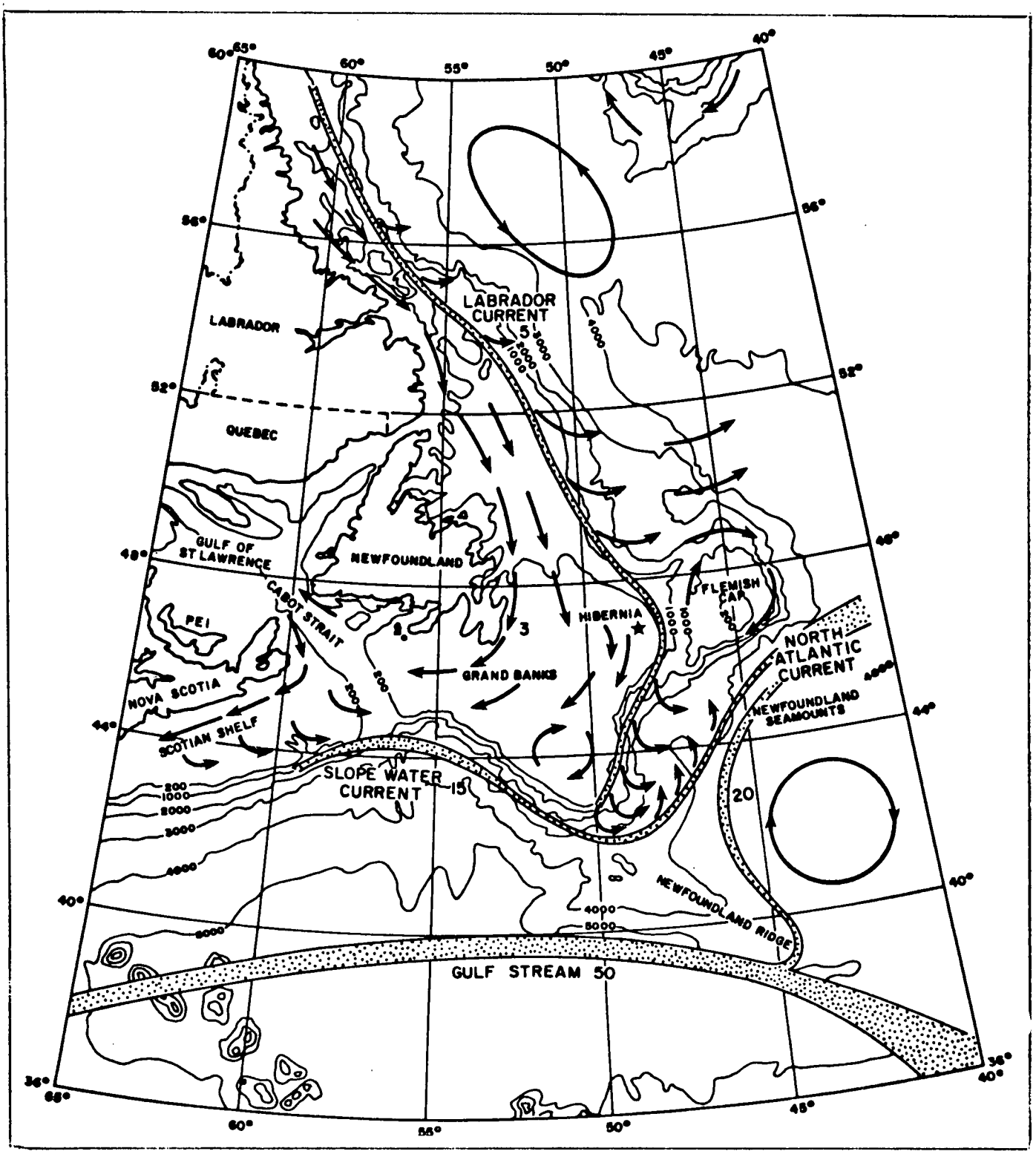

Figure 3. Map of iceberg hazard areas off Newfoundland. Currents are shown by arrows and dotted paths. Icebergs follow currents south to Grand Banks area from north of Labrador.

3.2.3 Waverider Information

Waverider buoy data are essential to quantify sea state objectively and to separate the effects of wind and waves on iceberg detectability. To minimize the potential for loss of data, provision has been made for two, recording waverider buoys. Directional buoys are not required because wave direction can be estimated reliably by observer, or from imagery or both. Experience with **BERGSEARCH '84** indicated that sea state was consistent over reasonably large areas, indicating that a buoy could be deployed in a convenient location for the duration of the experiment.

3.2.4 Reflectors

It is recommended that moored reflectors, arranged in a unique pattern, be used to fix a reference point on the imagery. Depending on how the reflectors are built, they could be used to assist in radar calibration, especially to assess effects of waves on small, bobbing targets.

4.0 COST ESTIMATES

Cost estimates for a nominal, six-week field experiment are given in Table 4, showing the fixed and variable costs. The sources of information for the estimates are given as well. The estimates are for typical values and are neither particularly generous nor conservative. However, they do assume that all the costs would have to be covered by the ESRF for the experiment and for the primary radar; other agencies might be willing to supply equipment. The cost of SAR has not been included because it is envisioned that this portion would be provided largely by the CCRS. Many of the items listed may be available at a reduced cost because of continuing operations in the area. No costs have been allowed for aircraft-of-opportunity, which might participate in the program. As in **BERGSEARCH '84**, it is expected that they would provide their data at no cost to the program in return for analysis of those data and for comparison with surface information.

Tables 5 and 6 show the cost reduction that would be possible by undertaking a two-week or four-week field program, instead of one of six weeks. Although savings could be achieved, clearly the substantial fixed costs would not allow savings of more than about 40% even for a shortened program. The disadvantage of a reduced program is that it is possible that the range of information required to solve the problem outlined in Chapter 1 would not be obtained.

TABLE 4

Cost estimates for six-week field program

	Basic/ Mobilization	Rate	/Unit	# Units	6-Week Usage Total	6-Week Total Cost	6-Week Section Totals	Information Source
1. RADAR AIRCRAFT								
Search radar	10.0	20	month	1.5	30.0	40.0		Eaton
Aircraft Install	50.0				0.0	50.0		INTERA
Basic flying		50	month	1.5	75.0	75.0		INTERA
Hourly flying		0.6	hour	90	54.0	54.0		INTERA
VCR Recorders	2.0				0.0	2.0		CANPOLAR
Air Stereo Camera	1.6	0.05	day	18	0.9	2.5		NORDCO
Film+processing	4.0				0.0	4.0	227.5	NORDCO
2. AERIAL PHOTOGRAPHY								
Atlantic KingAir	0.0	1.5	hour	30	45.0	45.0		Atlantic
Cameraman		0.25	day	6	1.5	1.5		Atlantic
Processing	5.0				0.0	5.0	51.5	Atlantic
3. SHIP, CREW, EQUIPMENT								
Polaris V & crew	5.0	5.5	day	15	82.5	87.5		NORDCO
Waverider buoy x2	3.0	5	month	1.5	7.5	10.5		NORDCO
Loran-C/Satnav	6.0	1.2	day	15	18.0	24.0		NORDCO
Mooring Equip.	2.0				0.0	2.0		NORDCO
Reflectors, Buoys	10.0				0.0	10.0		CANPOLAR
Cameras - 35mm	1.5				0.0	1.5		CANPOLAR
Polaroid x2	1.5				0.0	1.5		CANPOLAR
Shipbd. Stereo	0.0	0.05	day	40	2.0	2.0		NORDCO
Film + Process	2.0				0.0	2.0		CANPOLAR
Optical Ranger	1.0				0.0	1.0		CANPOLAR
Ship Personnel:								
WRB tech.		0.35	day	20	7.0	7.0		NORDCO
Ice Obs.		0.35	day	20	7.0	7.0		CANPOLAR
Ship Communicat.	5.0				0.0	5.0		CANPOLAR
Data Logger	4.0				0.0	4.0		CANPOLAR
Misc. Ship Equip.	20.0				0.0	20.0	185.0	CANPOLAR
4. GROUND SUPPORT								
Facility rental		5	month	2	10.0	10.0		CANPOLAR
Equipment	8.0	5	month	2	10.0	18.0		CANPOLAR
Consumables	5.0				0.0	5.0		CANPOLAR
Personnel (2)		0.35	day	65	22.8	22.8		CANPOLAR
		0.35	day	65	22.8	22.8	78.5	CANPOLAR
5. DATA TRANSCRIPTION & REPRODUCTION								
Full Bandwidth		0.7	hour	30	21.0	21.0		McMaster
Imagery		0.004	image	500	2.0	2.0	23.0	CANPOLAR
6. TRAVEL & LIVING								
Travel		1	trip	8	8.0	8.0		CANPOLAR
Living		0.1	day	125	12.5	12.5	20.5	CANPOLAR
7. ANALYSIS, INTERPRETATION & REPORT								
Senior scientists	10.0	0.5	day	55	27.5	37.5		CANPOLAR
Junior scientists	5.0	0.35	day	92	32.2	37.2		CANPOLAR
Research asst.'s	0.0	0.25	day	149	37.3	37.3		CANPOLAR
Travel	4.0	1.0	trip	8	8.0	12.0		CANPOLAR
Telephone	1.5	0.5	month	6	3.0	4.5		CANPOLAR
Subcont. Direct Expenses	1.5	3.0	month	3	9.0	10.5		CANPOLAR
Report Preparation	6.0	2.0	month	3	6.0	12.0	151.0	CANPOLAR
TOTALS:	174.6				562.4	737.0	737.0	

TABLE 5

Cost estimates for four-week field program

	Basic/ Mobilization	Rate	/Unit	# Units	4-Week Usage Total	4-Week Total Cost	4-Week Section Totals	Information Source
1. RADAR AIRCRAFT								
Search radar	10.0	20	month	0.0	0.0	10.0		Eaton
Aircraft Install	50.0			0.0	0.0	50.0		INTERA
Basic flying		50	month	0.0	0.0	0.0		INTERA
Hourly flying		0.6	hour	0.0	0.0	0.0		INTERA
VCR Recorders	2.0			0.0	0.0	2.0		CANPOLAR
Air Stereo Camera	1.6	0.05	day	0.0	0.0	1.6		NORDCO
Film+processing	4.0			0.0	0.0	4.0	67.6	NORDCO
2. AERIAL PHOTOGRAPHY								
Atlantic KingAir	0.0	1.5	hour	0.0	0.0	0.0		Atlantic
Cameraman		0.25	day	0.0	0.0	0.0		Atlantic
Processing	5.0			0.0	0.0	5.0	5.0	Atlantic
3. SHIP, CREW, EQUIPMENT								
Polaris V & crew	5.0	5.5	day	0.0	0.0	5.0		NORDCO
Waverider buoy x2	3.0	5	month	0.0	0.0	3.0		NORDCO
Loran-C/Satnav	6.0	1.2	day	0.0	0.0	6.0		NORDCO
Mooring Equip.	2.0			0.0	0.0	2.0		NORDCO
Reflectors, Buoys	10.0			0.0	0.0	10.0		CANPOLAR
Cameras - 35mm	1.5			0.0	0.0	1.5		CANPOLAR
Polaroid x2	1.5			0.0	0.0	1.5		CANPOLAR
Shipbd. Stereo	0.0	0.05	day	0.0	0.0	0.0		NORDCO
Film + Process	2.0			0.0	0.0	2.0		CANPOLAR
Optical Ranger	1.0			0.0	0.0	1.0		CANPOLAR
Ship Personnel:								
WRB tech.		0.35	day	0.0	0.0	0.0		NORDCO
Ice Obs.		0.35	day	0.0	0.0	0.0		CANPOLAR
Ship Communicat.	5.0			0.0	0.0	5.0		CANPOLAR
Data Logger	4.0			0.0	0.0	4.0		CANPOLAR
Misc. Ship Equip.	20.0			0.0	0.0	20.0	61.0	CANPOLAR
4. GROUND SUPPORT								
Facility rental		5	month	0.0	0.0	0.0		CANPOLAR
Equipment	8.0	5	month	0.0	0.0	8.0		CANPOLAR
Consumables	5.0			0.0	0.0	5.0		CANPOLAR
Personnel (2)		0.35	day	0.0	0.0	0.0		CANPOLAR
		0.35	day	0.0	0.0	0.0	13.0	CANPOLAR
5. DATA TRANSCRIPTION & REPRODUCTION								
Full Bandwidth		0.7	hour	0.0	0.0	0.0		McMaster
Imagery		0.004	image	0.0	0.0	0.0	0.0	CANPOLAR
6. TRAVEL & LIVING								
Travel		1	trip	0.0	0.0	0.0		CANPOLAR
Living		0.1	day	0.0	0.0	0.0	0.0	CANPOLAR
7. ANALYSIS, INTERPRETATION & REPORT								
Senior scientists	10.0	0.5	day	0.0	0.0	10.0		CANPOLAR
Junior scientists	5.0	0.35	day	0.0	0.0	5.0		CANPOLAR
Research asst.'s	0.0	0.25	day	0.0	0.0	0.0		CANPOLAR
Travel	4.0	1.0	trip	0.0	0.0	4.0		CANPOLAR
Telephone	1.5	0.5	month	0.0	0.0	1.5		CANPOLAR
Subcont. Direct Expenses	1.5	3.0	month	0.0	0.0	1.5		CANPOLAR
Report Preparation	6.0	2.0	month	0.0	0.0	6.0	28.0	CANPOLAR
TOTALS:	174.6			0.0	0.0	174.6	174.6	

TABLE 6

Cost estimates for two-week field program

	Basic/ Mobilization	Rate	/Unit	# Units	2-Week Usage Total	2-Week Total Cost	2-Week Section Totals	Information Source
1. RADAR AIRCRAFT								
Search radar	10.0	20	month	1.0	20.0	30.0		Eaton
Aircraft Install	50.0			0.0	0.0	50.0		INTERA
Basic flying		50	month	0.8	37.5	37.5		INTERA
Hourly flying		0.6	hour	40.0	24.0	24.0		INTERA
VCR Recorders	2.0			0.0	0.0	2.0		CANPOLAR
Air Stereo Camera	1.6	0.05	day	0.0	0.0	1.6		NORDCO
Film+processing	4.0			0.0	0.0	4.0	149.1	NORDCO
2. AERIAL PHOTOGRAPHY								
Atlantic KingAir	0.0	1.5	hour	15.0	22.5	22.5		Atlantic
Cameraman		0.25	day	3.0	0.8	0.8		Atlantic
Processing	4.0			0.0	0.0	4.0	27.3	Atlantic
3. SHIP, CREW, EQUIPMENT								
Polaris V & crew	5.0	5.5	day	7.0	38.5	43.5		NORDCO
Waverider buoy x2	3.0	5	month	1.0	5.0	8.0		NORDCO
Loran-C/Satnav	6.0	1.2	day	0.0	0.0	6.0		NORDCO
Mooring Equip.	2.0			0.0	0.0	2.0		NORDCO
Reflectors, Buoys	10.0			0.0	0.0	10.0		CANPOLAR
Cameras - 35mm	1.5			0.0	0.0	1.5		CANPOLAR
Polaroid x2	1.5			0.0	0.0	1.5		CANPOLAR
Shipbd. Stereo	0.0	0.05	day	14.0	0.7	0.7		NORDCO
Film + Process	2.0			0.0	0.0	2.0		CANPOLAR
Optical Ranger	1.0			0.0	0.0	1.0		CANPOLAR
Ship Personnel:								
WRB tech.		0.35	day	9.0	3.2	3.2		NORDCO
Ice Obs.		0.35	day	9.0	3.2	3.2		CANPOLAR
Ship Communicat.	4.0			0.0	0.0	4.0		CANPOLAR
Data Logger	4.0			0.0	0.0	4.0		CANPOLAR
Misc. Ship Equip.	20.0			0.0	0.0	20.0	110.5	CANPOLAR
4. GROUND SUPPORT								
Facility rental		5	month	1.0	5.0	5.0		CANPOLAR
Equipment	6.0	5	month	1.0	5.0	11.0		CANPOLAR
Consumables	5.0			0.0	0.0	5.0		CANPOLAR
Personnel (2)		0.35	day	30.0	10.5	10.5		CANPOLAR
		0.35	day	30.0	10.5	10.5	42.0	CANPOLAR
5. DATA TRANSCRIPTION & REPRODUCTION								
Full Bandwidth	5.0	0.7	hour	0.0	0.0	5.0		McMaster
Imagery		0.004	image	0.0	0.0	0.0	5.0	CANPOLAR
6. TRAVEL & LIVING								
Travel		1	trip	4.0	4.0	4.0		CANPOLAR
Living		0.1	day	0.0	0.0	0.0	4.0	CANPOLAR
7. ANALYSIS, INTERPRETATION & REPORT								
Senior scientists	10.0	0.5	day	24.0	12.0	22.0		CANPOLAR
Junior scientists	5.0	0.35	day	40.0	14.0	19.0		CANPOLAR
Research asst.'s	0.0	0.25	day	68.0	17.0	17.0		CANPOLAR
Travel	4.0	1.0	trip	4.0	4.0	8.0		CANPOLAR
Telephone	1.5	0.5	month	3.0	1.5	3.0		CANPOLAR
Subcont. Direct Expenses	1.5	3.0	month	2.0	6.0	7.5		CANPOLAR
Report Preparation	6.0	2.0	month	0.0	0.0	6.0	82.5	CANPOLAR
TOTALS:	175.6			0.0	244.8	420.4	420.4	

5.0 PROJECT MANAGEMENT STRUCTURE

An organizational structure for the project is laid out in Figure 4. Unlike **BERGSEARCH '84**, this structure has a single, prime contractor responsible to the ESRF for project management and for subcontract arrangements. The advantage of this arrangement would be that co-ordination of the various diverse aspects of the project could take place cost effectively. However, care would be required to assure that various commercially competitive interests are fairly represented and that scientific objectivity is maintained.

The prime contractor for the project should have at least the following qualifications:

- expertise in the area of iceberg detection by radar;
- project management expertise, especially in field situations;
- ability to bring all the required subcontractors into the program; and
- financial responsibility.

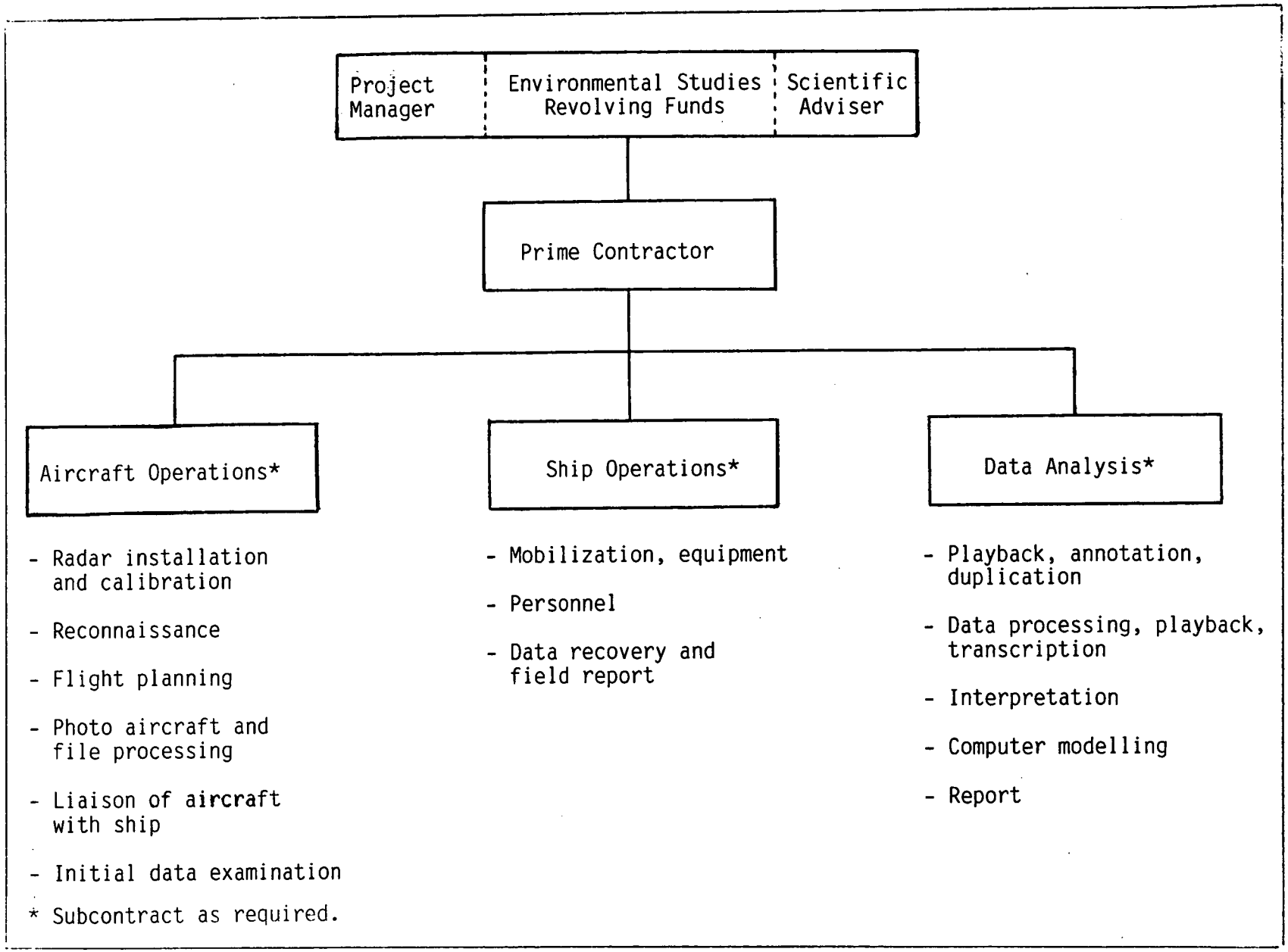

Figure 4. Possible project organization.

6.0 REFERENCES

Rossiter, J.R., L.D. Arsenault, E.V. Guy, D.J. Lapp, E. Wedler, B. Mercer, E. McLaren, and J. Dempsey. 1985. Assessment of airborne imaging radars for the detection of icebergs, Environmental Studies Revolving Funds, Report No. 016. Ottawa. xvii + 321 p.

Currie, B.W., and S. Haykin. 1985. Experimental evaluation of Eaton airborne radar for iceberg detection. CRL Report No. 142, McMaster University, Hamilton, 2 vols.

CANPOLAR Consultants Ltd. and INTERA Technologies Ltd. 1985. Continuation of analysis of the spring '84 ESRF aircraft radar iceberg data 'Examination of SAR asimuth smear', Report to Energy, Mines and Resources Canada. 60 p.

APPENDIX A

Side-Looking Airborne Radar (SLAR)

SIDE-LOOKING AIRBORNE RADAR (SLAR)

Prepared by

CANPOLAR Consultants Ltd.

Toronto, Ontario

March 1986

SIDE-LOOKING AIRBORNE RADAR (SLAR)

INTRODUCTION

In this section real-aperture SLAR systems that are available for iceberg detection are reviewed. A summary of previous work is given by Rossiter et al. (1985), including the results of **BERGSEARCH '84.**

These are all operational systems, and several have been used by several agencies (MARS, AES, IIP) for ice and iceberg detection for a number of years. They therefore provide a baseline against which newer radars can be compared.

The major limitation of real-aperture radars is their fixed azimuthal beamwidth, which gives azimuthal resolution that increases linearly with range to target. Since the beamwidth is controlled by the size (and, to some extent, by the construction) of the antenna, there is a practical limit to the beamwidth of approximately 0.45^{o}, giving resolution of about 8 m/km.

SLAR's differ from search radars in having a fixed antenna which senses only perpendicularly to the aircraft's motion. New area is covered as the aircraft moves, and no processing of data is carried out in real time.

SPECIFICATIONS

Five radars were examined for this study: Motorola AN/APS-94D, -94E, and -135, the Canadian Astronautics Limited (CAL) SLAR-100, and the INTRADAN MAPR. Specifications are given in Table 1. The three Motorola radars participated in **BERGSEARCH '84**, and their performance appeared to be comparable at the relatively short ranges used in that experiment. The CAL radar is new. It is currently undergoing acceptance trials, but is not likely to be available before Summer 1986. The INTRADAN radar has been used extensively for ice surveillance, but has not been evaluated for iceberg detection.

DISCUSSION

The major advantages of SLAR are the large swath coverage possible, given adequate power, and the relative simplicity compared to SAR and surveillance radar. Although the simplicity might lead to lower operational cost, there is no evidence of improvement in reliability or significantly lower size, weight and power consumption. Use of the widest swath coverage (100 and 150 km per side) is probably not practical for detecting small icebergs for several reasons: the azimuthal resolution degrades substantially; the depression angle of observation becomes very small; and the higher flying altitude required is not optimum for nearer targets.

The results of **BERGSEARCH '84** showed that although the SLAR's did not perform as well as the SAR's, the differences were not enormous. Of significance was the relatively poor output film format used by the SLAR's. It was felt that significantly better practical performance could be obtained with higher resolution plotters and monitors. Also none of the SLAR's used in **BERGSEARCH '84** had data tape recording facility which limited quantitative analysis of the results. Tape recording should be included in future evaluation experiments.

The SLAR's usually are flown at altitudes of 4,000 to 20,000 feet. Lower altitudes, and hence smaller depression angles, tend to reduce the sea clutter. However, lower depression angles may also increase wave obscuration, and lower altitudes preclude use of the widest swaths. Of practical concern is the increased turbulence often associated with lower altitudes. The Motorola SLAR's have gimballed antenna motion compensation (for yaw); the newer SLAR's compensate digitally with INS information; and correct for roll though adjustment in the STC applied. It is not clear how big a performance improvement digital compensation provides. However, it presumably reduces maintenance over mechanically compensated systems.

SLAR's with digital recording capability have some pulse-to-pulse integration capability (typically 64 pulses) in azimuth. Analog systems provide integration through visual integration of film output. Integration times are a small fraction of a second, and output is controlled largely by the antenna azimuthal beam pattern, including side lobes.

SLAR's differ in two additional ways from SAR's, which use doppler processing. SAR imagery of floating icebergs consistently shows azimuthal smearing of iceberg targets, presumably because of their motion and/or motion of the surrounding ocean (CANPOLAR and INTERA, 1985). This phenomenon could conceivably reduce the intensity of weak target echoes below a detection threshold. On the other hand, rain echoes appear shifted out of the SAR doppler pass band, and therefore do not appear on imagery, whereas they occasionally do appear on SLAR images.

Iceberg data interpretation for SLAR is performed primarily by annotation of small targets on film. These are often difficult to see and can be missed or confused with dust, etc. To date no automated target detection on enhancement schemes have been attempted. Acquisition of digital data from more modern SLAR's may make this possible.

RECOMMENDATIONS

SLAR's are currently being used for operational ice surveillance by the two major agencies charged with iceberg detection (AES and IIP). These radars will likely be used for iceberg detection for several years, and therefore should be used as a basis for comparison with other radars. Experimental use should include at least one of the newer digital SLAR's (SLAR-100 and/or MAPR) and data should be recorded on digital tape to permit post-processing and quantitative comparison. The advantages and disadvantages of wide swath coverage should be examined as well as optimum altitudes. Advantages of multiple passes should be better quantified.

REFERENCES

Rossiter, J.R., Arsenault, L.D., Guy, E.V., Lapp, D.J., Wedler, E., INTERA Technologies Ltd., Dobrocky Seatech Ltd., F.G. Bercha and Associates Limited (1985) "**BERGSEARCH '84** Assessment of Airborne Imaging Radars for the Detection of Icebergs", Environmental Studies Revolving Funds, Report No. 016, 321 pp.

CANPOLAR Consultants Ltd. and INTERA Technologies Ltd. (1985) "Continuation of Analysis of the Spring '84 ESRF Aircraft Radar Iceberg Data 'Examination of SAR Azimuth Smear'", prepared for Energy, Mines and Resources under contract 05SQ.23413-4-9082, 59 pp.

TABLE 1: SLAR Systems Specifications

All are X-band and look right and left simultaneously. Specifications from operators; some are approximate and/or subject to change.

Radar, Manufacturer and Model	Motorola AN/APS-94D	Motorola AN/APS-94E	Motorola AN/APS-135 (SLAMMR)	Canadian Astronautics Limited SLAR-100	INTRADAN (TERMA) MAPR
Operator	MARS Ltd.	AES	USCG-IIP	AES	INTERA Technologies Ltd.
Aircraft	Grumman G-1	Electra	HC-130	Dash-7, Electra	Cessna 441
Peak transmit power (kw)	65	45	200	200	20
Polarization	HH	HH	VV	HH	HH
Azimuth resolution (m/km)	8	8	8	7	9
Range resolution (m)	30	30	30	35	40
Antenna gain (dB)	35	35	35	37	34
Swath widths (km) each side	25, 50, 100	25, 50, 100	25, 50, 100, 150	25, 50, 100	25, 50, 100 (output) 20, 40, 80 (monitor)
Pulse repetition frequency (Hz)	750 avg.; 700-800	750	750	800 avg. (770-830)	1000 (slaved to ground speed)
Minimum detectable signal (dBw)	-130	-128	-129	-131	-130
Pulses integrated	64 (digital)	-	-	64	approx. 64

...continued

TABLE 1: SLAR Systems Specifications...continued

Radar, Manufacturer and Model	Motorola AN/APS-94D	Motorola AN/APS-94E	Motorola AN/APS-135 (SLAMMR)	Canadian Astronautics Limited SLAR-100	INTRADAN (TERMA) MAPR
Antenna length (m)	5	5	5	5.1	3.7
Antenna elevation beam pattern	csc^2	csc^2	csc^2	modified csc^2	Gaussian
Motion compensation	Gimballed antenna for yaw -------->			Digital	Digital
System weight (kg)	385	?	?	250 + mounting hardware	250
Power consumption approx. (kw)	1.5	1.5?	1.5?	1.5	1.3
Display type(s)	Wet negative film ---------->			Edo-Western dry silver film; CRT monitor (optional)	Visor-S print or film; CRT monitor
Useable film width (mm)	200	200	200	200	200
Film Resolution (mm)	0.07	0.07	0.07	0.07	0.1
Annotation	Time marks; printer notes	Time marks	Lat/long grid; ADAS block	Lat/long grid; 64 char. ADAS block	Event marks
Data recording	Miller CCT	Kennedy CCT	No	Digital optional	CCT
Downlink	Fax	Fax	-	Digital downlink	Digital downlink
Cost (approximate)	N/A	N/A	N/A	Not yet specified	$400 k purchase

APPENDIX B

Review of SAR Systems with Respect to Iceberg Detection Capability

REVIEW OF SAR SYSTEMS WITH RESPECT TO ICEBERG DETECTION CAPABILITY

Provided by
INTERA Technologies Ltd.
Calgary, Alberta

Provided for
Canpolar Consultants Ltd.
Toronto, Ontario

October 1985

R85-181

TABLE OF CONTENTS

Figure 1. Bergsearch '84 STAR-1 Data.
This image, taken from a standard Video display on a VAX-780, shows both ice and icebergs in heavy sea clutter. The bergs show the typical iceberg smear in the along track (up/down on this photo) direction.

Figure 2. Enhanced Bergsearch '84 STAR-1 Data.
This image shows the same data as are shown in figure 1, but after digital enhancement on the ERIM VAX-780. This form of analysis could be accomplished onboard user's vessels on the downlink/receiver (STAR-VUE) currently being field tested by INTERA.

1. INTRODUCTION

Airborne Synthetic Aperture Radar (SAR) systems have become standard tools in ice reconnaissance in most areas of the North, but have not yet been adapted for iceberg reconnaissance. There are numerous non-technical reasons for this, but there are also gaps in the understanding of how they function for this task which must be filled in. A combination of further study of existing data, analyses of scenarios of use and further data collection and analysis are required to adequately establish the place of SAR of iceberg detection.

SAR systems offer many advantages for iceberg reconnaissance. Firstly, they are the established best sensor for ice mapping, a task often needed in parallel with iceberg mapping. They cover a larger area more rapidly and with a finer resolution than any other all-weather sensor. However, SAR has been developed to map stationary targets in a stationary background. The motion of both the sea and the icebergs combines to produce an effect known as 'iceberg smear'. This is an apparent broadening of target response in the azimuth or along-track dimension of the SAR image. Although visually undesirable, it is not clear if this effect inhibits SAR iceberg detection. Indeed, it is known that it has certain significant positive aspects. However, the overall effect is not totally understood.

This report is aimed at establishing a SAR iceberg detection experiment for the spring of 1986. The first task undertaken is a review of available SAR systems (and data analysis systems) which could be used for this. In fact, this means either STAR-1, or, if it becomes available, the new CCRS radar which shares many significant features with STAR-1.

There is a substantial review of SAR 'smear' and ways to handle it, since this is the main outstanding feature of SAR imagery. Some study results on the handling of SAR

imagery with smear will be presented. The report concludes with a recommended study plan which could lead logically into an extended data collection and analysis program which would further delineate SAR's already demonstrated very fine performance.

2. SAR SYSTEM REVIEW

Synthetic Aperture Radars SAR(s) can produce very fine resolution images of the earth's surface and are, as a result, prime candidates for iceberg reconnaissance. Experiments have shown, however, that the complex interaction between the radar, the ocean surface and the iceberg creates effects which limit the radar's effectiveness compared to land-based targets, namely, iceberg "smear". It is therefore necessary to review briefly not only the normal specifications for radars, but those operational aspects which are related to imaging and smearing of icebergs.

There are very few SAR's actually operating that are potentially available to conduct iceberg surveillance or experiments (see Table 1). With the decommissioning of the SAR-580, STAR-1 is the only available system with real-time processing. In 1986, two more radars will appear, based on the same MacDonald Dettwiler and Associates real-time, digital, azimuth processor used on STAR-1; the CCRS's C-band IRIS (MDA's new SAR radar series) and INTERA's STAR-2 using an X-band IRIS. The C-band system will be designed to conduct experiments from the CCRS CV-580, whereas STAR-2 will be optimized to survey large areas rapidly.

Because the motion of icebergs and the ocean is such a critical element in SAR imaging of icebergs, it is necessary to concentrate on those SAR parameters which most affect imaging of moving scenes. These include the dwell time of the beam, which of course includes beam width, aircraft speed and altitude.

The real aperture radar transmits a pulse of duration T, which can locate a target in range with a resolution of roughly cT/2 (c = speed of light). The azimuth or along-track position can be located to within the beam width of the antenna "β" which is related to antenna length "L" and wavelength λ as

$$\beta = \lambda / L$$

Table 1. Summary of airborne SAR systems in use or in development.

SYSTEM	FREQUENCY POLARIZATION	RESOLUTION (M) Az	RESOLUTION (M) Rg	LOOKS NO.	SWATH WIDTH KM	PLATFORM	ALT. RANGE (KM)	REC. PROC.	AVAILABILITY
STAR-1 INTERA	X HH	6	6,12	1-7	25,50	Cessna 441	1-10	Digital real-time downlink	yes
STAR-2 INTERA	X HH	8	4,16	1-7	16,65	Cessna 441	1-10	Digital real-time downlink	mid-1986
Goodyear GEMS AN/APQ-120 Aero Service	X HH	10	12	1	37	Caravelle	8-13	Optical ground processor	yes
IRIS MDA/CCRS	C HH/V C VV/H	6,11	7,19	1-7	27,65	CV-580	1-6	Digital real-time	early-1986

The transmitter will typically illuminate a target many times during a beam width and those returns will be incoherently added to improve signal to noise ratio.

In a synthetic aperture radar, range resolution is a function of signal processing which happens at very high frequency. It can effectively be ignored for most iceberg considerations and the range resolution is used as specified. Azimuth resolution in SAR is achieved by recording returns from targets for a number of pulses, then coherently processing them into a single output value. In the case of all the SAR's using the MDA processor, this is done several times for each target and these returns are incoherently added, as in a SLAR, to improve "signal to noise". This is variously known as incoherent averaging or multi-looking. The movement of the aircraft drives this process, but the aircraft speeds are only 1-2 orders of magnitude faster than the wind/wave effects of the ocean surface. Therefore, although an image is formed, it is corrupted by the ocean surface motion. Therefore, in addition to the normal specifications for SARs, considerable detail will be given on the SAR's motion sensitive aspects of dwell time, doppler pass band etc.

2.1 STAR-1

As STAR-1 is the only radar studied that is currently flying, a greater amount of information is available to describe it. Further, as the azimuth processor used is the basis for the processors of the other two radars soon to be available, it is relevant to the performance expected from future radars to study STAR-1 in detail.

In Table 1, the STAR-1 system is described in overview. Those statistics, combined with some further details are discussed below.

2.1.1 Physical Beamwidth (β)

The physical beamwidth of the antenna, combined with range, determines how long a target is illuminated. For STAR-1, it is calculated as follows:

$\beta = \lambda / L$

$\lambda = 3.10^{-2}$ m (wavelength)

L = 1 m (antenna length)

$\beta = 3.10^{-2} \simeq 1.8°$

2.1.2 Multilooking, Doppler Bandwidth and Effective Dwell Time

The doppler bandwidth of the full beam β as it transits a target is given by

$$\Delta fd = \frac{2V_r}{\lambda} \simeq \frac{2V\beta}{\lambda} \simeq V/\beta$$

where V = platform velocity. (STAR-1, V=120 m/s)

$\rho = L/2$ is the theoretical optimum azimuth resolution for a fully focused SAR

However, the STAR-1 azimuth processor is a multilook look processor in which each of 7 azimuth beams or sub-apertures is separately processed (coherently), co-registered spatially, and summed incoherently.

The sub-aperture beamwidth or single-look beamwidth is nominally 1/7 of the full beamwidth. Due to critical sampling constraints, it is actually about 1/14 of the physical beamwidth.

Since the ultimate determinant is the actual azimuth resolution (ρ_n = 6 m), we shall use it to determine the 'effective' single look beamwidth βe of STAR-1 in this discussion.

That is,

$$\beta e = \frac{\lambda}{L} = \frac{\lambda}{2\rho_n}$$ where ρ_n = nominal azimuthal resolution = 6m

This gives $\beta_e \simeq 2.5 \cdot 10^{-3} \simeq 0.15°$

The effective dwell time (integration time) T is given by

$$R\beta_e = VT$$

or $$T = \frac{\lambda}{2\rho_a} \frac{R}{V}$$

With STAR-1 operated in the High Resolution mode (1:125 000 scale), targets will be within the range bounds 20-45 km. Typically the ground velocity is 120 m/s $\pm$ 20 m/s.

Therefore the bounds on dwell time are:

$$\frac{R}{V} \simeq (140\text{-}450)\ s$$

and $$T \simeq (0.35 - 1.12)\ s$$

Using STAR-1 in the wide swath mode, the maximum range increases to 70 km for the second half of the swath (R $\simeq$ 45-70 km, and the dwell times increase to T $\approx$ (0.8-1.75)s.

2.1.3 STAR-1 Multilook Configuration

The STAR-1 azimuth processor can be set up such that each of the 7 looks can be turned on and off independently. It should be noted that the parameters previously described do not change with this selection. If N < 7 looks is chosen, the chosen looks are processed and summed, while the remainder are not included in the summation. Each of the 7 looks will coherently and independently process the azimuth doppler spectrum over the dwell time T. The looks are then co-registered spatially and

summed incoherently. This is equivalent to stacking the single look images on top of one another.

The time varying properties of the target may change over a period longer than T. This means that the azimuth smear may differ in width and intensity from one look to the next. For example, sinusoidal swell motion has a typical period of 10 sec. Thus each sub-aperture will be sampling a different swell velocity component ranging from zero to maximum velocity.

If such velocity were the only source of smear, then we would expect single-look imagery to show much more variability over an ensemble of moving targets than 7-look imagery. The latter would show an 'average' smear width for all targets since it is sampling and summing 7 portions of the wave form of each oscillating target.

During the ESRF program the early data (April 2,3) were collected at 7 looks, the later data (April 5,6,7) were collected at 3 looks. Unfortunately, no single-look data were collected. It appears that had a large sample of targets been imaged at 7 look and then 1 look settings, it would have indicated whether long period movement was responsible for the smear as opposed to short period phenomena such as scatterer decorrelation.

2.1.4 Dwell Time Consequences

The motion-induced azimuthal smear originates with an expression for target kinematics given by ($X=vt + 1/2 A^2 t^2$ where 'x', 'v' and 'A' are the displacement, velocity and acceleration of the target respectively. This expression is valid for constant acceleration and is inappropriate in general for oscillatory motion. However, provided the period of such motion $T_w >> T$, the expression is a reasonable approximation within T. Since T=0.35 - 1.1 sec, the approximation should be adequate for T_w > 8 sec as was observed during the ESRF project.

A very important consequence occurs when the target has a coherence time $\tau < T$. Only the coherent portion of the source signal is processed coherently and this causes the resolution to be degraded (ie. smear width increased) proportionately to (T/τ) in the limit of $\tau << T$.

This would, for example, apply for τ = 10-100 ms as has been observed from capillary scattering of waves. On the other hand, breaking waves are thought to have longer ($\tau \approx 1$ sec) while it is not at all clear 'a priori' what would be associated with iceberg decorrelation.

2.1.5 Bandwidth Limitations

The doppler frequency of a target whose radial velocity component is V_r is given by

$$f = 2Vr/\lambda$$

In order for this target to be imaged, f must be within the doppler bandwidth of the processor, Δfd

That is, $|f| < \Delta fd$

fd represents the total bandwidth of all the sub-apertures being summed. For example, if all 7 looks are being processed,

$\Delta fd = 1/2\,\lambda/P$ where V = 120 m/s

= 120 Hz $\rho = L/2$

ρ = 0.5 m

The factor (1/2) is due to use of the effective beamwidth, which is reduced from the full beamwidth, as noted earlier.

If the number of looks being processed is less than 7, the effective bandwidth is given by

$\Delta fd = (N/7)$ 120 Hz where n = 1 to 7

During the latter part of Bergsearch '84, STAR-1 was set at n=3. Hence

$$fd = 50 \text{ Hz}$$

This implies that for this data set, any targets with radial velocity component

$$Vr > \lambda/2\Delta fd$$

$$> 0.75 \text{ m/sec} \simeq (1.5 \text{ knots})$$

would not be imaged.

Should the target possess a radial velocity component such that its doppler frequency lies outside the bandwidth of the individual sub-apertures but within the total effective bandwidth, the target will be processed in adjacent sub-aperture(s). However, the target intensity will vary with the number of sub-apertures in which the target was processed. For example, if the target radial velocity was such as to shift its doppler frequency beyond the first sub-aperture, the image intensity would be reduced by 1/7 (or 1/3 if the processor was operating in the 3-look mode, for instance).

On the other hand, there is no differential mis-registration in spatial position caused by this bandwidth limitation.

The implication for the Bergsearch '84 data set of all this is that:

1. Since average iceberg velocities are typically less than 2 knots, they are not likely to be lost due to the 3-look processing, although their intensity could be reduced in some instances.

2. Moving vessels viewed from orthogonal directions could very easily be lost in one of these directions.

3. Rainfall return is often outside the passband and does not appear to cloud the image.

4. Icebergs which are rolling in swell may be lost for at least some looks, if their instantaneous velocity is sufficiently high.

5. Although the energy is smeared in azimuth, and sea/iceberg returns saturate the doppler spectrum, the contrast between smeared bergs and smeared sea returns is still quite high.

2.1.6. Special Far Range Doppler Processing

There is an additional complicating factor that slightly alters some of the previously described limitations for STAR-1 data analysis. Owing to the nature of the processor, the total multi-look bandwidth is a function of range. Thus the total bandwidth, fd=120 Hz is relevant to near range, while at far range, it is reduced to about 60 Hz. The consequences must be altered accordingly. For later models of the MDA processor, this limitation is far less noticeable.

The same factor is responsible for maintaining the total multilook dwell time constant at about 1.7 sec, with respect to range. This weakens the image stacking effect described in Section 2.1.3, as there is less difference in the time separation of the samples experienced by the different multi-look configurations.

These qualifications do not affect the rest of the arguments advanced; these depend upon the dwell-time, bandwidth and beamwidth of a single sub-aperture.

2.2 STAR-2

Intera has contracted MDA to produce an X-band IRIS, using the motion compensation and processor from the CCRS C-band IRIS, and the X-band transceiver from the Litton

V5 radar. The radar is scheduled for delivery and systems testing to be completed by mid 1986. At this time many of the details of the operation of the radar have not been specified. For example, although the system will be capable of operating in a jet, it will likely be placed in a turbo-prop. As this will change both ground speed and the aircraft ceiling, it could substantially change the system dwell time. For example, it was estimated in the previous section that the dwell time for STAR-1 would vary from 0.35 s at near range, with a tail wind, to 1.755 at maximum range with a headwind. In a jet at 350 knots and 40,000 ft, this would become a range of 0.2 to 1.3 sec.

Since STAR-2 will not be available until the second half of 1986, and the details of the operational parameters will not be defined until early 1986, the analysis conducted in the rest of this report will concentrate on STAR-1.

2.3 SAR-580-X-L-C RADAR

This radar system no longer exists. The aircraft is being used to develop the CCRS C-band IRIS, and the radar has been re-purchased by ERIM. It is planned to upgrade the radar somewhat, replacing some obsolete equipment (i.e. steam driven film recorders) and place it in a US military aircraft to do oceanographic experiments. It could be available to do experiments at some time in the future, but when, under what terms, and with what characteristics is not currently known.

2.4 C-BAND IRIS

The CCRS radar is not expected to be available to conduct experiments until the first quarter of 1986, at the earliest. Again, the details of its configuration will probably be unknown until that time. However, it is possible to make some assumptions. Using a C-band source, with a 1 metre antenna, the dwell time will increase, as does the

antenna beamwidth. By flying lower, and using a portion of the swath, it should be possible to achieve dwell times of the same order as STAR-1, if not slightly shorter. The somewhat higher response of the ocean at C-band could be more than offset by the ability of the C-IRIS to record cross-polarized returns.

2.5 DOWNLINKS AND DATA ANALYSIS

In the past, it was neither possible or practical to have imagery analyzed in near real-time, except as film aboard the aircraft. With the development of fully digital SAR and SLAR systems and downlink systems, this has changed. It is now practical to have all relevant information available not only in real-time aboard a vessel, but also in a form and in a system that makes its analysis straightforward and very practical.

Digital downlinks for SAR's have a line-of-sight range up to 200 n.mi. or more, depending on aircraft height. The latest generation are based on small, special purpose imagery processing computer systems. They place great analysis power in the hands of the shipborne user, while at the same time freeing him/her of the large data handling tasks. Image enhancement techniques which remove the effects of iceberg smear, for example, become quite practical.

These systems are both robust and relatively inexpensive and can be deployed on shore or on vessels. They are designed for the end-user to operate them, <u>without</u> months of intensive special training, thus supplying information directly to the person responsible for taking action to avoid iceberg hazards.

3. IMPLICATIONS OF SYSTEM PARAMETERS

3.1 RESOLUTION

In a SAR, as with other radars, finer resolution is generally desirable, but there is a price to pay. In this section we will discuss these trade-offs.

Resolution is a commonly understood term, but in detail is rather poorly defined for a SAR. For the purposes of this discussion, we will refer to the -3 db points on the impulse response, and assume care has been taken to reduce sidelobes to a negligible level. The range and azimuth resolutions are usually independent and, for the most part, are generated in separate parts of the radar. Range resolution is generated at RF 'speed' so surface motion can be ignored. This is not so for azimuth resolution. We will discuss these separately.

In all the SAR systems under active discussion (STAR-1 or later), range resolution is generated using a SAW device, and the range of resolutions is from 3 to 20 metres. In the simplest case, when detecting a target whose reflectivity σ_t is greater than that of the background σ_b, the size of the pixel of resolution pack should be small. To detect a target of a size A_t which is smaller than a resolution cell A_b, requires that

$$A_t \sigma_t > A_b \sigma_b$$

Clearly making A_b smaller makes smaller targets detectable, thus finer range resolution is desirable. Unfortunately, with the ocean as a background, this is not always the case. While the average sea return may go down with decreased area (A_b), the variance goes up. With very fine resolution, this results in returns from the ocean which look like targets. These so-called 'sea-spikes' seriously limit the applicability of fine resolution real aperture radars without extensive long-term averaging (more than 10 sec).

Azimuth resolution in a SAR is proportional to beamwidth, or doppler pass band. This means that increasing beamwidth will result in finer resolution, but it will take a longer time to create a longer synthetic aperture for a given velocity of aircraft. This is why fine resolution SAR systems are always associated with azimuth smear. This is not entirely negative since it has the effect of evening out sea returns and eliminating 'sea-spikes'. It has been pointed out by Lyzenga (ERIM Private Communication) that preferential smearing of sea-spikes compared to iceberg targets improves the contrast of the iceberg to the ocean.

3.2 DYNAMIC RANGE

The dynamic range associated with modern SAR systems is generally more than adequate for any surveillance task. Although doppler processing tends to result in a lower gain for moving targets than would be expected for stationary targets, SAR systems still see a very substantial range of target and background brightnesses.

3.3 MULTI-LOOKING

Insufficient experimental data have been collected to detail the exact effects of multi-look processing on SAR imagery of icebergs in sea clutter. The effect of trading between full doppler pass band processing and multi-looking can be simulated merely by averaging the output scene. However, the MDA processor has multiple looks which can be independently turned on and off, each covering a separate doppler pass band. This could (at least in an average statistical sense) be used to study the coherence times of the different components of azimuth smear. A better approach, however, would be to study directly the doppler spectrum of the CCRS radar signals, in the CCRS radar processor.

4. SMEAR MECHANISMS AND THEIR IMPLICATION

During a detailed study conducted for CCRS/Radarsat, an analysis of SAR smear mechanisms was conducted (Canpolar 1985). Numerous aspects of the interaction between the radar, the sea and the iceberg were analyzed to see which were candidates for causing the observed phenomena. In this section we will briefly review what was discovered during that study, and what remains to be done as a result.

The interaction between radars and stationary targets does not show smearing of targets return. From this observation and rudimentary analysis of SAR imaging mechanisms, it is obvious the combination of sea and berg motions cause the smear. In the report to CCRS/Radarsat, both the separate motion of the ocean and of icebergs was considered, as well as the joint effect. The conclusions from the theoretical analysis were that a combination of effects was the most probable candidate for berg smearing. Specifically, the icebergs and the sea around them (both of which are in motion) both return energy to the radar. However, the dihedral return from the berg and sea surface is probably the predominate source of azimuth smear. This results in a signal which, when capillary action is added to the effects examined, totally fills the doppler spectrum. We are then left with the following observations:

1. An iceberg which is not submerged in swell will directly return to the radar enery that is little smeared, but may be shifted from its 'stationary' position in the image by a relatively small amount.
2. The sea return from around a berg may be enhanced by the froth and splash, but the primary source of smear energy comes from the dihedral effect between the ocean and the berg. This return will saturate the doppler spectrum and produce smear as observed.

It should be noted that although the energy from the iceberg is thus smeared and the resultant target images are elongated in one dimension, the iceberg return is still there. This is an important point because it implies that the detectability problem is really one of image aesthetics. This point is emphasized in Figures 1 and 2. Figure 1 shows a digital image of icebergs (taken during Bergsearch '84) from STAR-1. The image has not been optimally displayed and so looks somewhat inferior to the icebergs scenes previously published. Figure 2 shows the same iceberg scene digitally enhanced by scientists at ERIM. There is a dramatic improvement in the aesthetics of the image, but in the detailed comparison, it is hard to say whether any of the bergs visible in the second image were not also visible in the second image.

The Bergsearch '84 data cannot be relied upon for answering questions on SAR capability and have not been as fully analyzed as possible. However, it should be noted that there was a very high detection success rate under the conditions of ESRF Bergsearch. The biggest uncertainty is 'how much does performance deteriorate with increasing seastate?' The observations on SAR's capability to detect icebergs are accordingly far from complete.

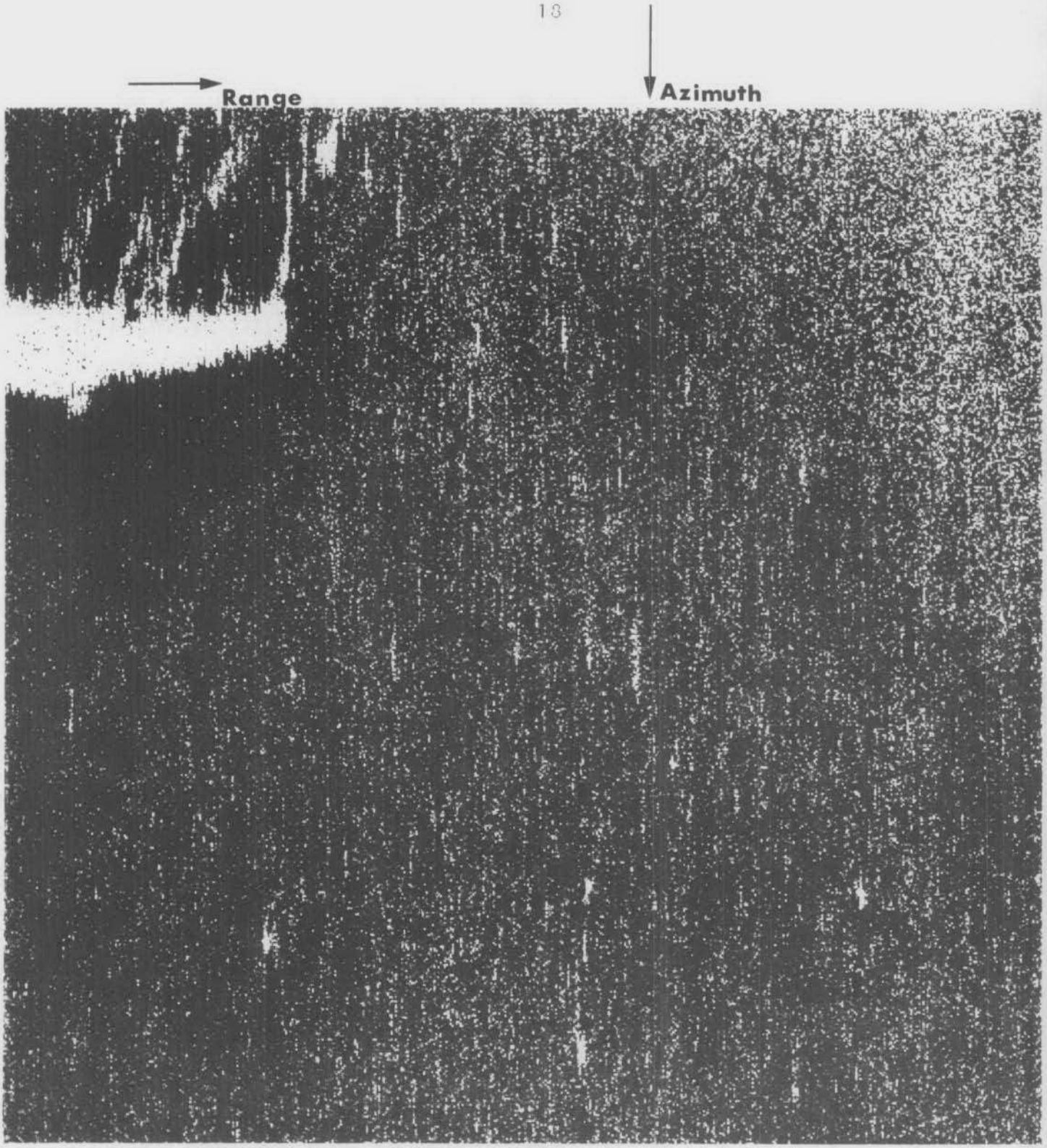

Figure 1. Bergsearch '84 STAR-1 Data.
This image, taken from a standard Video display on a VAX-780, shows both ice and icebergs in heavy sea clutter. The bergs show the typical iceberg smear in the along track (up/down on this photo) direction.

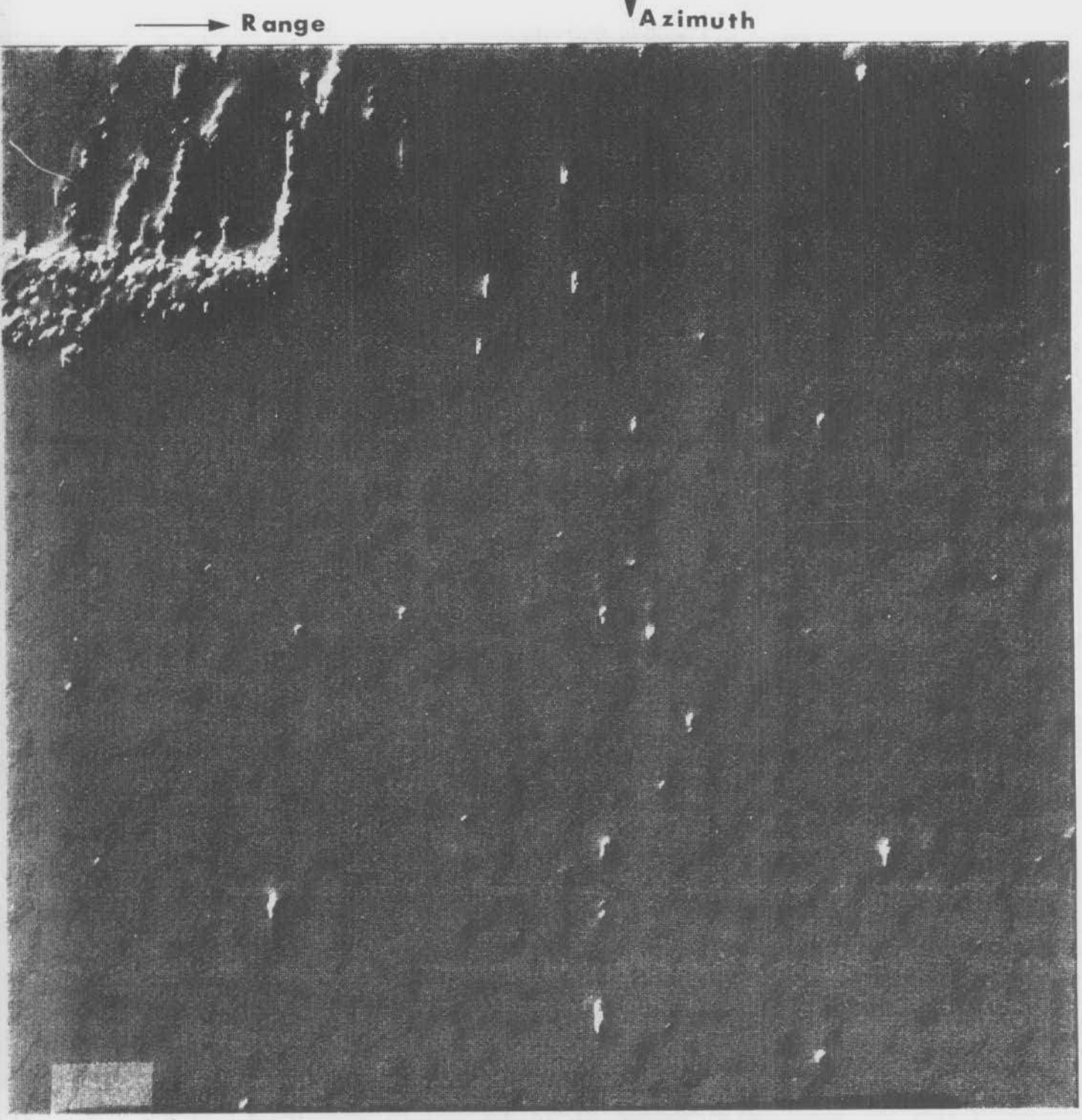

Figure 2. Enhanced Bergsearch '84 STAR-1 Data.
This image shows the same data as are shown in figure 1, but after digital enhancement on the ERIM VAX-780. This form of analysis could be accomplished onboard user's vessels on the downlink/receiver (STAR-VUE) currently being field tested by INTERA.

5. QUESTIONS REMAINING AND POSSIBLE SOURCES OF ANSWERS

There is an incentive to solve the problems of iceberg suveillance with SAR because:

1. SAR systems are available and are being used for regular ice reconnaissance;
2. Because they are being used, no long term development is needed to support a potentially small and unforeseen development on the east coast;
3. SAR can be reliably used to develop the needed ice reconnaissance on the east coast, which is the other half of the ice management problem; and
4. SAR covers large areas very rapidly, reliably and at a very reasonable cost.

For smaller icebergs there are two questions relating to operational requirements that should be clarified:

1. What is the cut-off size below which it is not necessary to accurately locate icebergs? It is possible to detect or predict whether small icebergs will be in an area using a combination of surveillance for larger icebergs and simple thermodynamic and drift modeling to predict the lifetime and drift of the small bergs. Large bergs will be tracked, small bergs will be given as an area population density, for example: What is the cut-off size? and
2. How, if at all, does this size vary with seastate, ice conditions, sea temperature etc?

This implies a study of a systematic approach to iceberg management, which will drive the surveillance requirements.

There are also several technical questions to answer about SAR imaging of icebergs.

1. It is clear that if an iceberg is covered with a wave while it is being viewed by the SAR, it will not be detectable. As a function of seastate, it is necessary to estimate the probability that icebergs of given size will not be detected due to submergence;
2. In the absence of smear of the iceberg return, modeling predicts that icebergs would be detectable to the resolution limit of the radar (say 6 x 6 m) in any seastate, as sea clutter 'saturates' at high wind speeds. That is, if the berg is seen above the water, it should return energy enough to be detected. Small bergs of 10-20 metres in very high seastates (30 knot winds or more) can only be observed with SAR; and
3. Although 'smear' does exist, it is in and of itself an indication of a berg. We have shown images above in which smear has been 'compressed' and the aesthetics of the image improved. The question is, does the smear energy take away from the berg return, or is it merely added to it, making bergs more easily detected, with appropriate image processing as is suggested by theoretical analysis.

6. RECOMMENDED FURTHER STUDY

6.1 FURTHER DATA ANALYSIS

There are a number of data sources which have not been adequately analyzed. Fhe Bergsearch '84 data have been compiled and, as part of a CCRS/Radarsat funded study, partially analyzed. However, some fundamental observations remain to be made. These include an analysis of berg signature in light and moderate seas to study the relative strength of the smear and berg return. There are also SAR/ship observations containing 'smear' which have not been adequately studied to establish relative returns.

Since the dihedral effect can be reduced to a bistatic radar problem using a 'perfect planer' iceberg, the literature on the doppler spectrum of bistatic radar observations of the ocean should be reviewed. This will further validate or disprove this model, and perhaps throw some light on the role of the froth and foam around icebergs.

Before more data are collected, both these studies should be completed.

6.2 FURTHER DATA COLLECTION

During the Bergsearch experiment of 1984, a number of trials were run on SAR and SLAR in an atmosphere of SAR vs SLAR without adequate concentration on the mechanisms by which images of icebergs are formed by SAR. It seems clear, especially in view of the research into SAR imaging mechanisms that has taken place in the intervening time, that a subsequent experiment is needed. Its objective should be clearly aimed at understanding the mechanisms for imaging icebergs with SAR and how to optimize those images. Below are listed a number of factors and a first cut at an experiment to isolate the effects.

6.2.1 Seastate

During Bergsearch '84 only moderate seastates were encountered. It would be desirable to have the same group of bergs imaged under low, medium and high sea states. Since the models and data show that the entire doppler spectrum saturates with energy at moderate seas, it could be argued that as long as the bergs are not under water during the time the SAR images them, the imagery will not degrade beyond the medium seastate, or at least will degrade much less rapidly than real aperture and search radars. This could be relatively easily verified.

6.2.2 Synthetic Aperture Dwell Time

During the Bergmap '84 experiment, the data collected by the SAR-580 and STAR-1 differed substantially in the way the ocean was imaged. The SAR-580 saw waves quite effectively, while STAR-1 did not. The difference was largely attributed to dwell time of the synthetic aperture. By flying STAR-1 at lower altitudes and steeper angles, shorter dwell times (with narrow swaths) may be achieved. Times that will be associated with jets could be simulated. There is likely a trade-off between increased sea-spikes and reduced azimuth smear at very short times. Exactly where this is would need to be determined empirically.

6.2.3 Number of Looks

As STAR-1 (and all MDA processors) are set up with independently operated looks, it is possible to examine in detail the operation of the multilooking. Looks 1 and 7 are farthest apart, with look in the middle. Although it is not possible to freeze the ocean surface, new passes every 20 minutes are possible, and with surface-truth, it should be possible to have a statistically valid experiment to compare the degree of signal to clutter improvement available in multi-looking.

6.2.4 Resolution

Neither the C-band IRIS or the STAR-1 SAR can provide a wide variety of range resolutions. C-IRIS is planned to have differing resolution in azimuth as well as range to preserve the number of looks on wide swath to the edge of the coverage. STAR-1 has constant resolution but varies the amount of the doppler spectrum per look beyond a 37 km range. It is therefore not easy to simulate exactly the effect of variable resolution. In range this can be partially simulated by averages of pixels but no azimuthal effects can be simulated except as dwell time is also simulated. This should be considered with dwell time. Old SAR-580 data are more flexible in this respect, and should be analyzed.

6.2.5 Signal Processing

It is possible with special processing to greatly improve image quality. A study should be launched to test the applicability of signal processing strategies to detection of icebergs in SAR imagery. This would parallel work being done at CRC to study the imaging of ships on the ocean. The prime data source for this would again be old SAR-580 data.

7. SUMMARY

SAR systems are likely candidates for iceberg reconnaissance systems both because they are available and being used for ice reconnaissance, and because they offer the possibility of excellent and reliable iceberg detection and tracking over wide areas. The potential of SAR has, however, been clouded by the existence of unpleasant-looking 'smear' associated with iceberg signatures. A theoretical analysis of smear shows that it should not affect the detection capability of SAR, and may indeed help it. The visual effect is easily removed using simple image processing techniques that are available on inexpensive, field-deployable image analysis/downlink systems.

The main test of SAR for iceberg detection, Bergsearch '84, yielded an incomplete data set which has been incompletely analyzed. Specifically, it lacked data for very high seastates. Theoretically, SAR should be less obscured by high seastates than real aperture radars. This needs to be validated.

A recommendation for data analysis on existing data is made. Specifically, an attempt needs to be made to establish if the azimuth smear is '<u>in addition</u>' to the target return, as predicted by current theories, or if it takes energy from the target return by some other mechanism. Both the Bergsearch '84 and SAR data from other sources need to be analyzed.

The largest hole in the existing SAR data is for icebergs in heavy seas. An experiment to fill this hole would answer the question of whether SAR performance deteriorates further theoretically predicted good detectionability under these conditions.

Finally, since small bergs are only found close to large bergs, for short lifetimes, a systematic iceberg detection, tracking and prediction study should be considered.

APPENDIX C

Airborne Radars for Ice Surveillance

CRL REPORT SERIES

NO. CRL-146

AIRBORNE RADARS FOR ICE SURVEILLANCE

B.W. CURRIE AND S. HAYKIN

September 1985

This report was prepared for Canpolar Consultants Ltd.

TABLE OF CONTENTS

LIST OF FIGURES

LIST OF TABLES

1. GENERAL SURVEILLANCE-RADAR INFORMATION

1.1 TARGET COVERAGE

There are three angles generally referred to in airborne radar work: incidence, depression, and grazing. Incidence angle is the angle at which the radar signal impinges on the target, measured with respect to the vertical, and usually at the target location. Depression angle is the angle at which the radar signal is transmitted with respect to the horizontal at the radar. Grazing angle is the angle at which the radar signal impinges on the target, measured with respect to the horizontal at the target. Because of the curvature of the earth, depression and grazing angle are not exactly equal. Using the four-thirds earth radius approximation to account for signal propagation, Nathanson (1969) gives the following expressions for depression angle α and grazing angle ψ:

$$\alpha \simeq \sin^{-1}\left\{\frac{h}{R} + \frac{R}{2r_e}\right\} \qquad (1) \quad \text{depression angle}$$

$$\psi \simeq \sin^{-1}\left\{\frac{h}{R} - \frac{R}{2r_e}\right\} \qquad (2) \quad \text{grazing angle}$$

where h = radar altitude

R = slant range

r_e = 4/3 actual earth radius

For small ranges R, the term $R/2r_e$ can be ignored, and depression and grazing angles taken as equal.

Figure 1 diagrams a sideview of the coverage of the surveillance radar beam. As the radar antenna rotates, it illuminates an annulus centred on the radar location. The width of the annulus is determined by the vertical beamwidth of the antenna. To move the beam footprint in range, the antenna boresight can be varied by adjusting the tilt of the antenna. The maximum slant range Rs_{max} for a given radar altitude h is the range at which the grazing angle equals zero, called the radar horizon. From (2), this range is $Rs_{max} = \sqrt{2hr_e}$. Minimum slant range Rs_{min} is the radar altitude h, although target detection for grazing angles near 90^{o} is impractical due to high clutter power.

1.2 TARGET DETECTION

The essence of target detection is to have some measurable difference between the signals from the target and the background interference. For the radars of concern here, that difference must appear in the signal amplitude. The target and interference signals are characterized by a mean amplitude and a distribution about that mean. Detection generally involves the setting of a decision threshold as shown in figure 2. Associated with the threshold are a probability of detection (P_D) and a probability of false alarm (P_{FA}). The detection performance depends on the separation of the target and interference distributions, determined by their means, and called the target-to-interference ratio (TIR). Typically a TIR of 12 db gives

$P_D = 0.5$ at $P_{FA} = 10^{-6}$, while a TIR of 14 db gives $P_D = 0.9$ at

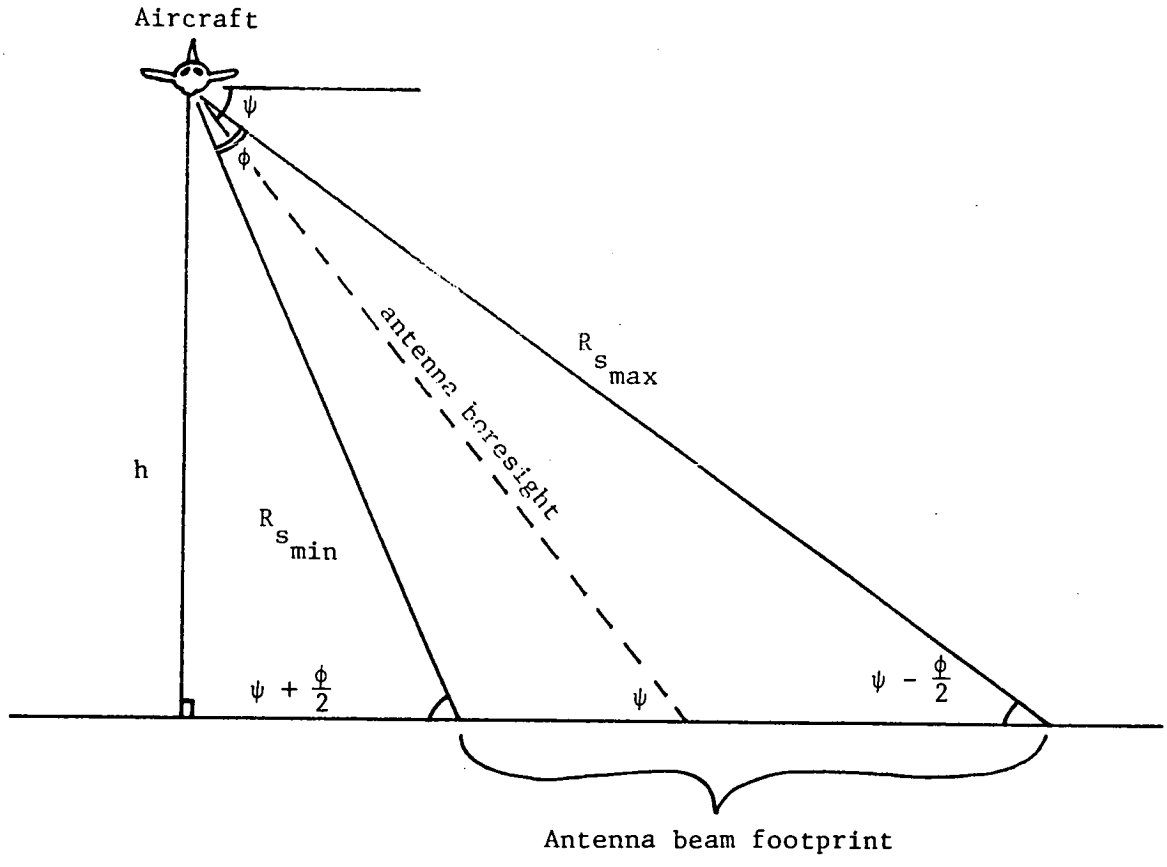

Figure 1: Geometry of surveillance radar coverage.

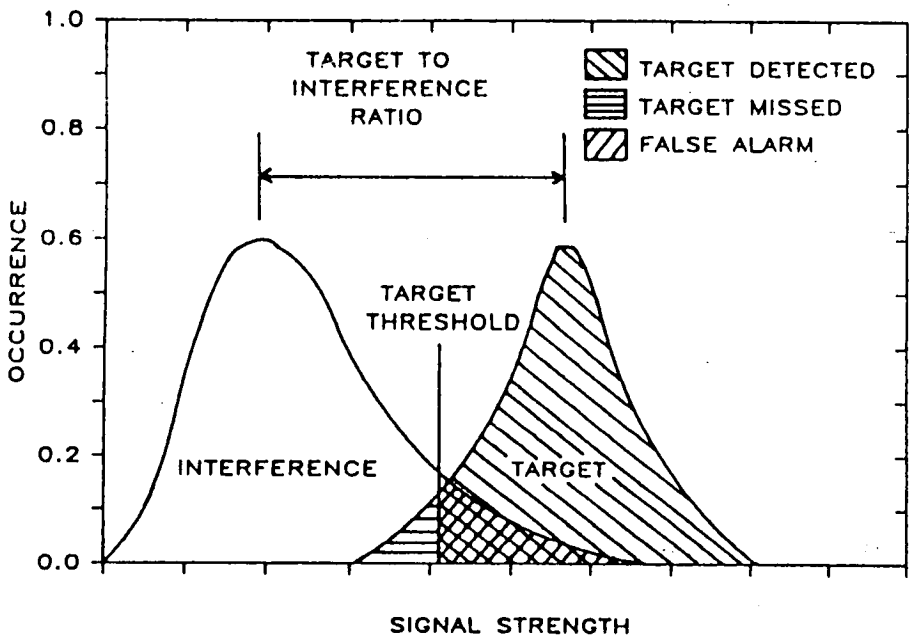

Figure 2: Target detection process. Target and interference returns are statistically distributed. Target-to-interference ratio is determined by the mean values. Probabilities of detection and false alarm are determined by the distributions and the target threshold setting.

$P_{FA} = 10\text{-}6$.

Consider now how these various return signal powers are estimated.

1.2.1 Noise

The background noise power in the radar is given by kTBF, where k is Boltzman's constant (1.4×10^{-23} W/Hz ^{o}K); T is the system noise temperature, usually taken as 290 ^{o}K; B is the receiver bandwidth, usually taken as $1/\tau$ where τ is the transmitted (compressed) pulse length; and F' is the receiver noise figure. For a typical pulse length τ of 30 ns (i.e. B = 33.3 MHz) and noise figure F' of 4 db ($= 10^{0.4}$), the system noise power N is

$$N = kTBF'$$

$$= 1.4 \times 10^{-23} \frac{W}{Hz\ ^{o}K} (290\ ^{o}K)\ 33.3 \times 10^{6}\ Hz\ 10^{0.4}$$

$$= 3.4 \times 10^{-13}\ W$$

$$= 3.4 \times 10^{-10}\ mW$$

$$= -94.7\ dbm \qquad (3)$$

The units dbm are 10 log P, where P is power in milliwatts. This noise power is constant, that is, independent of range and bearing. The amplitude of the noise signal is Rayleigh distributed, and successive noise samples taken in range can be considered to be uncorrelated.

1.2.2 Target

For a point target, the usual radar equation giving expected return power P_r is

$$P_r = \frac{P_t G^2 \lambda^2 F^4}{L(4\pi)^3 R^4} \sigma_t \qquad (4)$$

where P_t = transmitted power

G = antenna gain

= radar wavelength

R = range

L = system and atmospheric losses

F = propagation factor

σ_t = target radar cross-section

For a pulse compression radar, the term P_t should be the effective peak power transmitted, that is, actual peak power times the compression factor.

For a fixed target cross-section σ_t of say, 1 sqm, typical of a small target, the return power reduces as range R to the fourth power. For 50% detection performance at $P_{FA} = 10^{-6}$ for a target in noise only, the target to noise ratio, P_r/N, must be at least 12 db.

For typical radar parameters of

P_t = 4000 kW (effective)

G = 32 db

λ = 3.2 cm (X-band)

L = 4 db

F = 1

σ_t = 1 sqm

and requiring P_r = N + 12 db with N = -94.7 dbm, the maximum range of detection would be 13.3 nm. This range can be extended with target-to-noise ratio improvements derived from

signal processing, such as signal integration.

1.2.3 Clutter

For an airborne radar looking down on the ocean, the sea surface presents an area of clutter, not a point return as for the target. This area return is characterized by a normalized radar cross-section per unit area, σ^o, times the actual area of the radar resolution cell. The cell area is determined by the (effective) pulse length τ in range and the horizontal beamwidth θ in bearing, and is given by $(\frac{c\tau}{2})\ R\theta\sec\psi$, where c is the speed of light and ψ is grazing angle. To calculate the expected return clutter power, the term σ_t in equation (4) is replaced with the clutter cross-section σ_c, given by

$$\sigma_c = \frac{c\pi}{2} R\theta \sec\psi \sigma^o \qquad (5)$$

giving

$$P_r = \frac{P_t G^2 \lambda^2 F^4}{L(4\pi)^3 R^3} \frac{c\tau}{2} \theta\sec\psi \sigma^o \qquad (6)$$

Note that now the return clutter power drops as R^{-3}, not R^{-4} as for the point target.

The value of σ^o to be used depends on a number of factors, for example, wind and sea conditions, grazing angle, and polarization. For example, figure 3 graphs σ^o versus grazing angle for sea states 2 to 5, horizontal polarization, taken from tabulated values in Nathanson (1969). Consequently, reliable prediction of sea clutter power is difficult, and

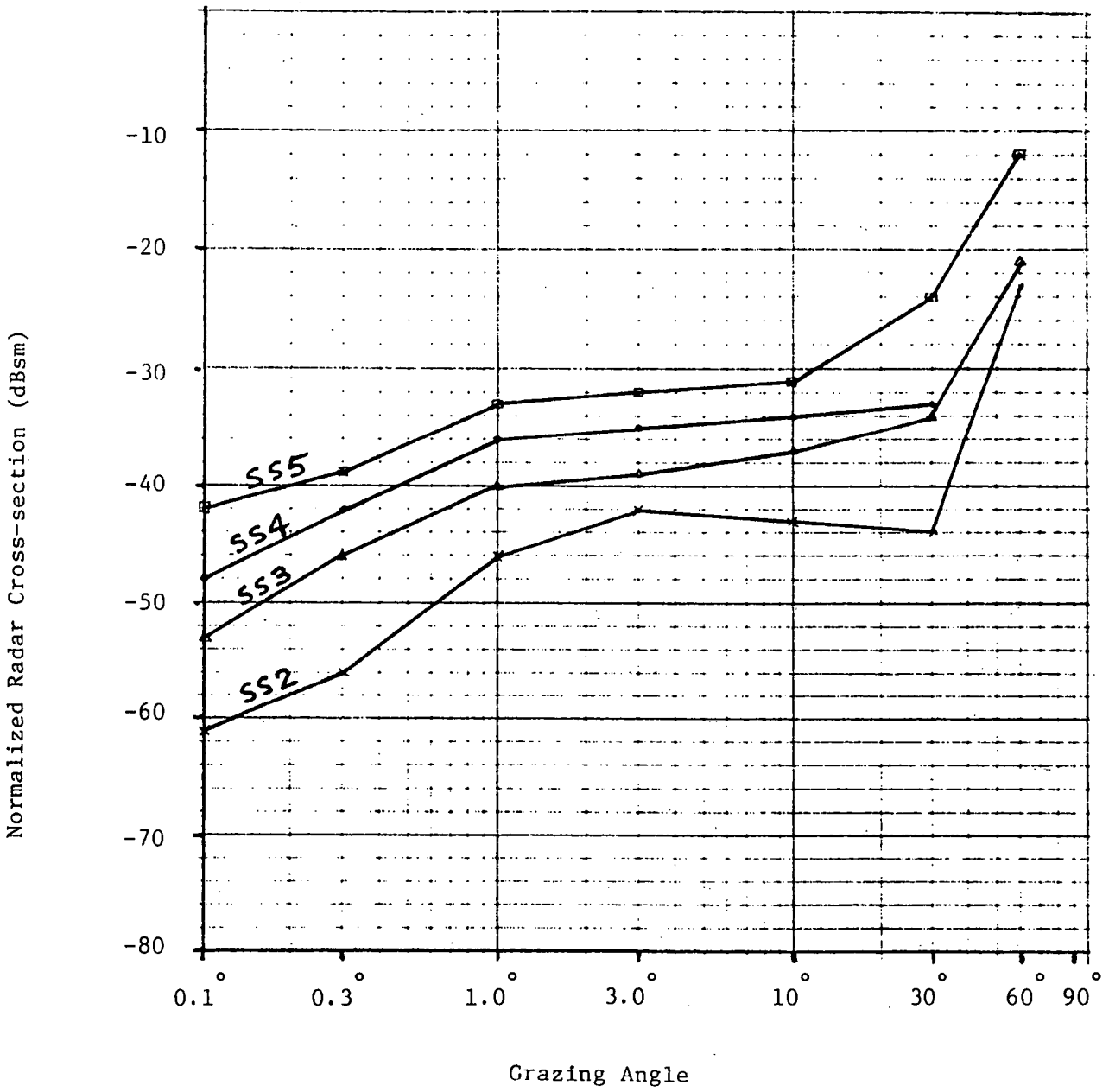

Figure 3: Normalized radar cross-section versus grazing angle for sea states 2 to 5. (from Nathanson [1]).

requires a detailed description of the operating conditions.

The statistics of sea clutter return depend on the same factors as does σ^o, and unlike noise, cannot be considered to be uncorrelated in range and time.

1.3 RADAR DESIGN CONSIDERATIONS

The basic aim in radar design is to maximize the return power from the target while reducing the clutter and noise powers. This involves two major topics: (1) selection of radar equipment parameters, which is governed by practical considerations, and (2) use of signal processing techniques to reduce the effects of clutter and noise. Topic 1 primarily involves reducing the mean clutter and noise powers, while topic 2 deals with the statistics of the clutter and noise returns.

1.3.1 Radar Parameters

Consider first the radar equipment parameters. For noise reduction, see equation (3), the noise figure F is about the only controllable variable, but modern radars are already at the practical limit of 3-4 db. The bandwidth B is dictated by the transmitted pulse length.

For the target, see equation (4), more parameters are available. To obtain reasonable beamwidths from a physically manageable antenna size, assume X-band operation, hence λ about 3 cm. The losses L, such as in waveguide components, is assumed to be minimized in the radar installation design. The antenna gain, G, can be increased, but with the mitigating requirements for a fan beam, a reasonable antenna size, and reasonably low sidelobes. Finally, the transmitted power, P_t,

can be increased. For an uncoded RF pulse, high power transmitters become impractical for airborne use due to increased size and power requirements. Pulse compression can instead be used to produce high effective peak powers while using only moderate actual peak powers. However, pulse compression systems require coherent transmitters, which have (actual) peak power limitations. Note that as the compressed pulse length reduces, the noise power increases since receiver bandwidth must also increase.

For clutter, see equation (6), the return power also increases with P_t so that increasing P_t only improves the target-to-noise ratio, not the target-to-clutter ratio. The same comment applies for antenna gain G and loss L. The major way of reducing mean clutter power is to reduce the radar resolution cell area, determined by pulse length τ and horizontal beamwidth θ. The pulse length can be reduced through pulse compression. The beamwidth θ is determined primarily by the physical size of the antenna, which obviously has a practical maximum. The antenna must also have a reasonably large vertical beamwidth to provide simultaneous illumination of the ranges of interest.

1.3.2 Signal Processing

Next consider techniques which operate on the statistics of the radar returns. Examining figure 2, for a fixed target-to-interference ratio, the P_D and P_{FA} are determined by the width of the distributions and the size and extent of the overlapping 'tails' on the distributions. If the

distributions can be made narrower and the tails reduced, the P_D and P_{FA} could be maintained with less separation between the distributions. That is, a lower target-to-interference ratio would be required. This resulting reduction in TIR is the signal processing improvement factor.

A basic method of reducing the width of the distributions (or more correctly, considering distributions of a new variable based on the return signal) is to average (or integrate) several return samples. The distributions of the averaged returns are narrower, yielding a TIR improvement factor. The noncoherent (i.e. amplitude only) integration improvement factor is between $\sqrt{n}$ and n, where n is the number of independent samples integrated. The effectiveness of the integration depends on the independence of the samples. Sea clutter, especially for short-pulse radars, has two component decorrelation times: the capillary waves decorrelate in the order of 10 ms, while the large sea waves give rise to spikey returns, with decorrelation times in the order of a few seconds. The desire is to decorrelate the sea clutter samples before integration so as to derive maximum integration improvement. Two decorrelation techniques used for the two components of the sea return are frequency agility and scan-to-scan processing.

Frequency agility With a typical pulse repetition frequency (PRF) of 2 kHz, successive pulse samples will only be 0.5 msec apart. With even the fast sea clutter fluctuations decorrelating in a few msec, successive-pulse sea clutter samples will be nighly correlated, yielding little integration

gain. Changing the radar frequency (by more than the inverse of the pulse length) between pulses will alter the phase relationship of the various capillary wave scatterers, and provide an independent return sample. However, frequency agility only decorrelates the capillary wave, i.e. fast fluctuating, component of the sea clutter. It does not decorrelate the slower spikey return (Trunk (1972), Ward (1982)). Frequency agility also improves the target return by reducing radar frequency-dependent fading and glint. Lind (1970) reported that frequency diversity was calculated to yield a 6 db improvement due to sea clutter decorrelation, and a further 8 db improvement in the target return.

Scan-to-scan integration The only effective way to handle the slowly fluctuating component of sea clutter is to wait for it to decorrelate with time. The total time taken however should be short enough that the target will not move significantly (e.g. to a different resolution cell). In this situation, scan-to-scan processing is useful. Samples from successive scans are spaced on the order of 0.2 to 2 seconds, so that over several scans even the sea spikes will decorrelate. Typically, to obtain more samples in a fixed period of time, the antenna is rotated faster (60-300 rpm) than in a 'normal' surveillance radar, yielding the term fast-scan processing. In addition to simple averaging, other detection schemes are used. For example, a threshold can be set and if the return exceeds the threshold on M out of N successive scans, a target is declared. This is the M-of-N detector.

Constant-False-Alarm-Rate (CFAR) Processing Figure 2 showed the detection process for a given target-to-interference ratio. Knowing the mean return amplitudes for the target and interference, and the shapes of the distributions, the theoretical P_D and P_{FA} can be calculated for a given threshold. In practice, the difficulty is setting the threshold when the mean amplitudes and distribution shapes change with time. Equations (4) and (6) show that the return power for the target and clutter depend on range R as R^{-4} and R^{-3} respectively. The clutter power, based on σ^o, varies dynamically with grazing angle and sea conditions. The purpose of the CFAR processor is to estimate the local mean interference level, which can then be subtracted from the return at that location to give a time-invariant return amplitude distribution, against which a fixed threshold can be applied to yield a predicted P_D and P_{FA}. A typical CFAR averages samples taken spatially about the target cell of interest in order to generate the mean interference amplitude estimate. If the CFAR processor underestimates the mean interference level, the threshold will be too low, and the P_{FA} will rise. Overestimation of the level will lower the desired P_D.

1.4 USE OF DIGITAL CIRCUITRY

As digital technology improves in speed and capability, more of the radar processing after video detection is being done digitally. Once the radar video has been digitized, the performance of the processing circuitry is predictable and repeatable. It is also amenable to computer simulation. Use of digital memories driving raster-scan

displays allows bright display of the radar video together with an alphanumeric overlay. A number of gray levels can be presented, and the memory allows a variety of scan-to-scan combination techniques with selectable decay rates.

Because of the repeatability of digital logic, the circuitry can be designed to contain built-in test functions to help isolate any failure, facilitating quicker repair.

2. REVIEW OF INDIVIDUAL RADARS

2.1 TEXAS INSTRUMENTS AN/APS-134(V)

The TI APS-134 radar is designed for maritime surveillance, with special attention to periscope detection. The radar in fact has three modes of operation:

Mode I is optimized for the low-altitude detection of periscope-size targets of limited exposure time. The compressed pulse equates to a range resolution of less than 1.5 feet, which closely matches the physical dimension of periscope and snorkel classes of targets. The rapid scan antenna rotates at 150 rpm to provide the necessary S/S processing gain in a short time. Maximum range in this mode is 32 nmi.

Mode II is the navigation and weather avoidance mode and is designed for maximum sensitivity against land and other distributed targets. The techniques associated with the fast-scan modes emphasize point target detection while rejecting distributed or area targets (i.e., sea clutter). Therefore, this mode employs a slow antenna rotational rate and an uncompressed waveform. Maximum range is 150 nmi.

Mode III provides high-altitude maritime surveillance to ranges of 150 nmi. Again, the use of pulse compression and fast-scan processing allows detection of patrol/fishing-boat size targets and larger under all sea conditions. These targets are continuously exposed and longer integration times (i.e. S/S processing intervals) can be employed. Thus, the antenna rotational rate can be slowed to 40 rpm to minimize processing losses.

Table 1 lists the system parameters of the AN/APS-134(V).

In mode I, the radar uses a 500 MHz bandwidth linear FM pulse compression technique, transmitting a 0.5 μs pulse, then compressing it to 2.5 ns (3 ns after weighting), a 23 db compression factor. The actual peak power is 500 kW, generated using a travelling-wave tube/cross-field amplifier assembly. This high power permits long range target detection in noise in the other modes. The design criteria dictated the need for periscope detection within 5 seconds; consequently a high antenna scan rate was used. However, Smith (1984) indicates that for continuous-exposure targets, scan speeds between 40 and 120 rpm can be used.

Because of the very narrow compressed pulse width of 3 ns, the digital signal processor and display cannot handle the very large bandwidth raw data. Instead, the video is thresholded for noise removal, then peak detected with pulse stretching in range to reduce the data rate. Clutter is removed through scan-to-scan integration. Three loops of range-gated automatic gain control provide user controllable constant-false-alarm-rate operation.

The display is a 512 x 512 raster. Because the radar video data has already been thresholded and targets extracted before display, this display resolution is felt to be sufficient. The display has an interesting mode called multi-level processing. The display has 8-bits per pixel, allowing theoretically 256 intensity levels. The display allows the background returns, e.g. land or sea, to integrate up to about

TABLE 1. AN/APS-134(V) SYSTEM PARAMETERS

Antenna	
Radar	
Gain	35 dB (nominal)
Azimuth beamwidth	2.4 degrees
Elevation beamwidth	4.0 degrees
Sidelobes	Down at least 20 dB
Polarization	Vertical
IFF (integral)	Standard IFF interrogator sets monopulse compatible
Scan speed	
Mode I	150 rpm
Mode II	6 rpm
Mode II	40 rpm
Transmitter	
Peak power	500 kW
Average power	500 W
Frequency	
Mode I, III (linear FM sweep)	9.5 to 10.0 GHz
Mode II (random frequency agility)	9.6 to 9.9 GHz
PRF (four-pulse stagger)	
Mode I	2,000 pps
Mode II, III	500 pps
Pulsewidth	0.5 μs
Receiver	
Noise figure (system)	4.5 dB
Intermediate frequency	
Mode I, III	1300 MHz
Mode II (dual conversion)	1300 MHz and 100 MHz
IF bandwidth	
Mode I, III	500 MHz
Mode II	2.4 MHz
Pulse compression gain (Mode I, III)	23.0 dB
Compressed pulsewidth (Mode I, III)	2.5 ns
AGC	Three loops, CFAR

one-third full intensity, but no more. Discrete targets can integrate up to the full intensity, making them visible as bright spots on the subdued radar background. This background clutter mapping may be very useful for ice pack mapping, with strong point targets such as icebergs being distinguishable from the pack.

The following images, figures 4 to 7 supplied by TI, show the effect of some of these processing and display features.

2.1.1 Performance

TI supplies graphs of radar performance, such as the one in figure 8. The graph shows the minimum target cross-section required for 50% probability of detection at a false alarm rate of one in a million, 10^{-6}. For example, a 1 sqm target can be detected out to 23 nm in sea state 3, with noise in fact being the limiting factor. Table 2 summarizes the maximum range of detection, maximum sea state, and maximum flight altitude versus target cross-section for 50% detection at $P_{FA} = 10^{-6}$. Note that as the target size of interest increases, the detection range and flight altitude, hence radar coverage, increase significantly.

2.1.2 Size, Weight, Reliability

Figure 9 shows an excerpt from the ASP-134 Specifications manual, listing the size and weight of the various components, which are pictured in figure 10. The total weight is 582 pounds. Figure 11 indicates the power budget for most of the components. The TI representative indicated that

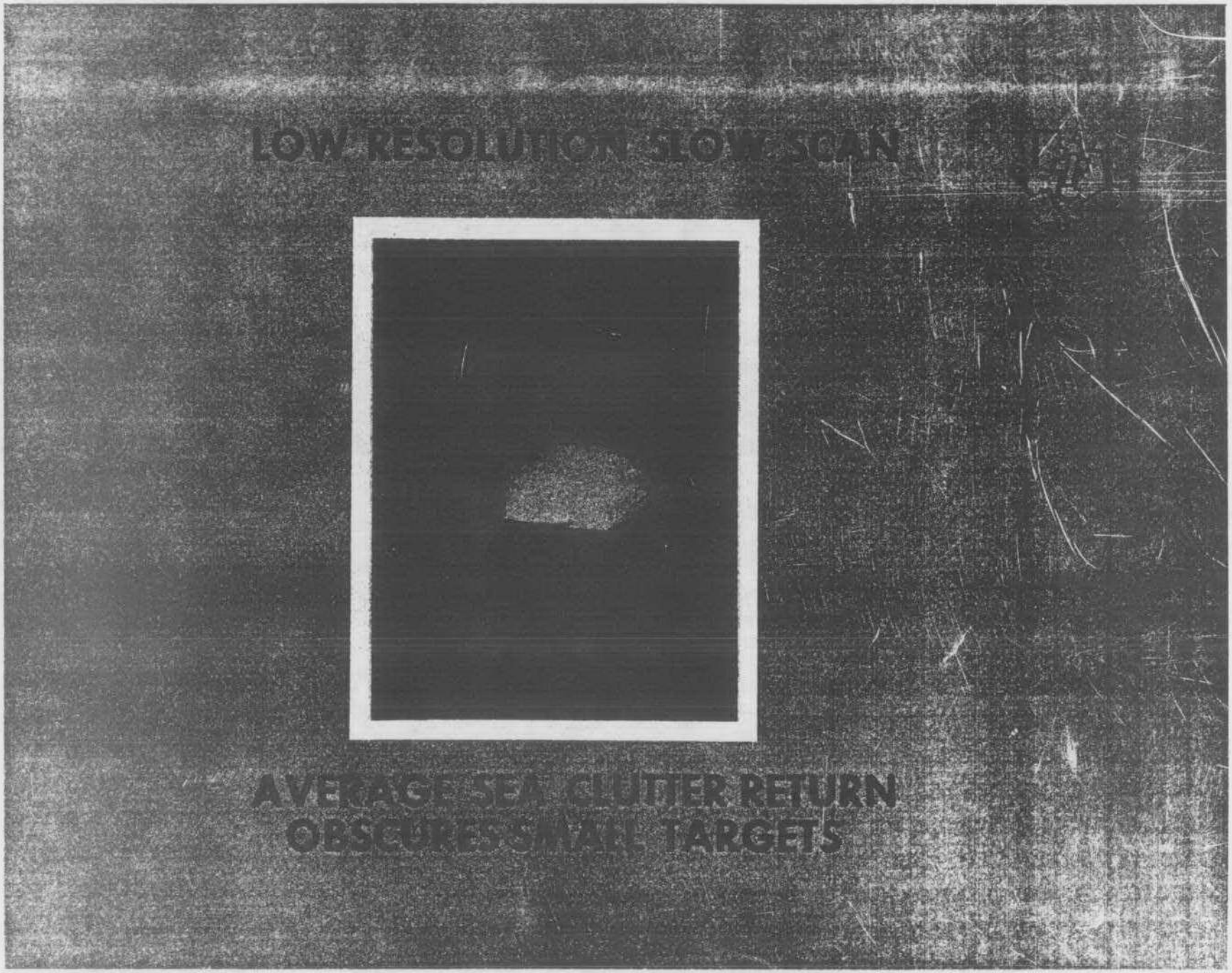
LOW RESOLUTION SLOW SCAN
AVERAGE SEA CLUTTER RETURN
OBSCURES SMALL TARGETS

FIGURE 4

FIGURE 5

53-1613

TEXAS INSTRUMENTS

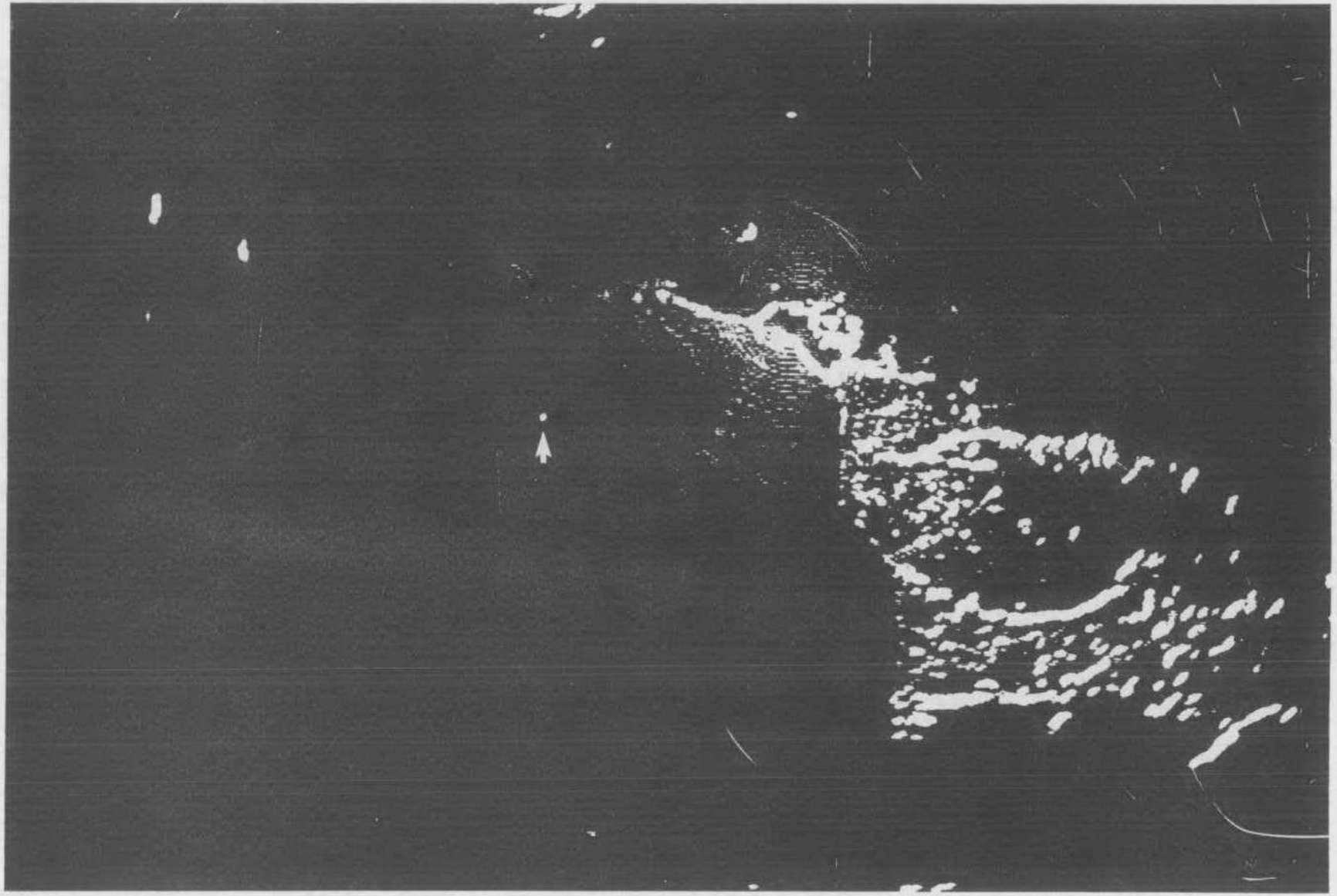

FIGURE 7: Example of multi-level display showing sea clutter background, but small point target is still clearly visible (indicated by arrow).

1346-263

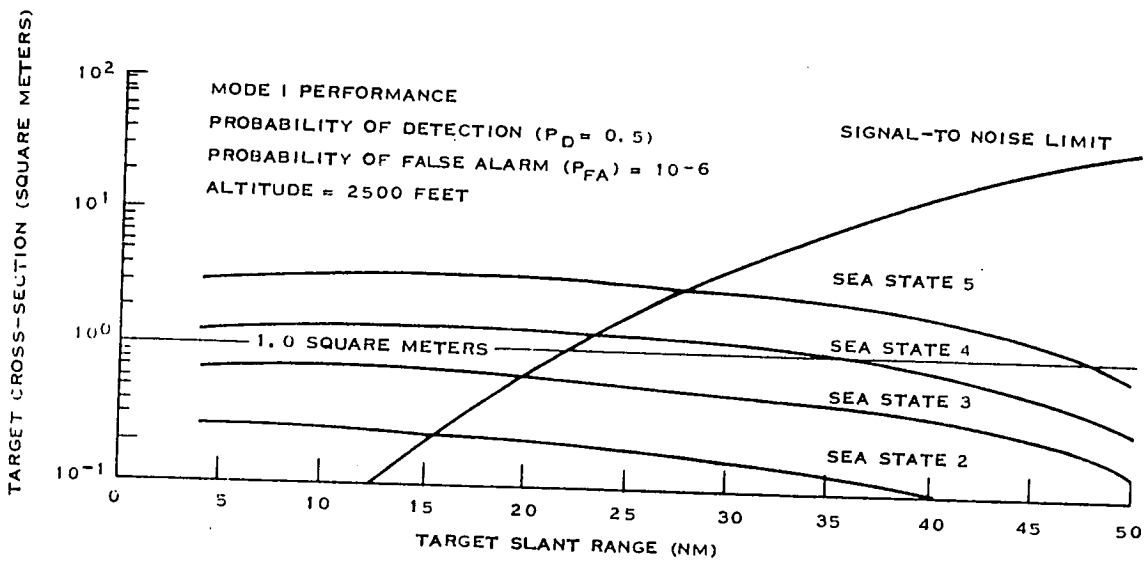

FIGURE 8: PERFORMANCE CURVE

TABLE 2. AN/APS-134(V) DETECTION PERFORMANCE

Target Type	Radar Cross Section (m^2)	Detection Range (nmi)	Sea State	Altitude (feet)
Periscope	1	23	3	2,500
Snorkel	10	38	4	8,000
Patrol/fishing boat	100	65	5	20,000
Small transport or destroyer	1,000	105	5	20,000
Cruiser	3,300	140	5	20,000
Aircraft carrier or weather	>5,000	>500	5	25,000

Probability of detection (P_d) = 0.5

Probability of false alarm (P_{FA}) = 10^{-6}

FIGURE 9: Site and weight specifications for TI APS-134 radar.

3.2.2 Physical Characteristics - The following table lists the maximum dimensions and weights of each WRA of the radar subsytem: (dimensions exclude connectors, filter retainers, handles and indicators):

WRA IDENTIFICATION	DEPTH (INCHES)	WIDTH (INCHES)	HEIGHT (INCHES)	WEIGHT (LBS.)
Power Supply	19.10	11.60	8.95	44
Synchronizer-Exciter	17.10	10.10	9.50	36
Transmitter	20.73	21.85*	12.72	174
Receiver-Pulse Compressor	16.10	13.30	10.60	48
Antenna	27.10	41.10	36.30	62
Signal Data Converter	19.60	15.50	7.70	55
Radar Control/ Display	22.50	23.10	15.70	107
Waveguide Pressurizer	5.00	12.60	14.25	21
Auxiliary Display	16.60	10.00	8.00	35
			Total Subsystem Wt.	582

*23.65 including protruding mounting bolt provisions.

3.2.3 Reliability - The contractor shall conduct a reliability program using MIL-STD-785A as a guide.

3.2.3.1 Reliability Mean Time Between Failure (MTBF) - The equipment including any built-in-test provisions, shall have 90 hours of mean (operating) time between failures.

3.2.3.2 Operating Life - The equipment shall have a life time of 15 years and an operational time of 5000 hours with reasonable servicing and replacement of parts.

AN/APS-134 (V) MARITIME SURVEILLANCE RADAR

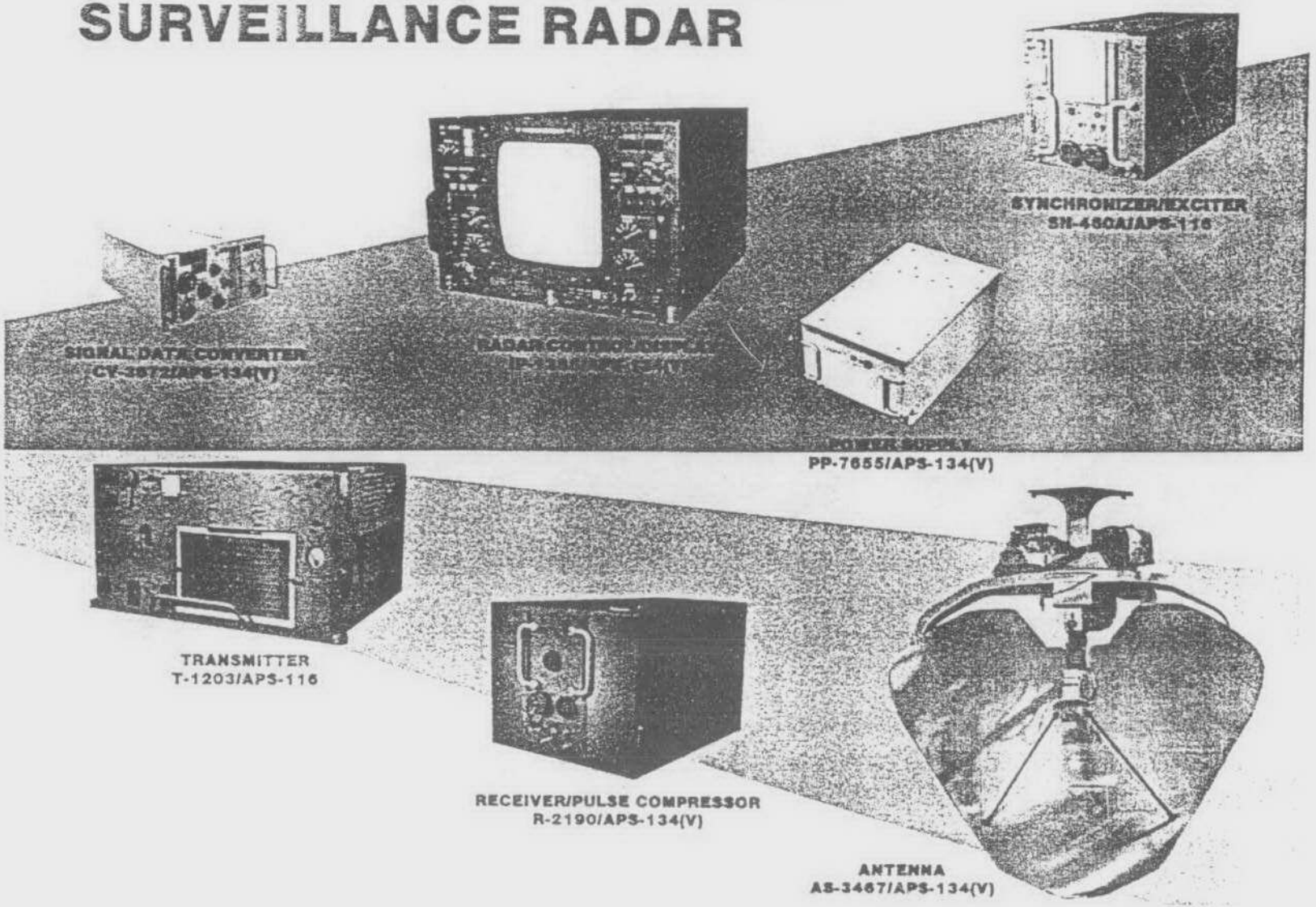

FIGURE 10

SIZE/WEIGHT/POWER

LRU	SIZE	WEIGHT	POWER
POWER SUPPLY	8.15 x 11.5 x 19.0	44 LBS.	365 WATTS
SYNCHRONIZER/ EXCITER	9.44 x 10.0 x 17.5	36 LBS.	155 WATTS
TRANSMITTER	12.6 x 21.8 x 20.6	174 LBS.	3495 WATTS
RECEIVER/PULSE COMPRESSOR	10.5 x 13.0 x 16.0	48 LBS.	149 WATTS
ANTENNA	41.0 x 36.0 x 27.0	62 LBS.	365 WATTS
SDC	19.6 x 15.4 x 7.6	55 LBS.	310 WATTS
		419 LBS.	4839 WATTS

FIGURE 11

the radar would not fit in a Beach 200, but would require an airframe in the next level up. He gave an example of the Dash 7 or 8, or Gulfstream G3. The radar specifications call for a mean time between failure (MTBF) of 90 hours, while the brochures indicate 100.

2.1.3 Cost

The TI AN/APS-134(V) sells for $1.5 million American.

2.1.4 Future Options

TI is presently negotiating the possibility of adding a synthetic aperture (SAR) processor as an add-on to the basic APS-134. The same radar/airframe could then perform either surveillance or mapping.

2.2 LITTON SYSTEMS (CANADA) LIMITED APS-504(V)5

The Litton V5 radar is intended for maritime patrol and anti-submarine watch applications. It is therefore designed to detect small targets. It uses pulse compression, and offers two ratios, 10 μs compressed to 30 ns (weighted), and 30 μs to 200 ns. Uncompressed pulse lengths of 0.2, 2, and 5 μs are available. The actual peak power transmitted is 8 kW, using a TWT. The transmitter has frequency agility.

The antenna rotates at 120 rpm to provide scan-to-scan integration for sea clutter control. Sector scan is available through transmitter blanking. There is also pulse-to-pulse integration. The radar has digital CFAR. The display is an 800 x 800 raster, with 4 bits per pixel, that is, 16 intensity levels. The display also has alphanumerics, organized as shown in figure 12.

The major features of the radar are summarized in figure 13, four pages copied from the Product Description for the APS-504(V)5. In the U.S., the radar is designated as AN/APS-140(V).

2.2.1 Performance

This V5 radar is very new, and the company is using its engineering prototype for its first contract. Consequently there is little actual performance data. A company brochure suggests "detection performed better than 30 nm on 1 to 5 sqm radar targets in high sea states". There has been some testing at the CN Tower in Toronto, in which a 2 sqm (lens) radar reflector was towed by boat and tracked out to about 20 nm.

DISPLAY FEATURES

ALPHANUMERICS

H - Heading from Navigation System
S (or N) Latitude - from ARINC bus
E (or W) Longitude - from ARINC bus
A - Aircraft/Mission number - from ARINC bus
D - Date - from ARINC bus
Z - Time - from ARINC bus
M - System mode
P (if present) - indicates system under pilot control

Receiver Processing Characteristics (LIN/LOG/CFAR/Sea/Land/Freeze)
D - Display mode (PPI/Sector)
R - Range scale selected

1
2
3
4
5
6
7
8
9

Data entered by user via keypad unit

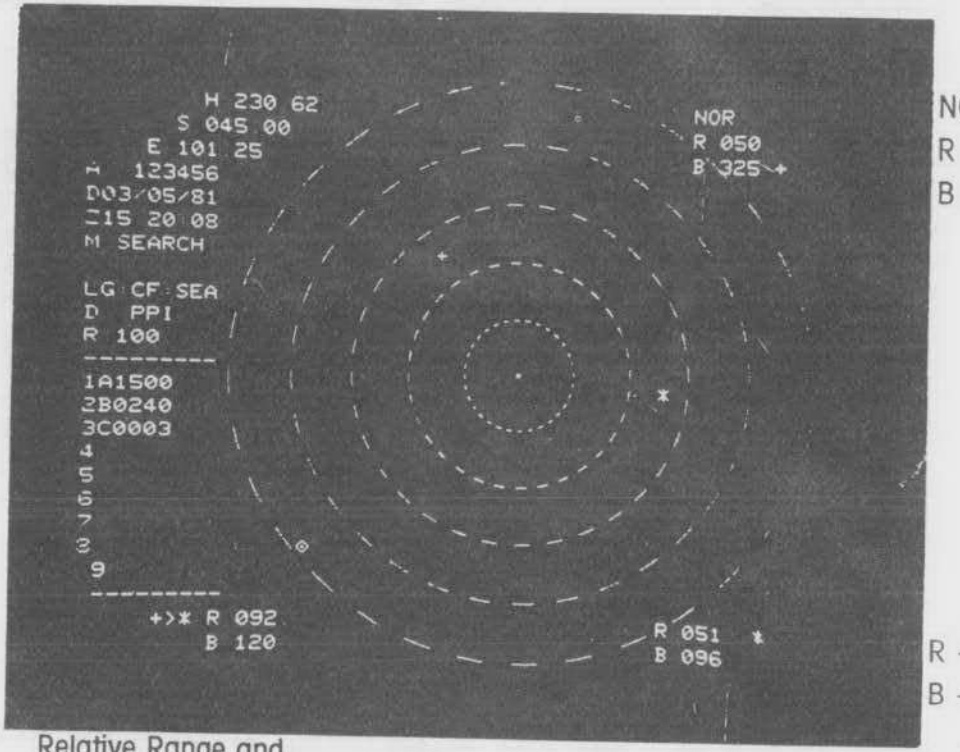

Relative Range and Bearing from Cross to Asterisk Cursors

NOR or LOS - orientation of display
R - Range from origin to cross
B - Bearing from origin to cross

R - Range from origin to asterisk
B - Bearing from origin to asterisk

◇Aircraft Heading Marker
□Origin (in ground stabilization mode)
+ Cross Cursor
* Asterisk Cursor

FIGURE 12

2.0 THE APS-504(V)5 AIRBORNE SEARCH RADAR SYSTEM

2.1 General

The APS-504(V)5 radar transmits within the frequency band of 8 to 10 GHz. Its peak power is 8 kilowatts.

2.1.1 Line Replaceable Units

The APS-504(V)5 radar consists of the following Line Replaceable Units:

Antenna Group consisting of:
- Pedestal and Yoke Assemblies
- Antenna

Transmitter/Receiver Group consisting of:
- Exciter/Receiver Unit (ERU)
- Power Amplifier Unit (PAU)

Signal Processing Group consisting of:
- Digital Filter Preprocessor (DFP)
- Synchronizer, Processor and Converter Unit (SPC)

Radar Control Unit (RCU)

Operator Display Unit

Waveguide Switch and Dummy Load Assembly

Optional units available are:
- Pressure Regulator and N2 Bottle
- Pilot's Display Unit with Pilot Control Unit
- Video Cassette Recorder (VCR) with Remote Control
- Video Tape Recorder Playback System (Ground) Unit

2.1.2 Features

Search Modes (ASW and MPA) employing:
- Pulse compression
- Frequency Agility
- Scan to scan integration
- Multiple pulse widths
- PRF and Ant RPM matched to mode and range
- CFAR processing
- Pitch and roll stabilized antenna
- Display of variable sector with:
  - Radiation restricted to sector displayed
  - Display origin offset control
  - Display orientation (LOS or North)
  - Ground stabilization of display
- Built in Test auto cycled and displayed

2.1.3 Options

IFF

Track While Scan

Target Reporting Data Link

Growth Potential

Pulse Doppler

Synthetic Aperture

2.2 Significant System Features

Operator's Display

Type:	TV-type X-Y raster display - RS 343A 875-line.
Size:	10 inch (25.4 cm) diagonal standard; other sizes available.
Phosphor:	P43 or similar for viewing in high ambient light conditions.
Lines per Frame:	875
Active Lines per Frame:	800
Grey Scales:	16
Interlace:	2:1 (New radar data every line; both odd and even raster fields composed of independent information).
Refresh (frame):	30 Hz
Presentation:	Alphanumeric Display combined with radar data.

Ranges	**Range Markers**
3 nmi	1 nmi
6 nmi	1 nmi
12 nmi	2 nmi
25 nmi	5 nmi
50 nmi	10 nmi
100 nmi	20 nmi
200 nmi	20 nmi

Transmitter/Receiver

Frequency:	8.9 to 9.4 GHz
Power	8 kW
Pulse Widths:	10 µsec/30 nsec, 30 µsec/200 nsec, 200 nsec, 2 µsec, and 5 µsec.
Compression Ratios:	500, 210
Agile Range:	500 MHz
Receiver Noise Figure:	4 dB typical, 5 dB maximum.
Bandwidth:	Matched to pulse requirements.
Processing:	RF STC, logarithmic IF.
PRF:	Optimized for range and mode.

Antenna

Type:	Flat plate (planar array), size tailored to requirements.
Rotation Rates:	Tailored to mode and range scale.
Tilt Control:	± 16 degrees.
Stabilization:	Compensation for pitch and roll.
Polarization:	Horizontal

Synchronizer, Processor and Scan Converter (SPC Unit)

Video Signal Processing:	CFAR Peak Detection Azimuth Filtering (pulse to pulse integration) Adaptive Data Compression Scan to Scan Integration
Scan Conversion:	Rho-Theta to X-Y
System Functions:	Synchronization and timing.
Memories:	Display Refresh Memory for Radar Data - 1024 x 1024 x 4-bits. Alphanumerics and Graphics overlay Memory 512 x 512 x 1-bit.
Output:	4 outputs formatted in RS 343A 875 line TV video.
Interface:	MS 1553B Data Bus or ARINC 571
Miscellaneous:	Ground Stabilization

Radar Control Unit (RCU)

Control functions provided:	Mode and Range Scales Range Delay Antenna Tilt Sector Scan Presentation Width STC, CFAR Scan to Scan Integration Ground Stabilization Built-in Test Overlay Brightness Altitude Correction Cursor Select Frequency Agility On/Off Optional Control Grip

Pilot's Display and Control Units (Options)

Repeater Display

Function:	Provides full repeat of Operator's Display.
Type:	TV 875 line to RS 343A standard.
Size:	12.7 cm diagonal (5 inch)
Features:	Visible in high ambient light Freeze Mode.

Pilot's Control Unit

Controls:	Antenna tilt, Range selection Cabin (permits pilot to select a preset mode as set on main Radar Control Unit).

Video Cassette Recorder and Remote Control Unit (Option)

Video Cassette Recorder

Function:	To record radar video for later replay in the air or on the ground.
Format:	875 line TV video
Input:	875 line, compatible with radar system.

Remote Control Unit

Function:	To allow cabin operation of the VCR.
Features:	Record, playback. Variable speed playback Bi-directional scanning.

The radar was at 1100 feet. Litton personnel also indicated that a theoretical evaluation of the V5 had been commissioned by Fokker aircraft, but that the report was proprietary.

2.2.2 Size, Weight, Reliability

Figure 14 shows the various components of the APS-504(V)5 system. The specifications give the weight as not exceeding 370 pounds. Table 3 lists size and weight for the various components, taken from the specifications. Figure 15 shows airframes in which Litton has installed V2 and V3 radars. The V5 prototype is installed in a NOMAD.

Because of the newness of the radar, MTBF figures for the V5 have not yet been established. Litton personnel indicated that an MTBF of 200-300 hours is typical for an airborne radar, albeit not of this complexity.

2.2.3 Cost

The Litton APS-504(V)5 sells for $1 million dollars Canadian.

2.2.4 Future Options

Litton presently supplies receiver/transmitters to MacDonald Dettwiler Associates (MDA) for use in a synthetic aperture radar system. Litton indicated that the V5 might be available in the future with an optional SAR processor.

APS-504(V)5 AIRBORNE RADAR SYSTEM CONFIGURATION

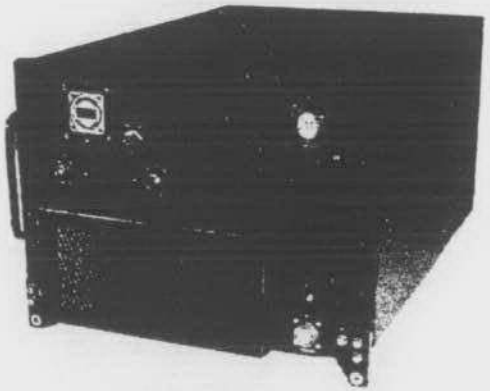

Power Amplifier Unit

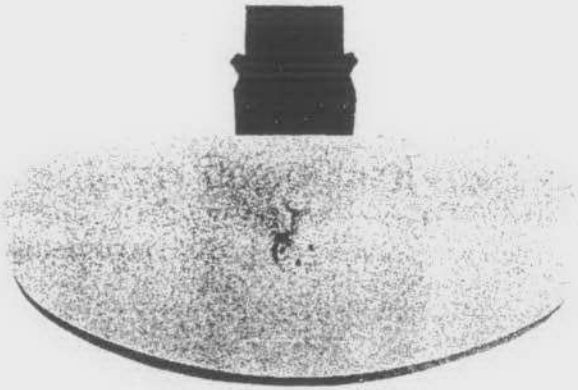

Antenna/Pedestal Unit

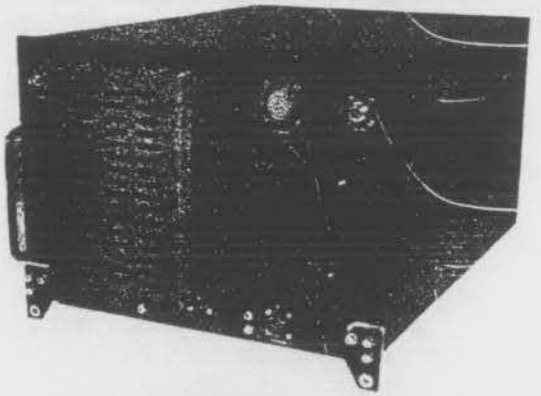

Emitter/Receiver

Radar Control Group

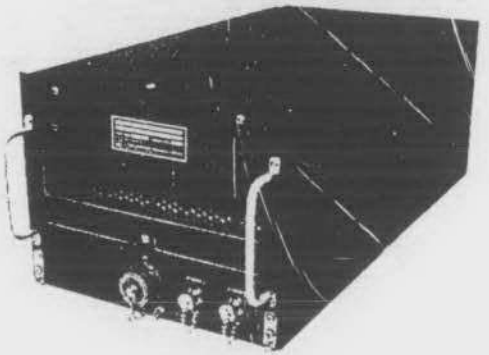

SPC Unit (Synchronizer, Processor and Converter)

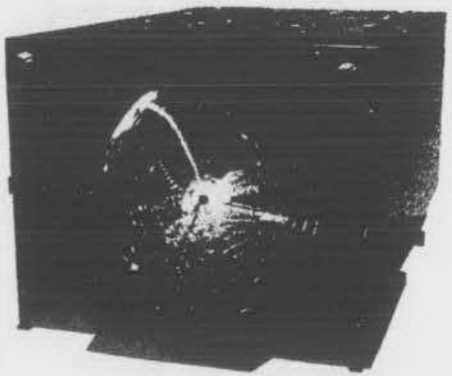

Operator's Display

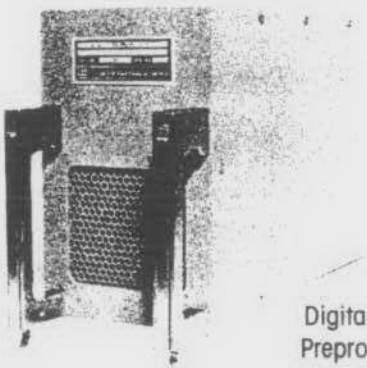

Digital Filter Preprocessor

LC 84/200

FIGURE 14

TABLE 3: SIZE AND WEIGHT OF APS-504(V) SYSTEM COMPONENTS

UNIT	SIZE			WEIGHT
	Height (in.)	Depth (in.)	Width (in.)	(pounds)
Emitter/Receiver	11	20	15.5	50
Power Amp	11	20	15.5	90
Antenna	36.4	47.5	47.5	65
Digital Filter Preprocessor	8	11	19	32
Radar Control Group	7	14	19	25
SPC	7.62	22	10.2	45
Pilot's display	6	14	6	18
Operator's display	8	18	10	35
			TOTAL WEIGHT:	360 lbs.

FIGURE 15

AIRCRAFT FITTED WITH LITTON RADARS

F-27

NOMAD

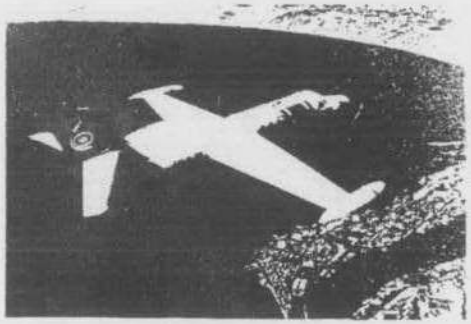

WESTWIND

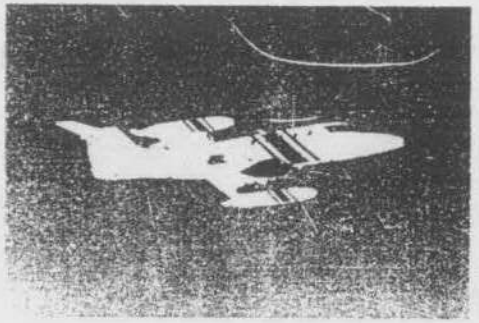

LEAR JET

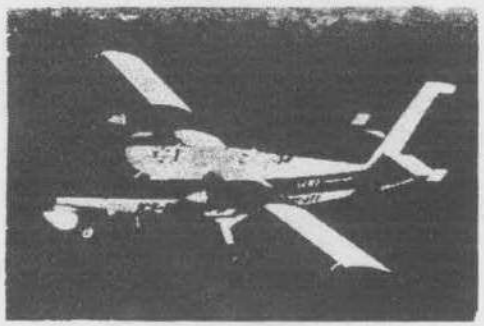

TWIN OTTER

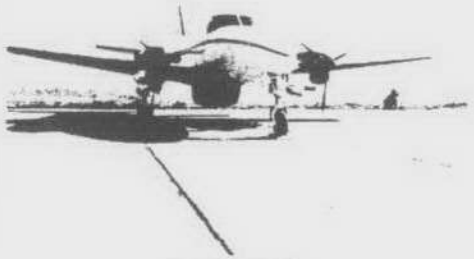

BEECH 99

BEECH T200/U.S. NAVY

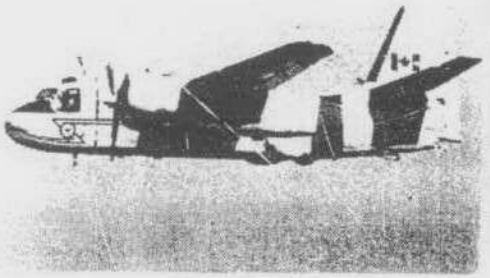

TRACKER

TCOM AEROSTAT/U.S. COAST GUARD

UC-880/U.S. NAVY

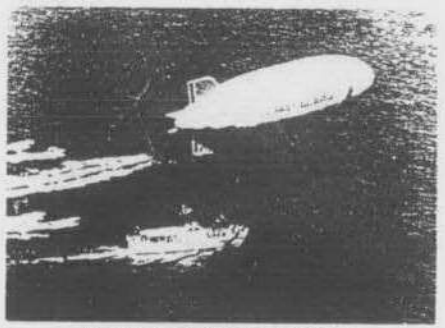

GOODYEAR AIRSHIP

Also being marketed with:

- Swearingen Metro 3
- DHC-7
- Fairchild - SAAB 340
- Gulfstream Commander 1000

LC 84/200

2.3 EATON AN/APS-128( ) PULSE COMPRESSION RADAR

The Eaton APS-128 PC, where PC indicates the pulse compression version, is intended for use in maritime patrol aircraft. There are two pulse compression ratios, 5 μs compressed to 100 ns (weighted), and 17 μs compressed to 100 ns. The larger pulse is used for long ranges. The actual peak transmitted power is 8 kW, using a TWT. The transmitter has frequency agility.

The antenna rotates at 60 rpm for 360° search, or 15 rpm wiper action for sector scan. Pulse-to-pulse integration is used, as well as scan-to-scan integration. Digital CFAR is employed. The display is 540 x 540 x 3 bits for radar data, and an additional bit for alphanumerics, all shown on an 875-line raster monitor. Using the digital tactical system (DITACS), a number of display tableaus are possible. Figure 16 shows an example in which a cursor can be used to designate targets, e.g., R01, whose latitude and longitude are then computed (relative to the aircraft's INS) and displayed under TARGET at the right. These designated target coordinates could be downlinked by radio to a surface receiver. The display also has the capability to offset the sweep centre by up to five radii, to allow for example close-up examination of a target at up to 50 nm using an equivalent 10 nm range scale.

The major parameters of the radar are summarized in figure 17.

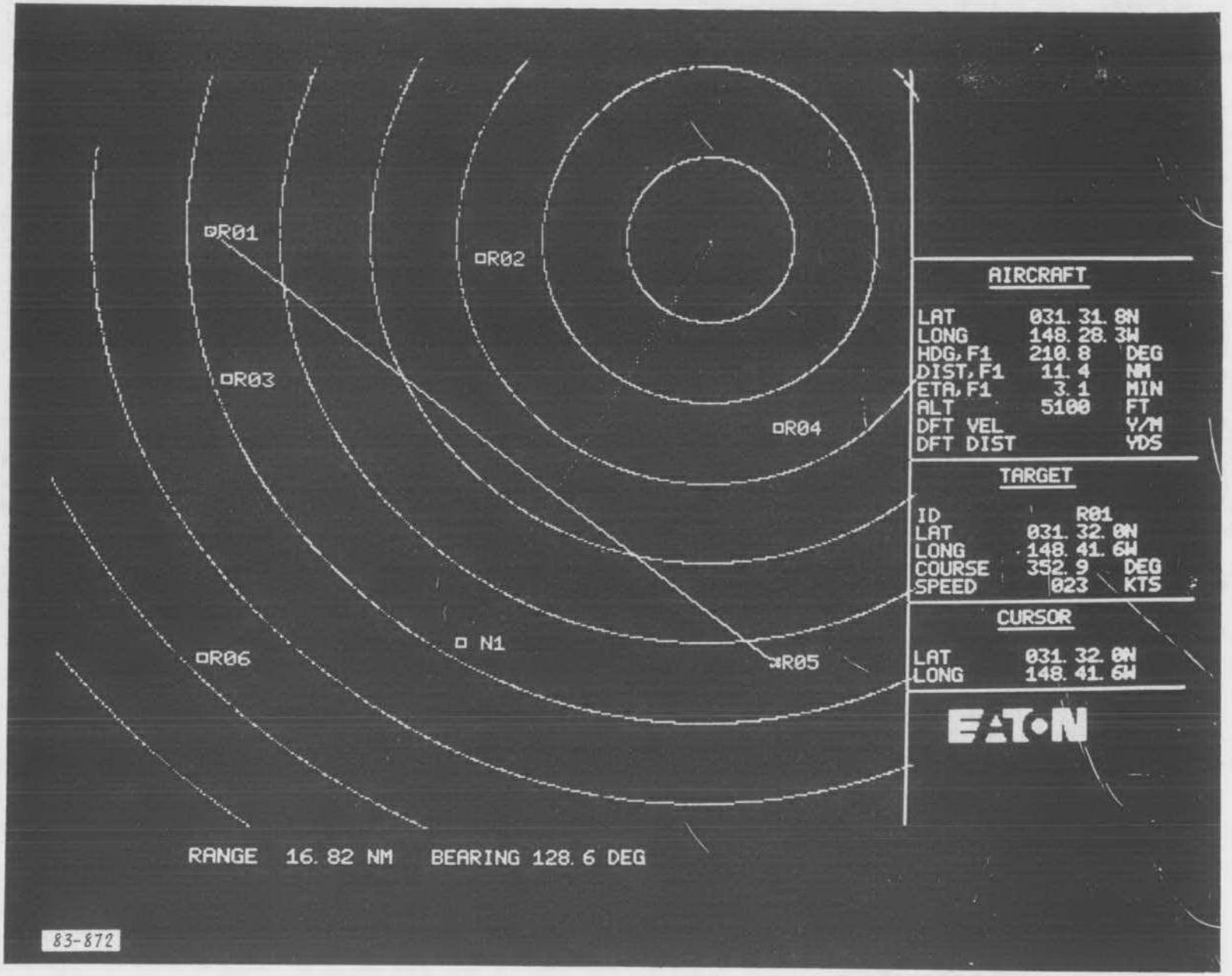

Figure 16: DITACS Display Presentation in GEO NAV Mode

FIGURE 17

Table 2-1. AN/APS-128 Radar System Specifications

A. Weight/Volume Summary	Weight (lb)	Dimensions (inches)
Antenna/pedestal	45	25 x 44 swept diameter
Receiver/transmitter	84	10 x 16 x 20
R/T tray	4	1.75 x 16.7 x 20.9
Digital Scan converter	35	9.1 x 10.2 x 21.5
DSC tray	3	2.0 x 10.8 x 21.4
TV Display (14 inch)	45	13.0 x 12.0 x 18.0
Radar Control Unit	7	5.8 x 11.3 x 5.5
Contact Control Unit	9	8.0 x 9.6 x 4.0

B. Input/Output Signals	
1. Inputs	
115 volts, 400 Hz, three phase	1100 VA
28 vdc	11 amp
1553B Data	
Pitch, roll data	Three-wire synchro preferred (50 or 200 mv/degree)
2. Outputs	
1553B Data	
TV composite video	EIA Standard
C. Technical Parameters	
1. Antenna/pedestal	
Dimensions	14 x 42 inch Flat-plate array
Gain	32.0 dB horizontally polarized
Beam width	2.3 degrees in azimuth 7.0 degrees in elevation

Table 2-1. AN/APS-128 Radar System Specifications (cont)

Rotation rate	15 and 60 RPM continuous
Sector scan	30 to 300 degrees at 15 RPM
Stabilization	Pitch and roll to ±20 degrees
Tilt	±15 degrees
2. Transmitter	
Type	Traveling Wave Tube
Frequency	9.235 to 9.519 GHz, fixed, selectable in 16 steps
Frequency agility (minimum)	100 MHz peak-to-peak
Power output (peak)	10 kw nominal
Pulse widths	5 usec uncompressed 0.1 usec compressed
PRF	2000, 1500, 800, 400 Hz
3. Receiver	
Type	Linear FM Compressive (50 to 1)
Local Oscillator	SAW Device (L-band)
Noise figure	3.5 dB receiver 5.0 dB system
Bandwidth	Matched to pulse width
Response	Lin-log
Processing	STC, CFAR, Frequency agility
4. Radar and Contact Control	
See part 7 (MIL-STD-1553B Interface) of this table.	
5. Digital Scan Converter	
Coordinate conversion	2048 x 2048 picture elements (pixels)

FIGURE 17 (Continued)

Table 2-1. AN/APS-128 Radar System Specifications (cont)

Centering	Aircraft or target (offset)
Ground stabilization	At all ranges in aircraft or target centered modes
Memory storage	540 x 540 x 3 bits - radar data 540 x 540 x 1 bit - synthetic data (alphanumerics and symbology)
Offset (zoom)	Up to 5 radii of offcentering (with ground stabilization)
Sweep integration	25 to 40 sweeps dependent on mode

6. TV Display

Type	High resolution, high intensity green phosphor
Size	10 to 14-inch diagonal
Line rate	875 lines
Phosphor	P-1/P-39 mixture
Filter	Contrast enhancement filter

7. MIL-STD-1553B Interface Inputs/Outputs

a) Outputs

Type	Function	Description	Comments
Radar Control	Mode	STBY, WX, SRCH, FA, CFAR	Discretes
	Range	5, 10, 25, 50, 100, 200	Discretes
	Integration	FAST, MED, SLOW	Discretes
	Display	GND, STAB, ACFT, HEAD, OFF-CENT, CENTER	Discretes
	Sector Scan	Bearing, Width	Binary LSB = $\frac{360°}{128}$
	Sector Scan	On	Discrete

2.3.1 Performance

Eaton uses computer analysis to predict the performance of its radars. The following figures, 18 to 22, show such predictions, taken from Eaton literature. Eaton personnel indicated that the 100 nsec pulse length design objective was deliberately chosen to avoid the more spikey sea clutter return, and the required high speed digital signal processing rates. Eaton feels that to detect small targets in strong sea clutter, the radar can be flown at a lower altitude, thereby reducing the grazing angle, hence the clutter level. Consequently in the given performance curves, the performance improves as the altitude is reduced.

2.3.2 Size, Weight, Reliability

Figure 23 shows the components of the Eaton APS-128( ) PC radar. The total weight is less than 220 pounds. Figure 17, already given, listed the sizes and weights of the various components. Figure 24 lists airframes in which the basic APS-128 has been installed. The pulse compression version of the APS-128 is quite new, so MTBF figures are not available. However, the pulse compression version differs from the basic APS-128 D only in the receiver/transmitter unit. Japan has reported an MTBF on 15 APS-128D's of 442 hours.

2.3.3 Cost

The Eaton APS-128( ) pulse compression radar sells for $450,000. American, with an additional $65,000. American for the DITACS display system.

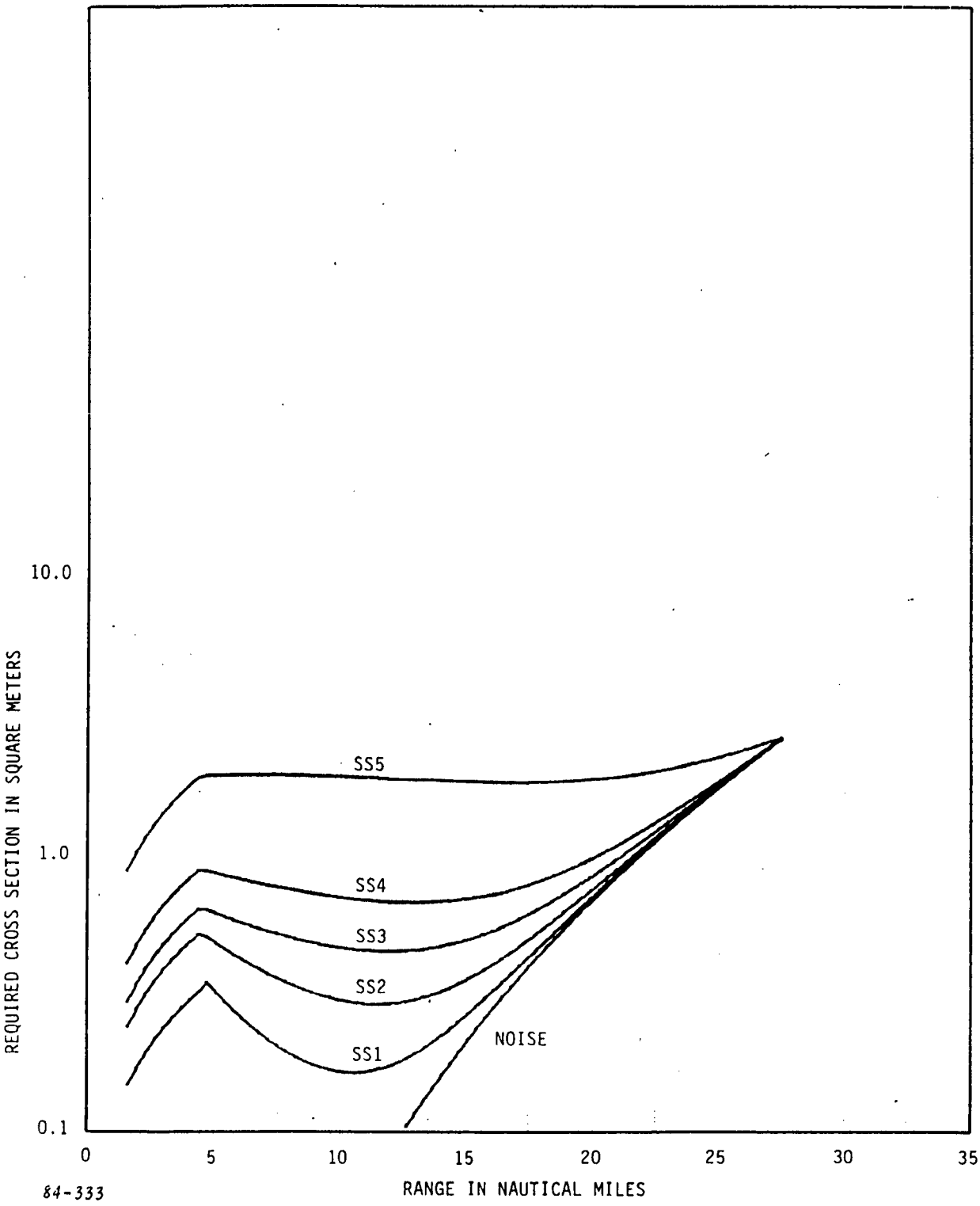

Figure 18: AN/APS-128 PC Radar at 500 ft Altitude-Low Noise Front End, 0.1 usec PW, 10 kw Power

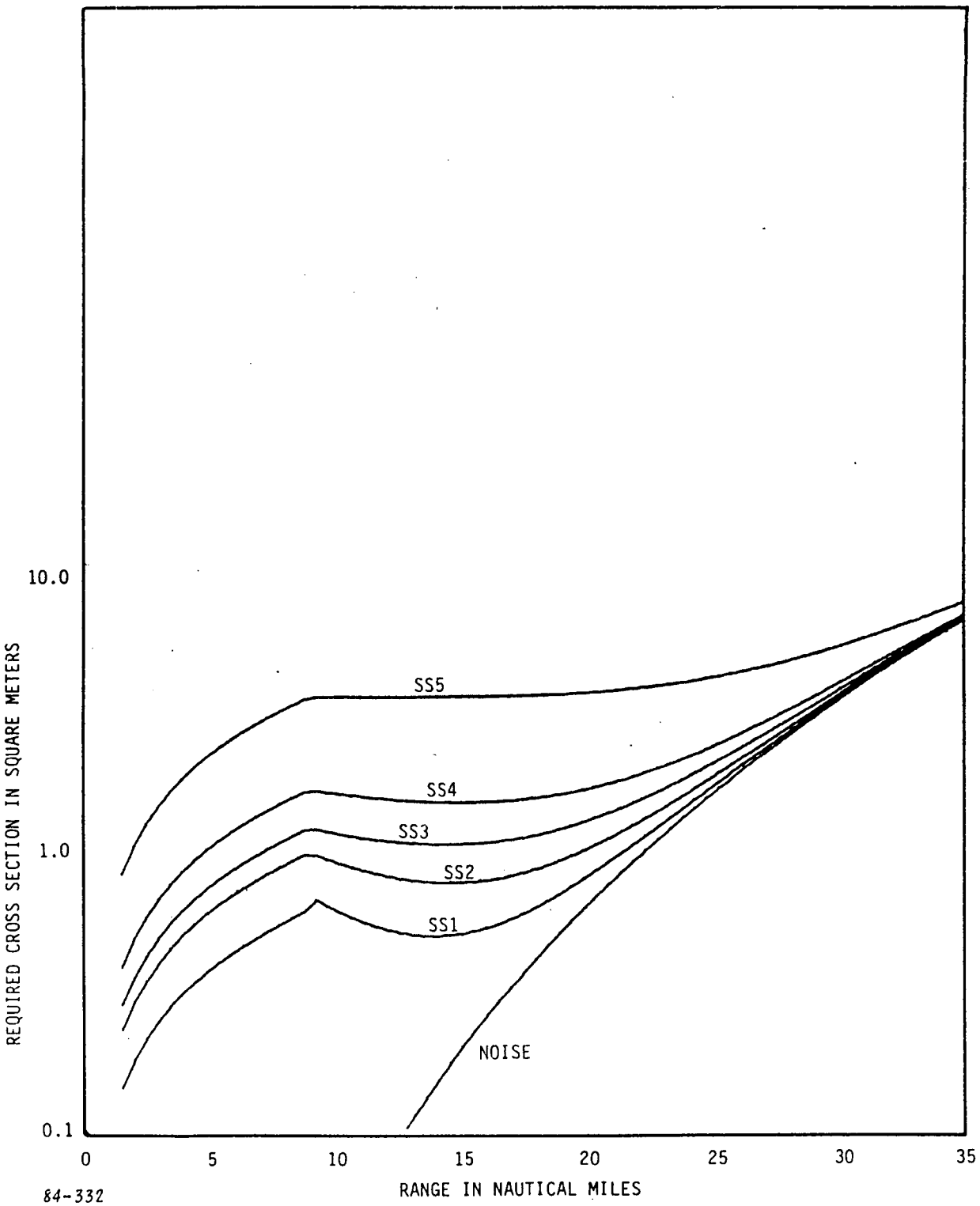

Figure 19: AN/APS-128 PC Radar at 1000 ft Altitude-Low Noise Front End, 0.1 usec PW, 10 kw Power

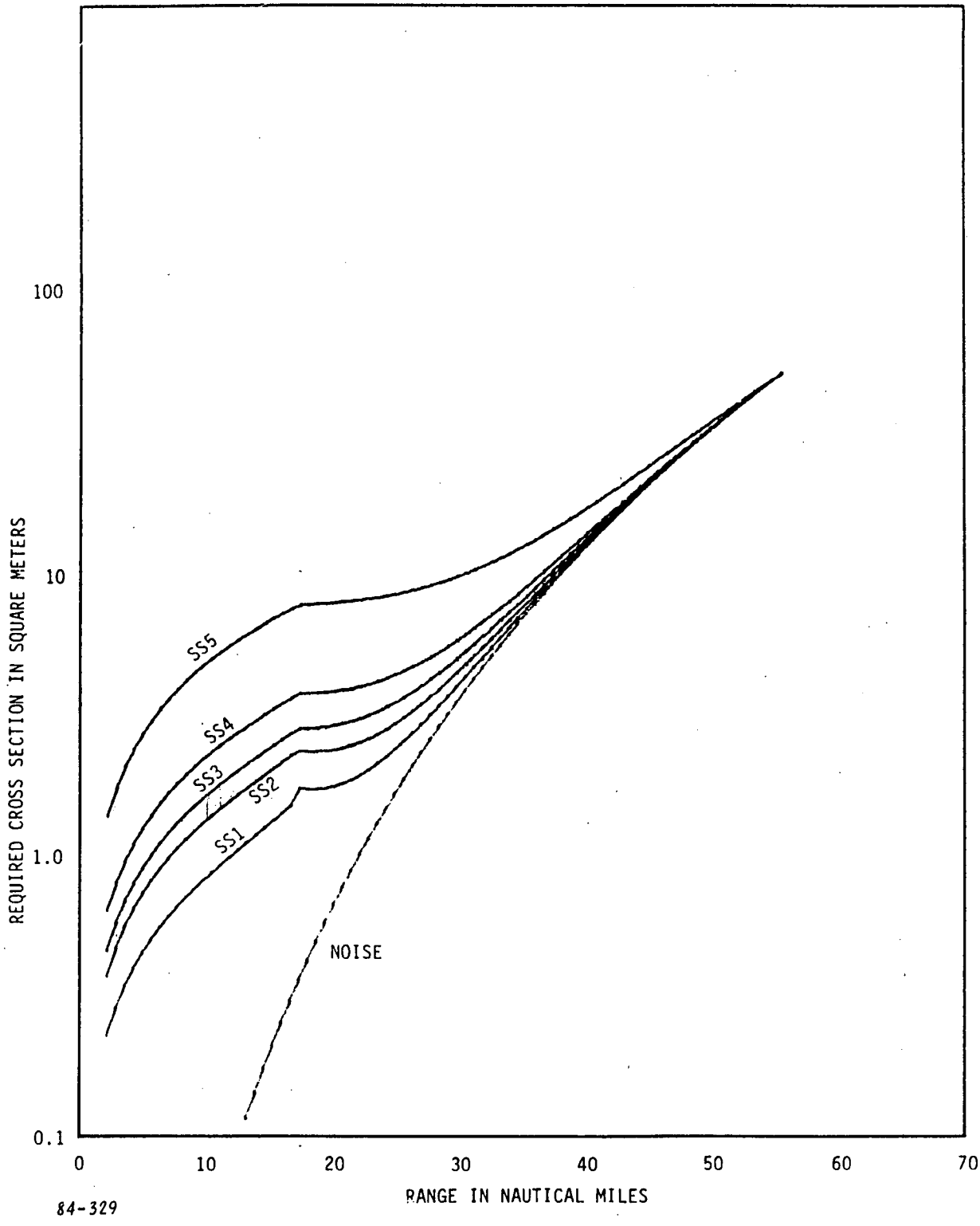

Figure 20: AN/APS-128 PC Radar at 2000 ft Altitude-Low Noise Front End, 0.1 usec PW, 10 kw Power

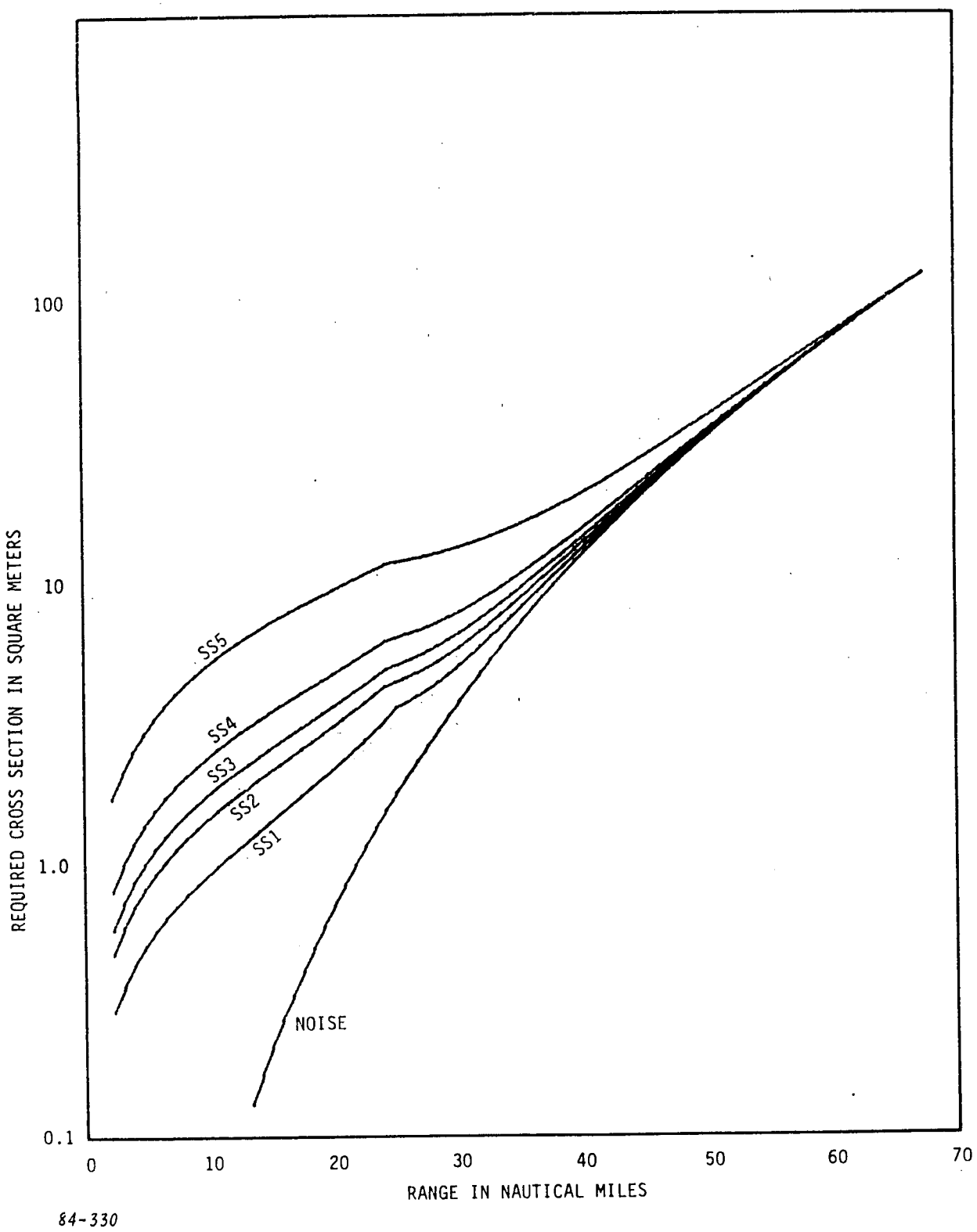

Figure 21: AN/APS-128 PC Radar at 3000 ft Altitude-Low Noise Front End, 0.1 usec PW, 10 kw Power

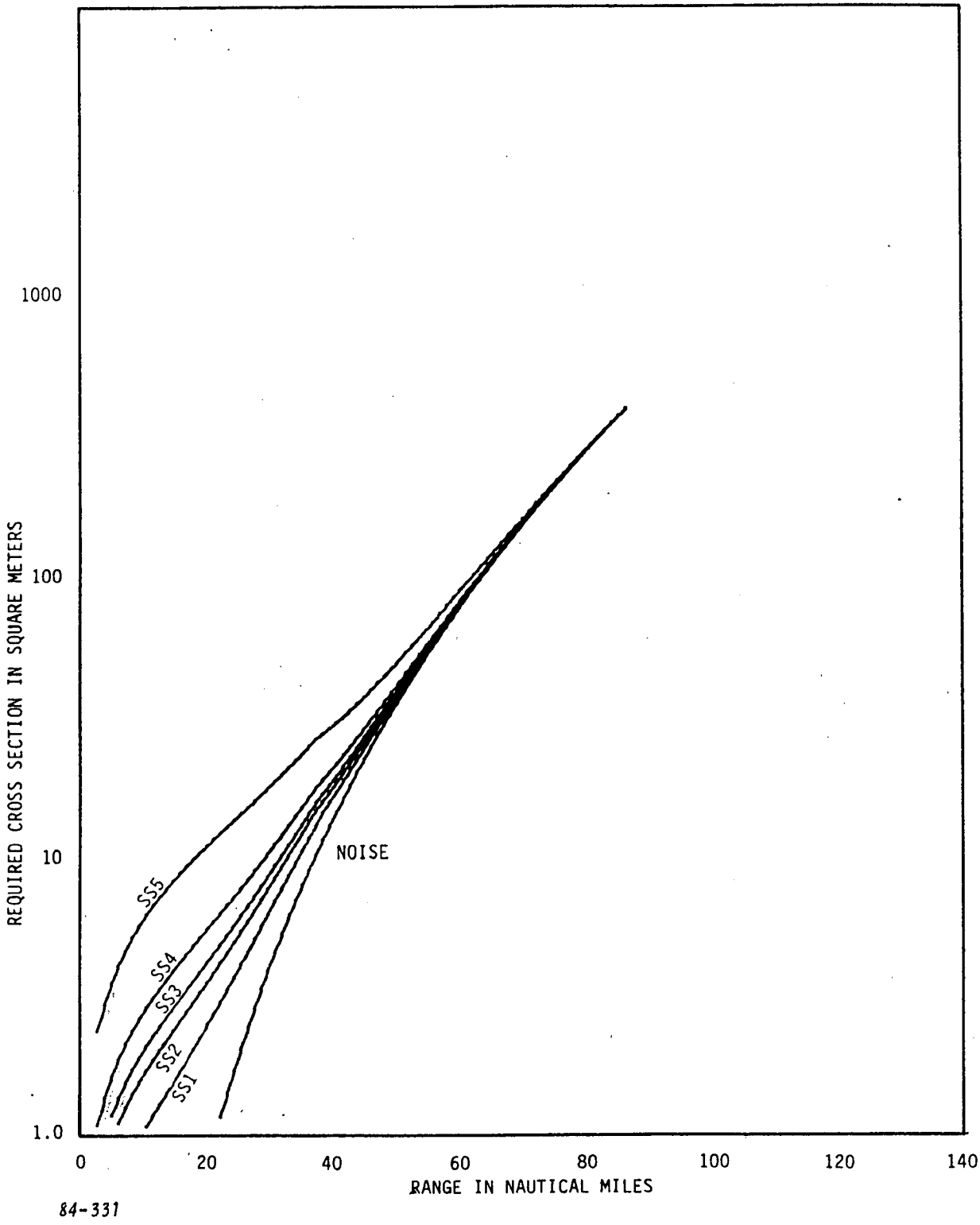

Figure 22: AN/APS-128 PC Radar at 5000 ft Altitude-Low Noise Front End, 0.1 usec PW, 10 kw Power

AN/APS-128 DITACS System Components

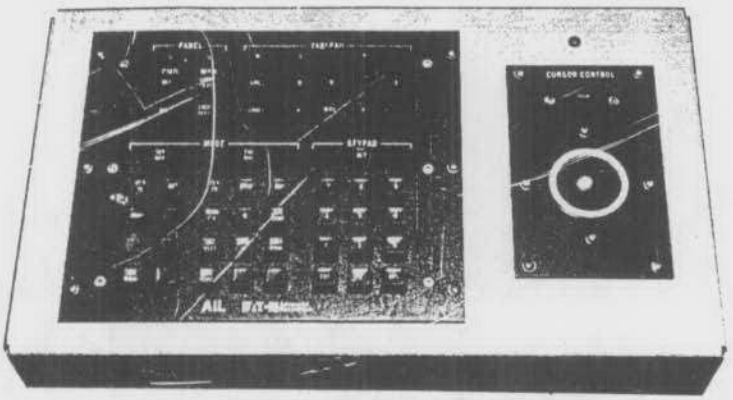

DITACS
CONTROL

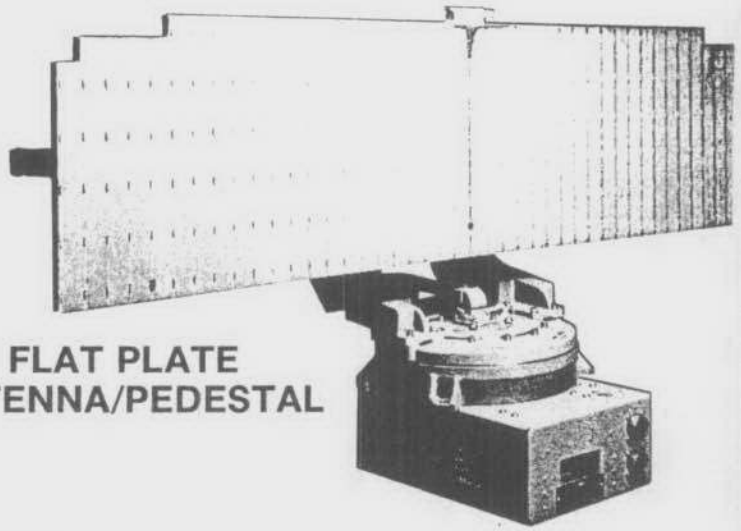

FLAT PLATE
ANTENNA/PEDESTAL

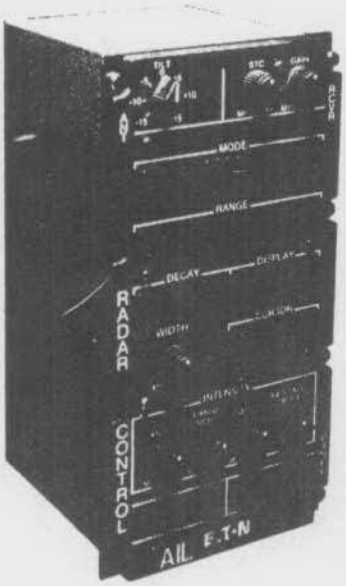

RADAR
CONTROL

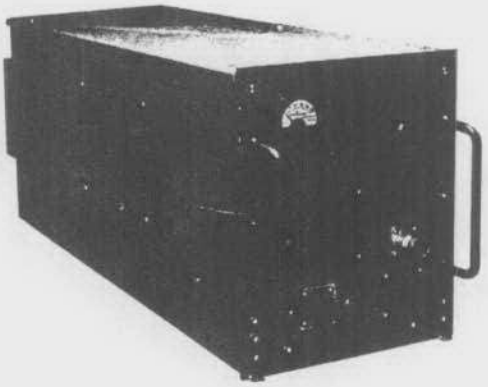

DIGITAL
SCAN CONVERTER

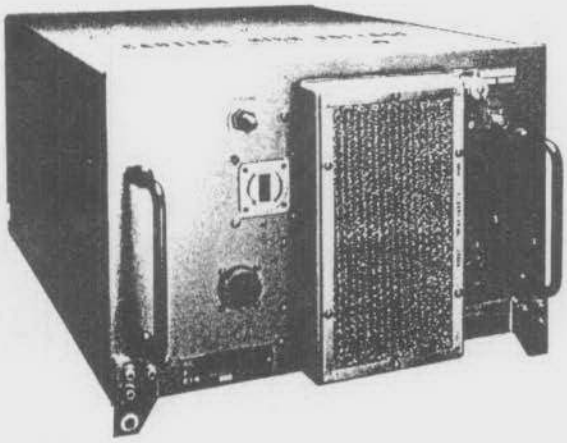

TRANSMITTER-RECEIVER

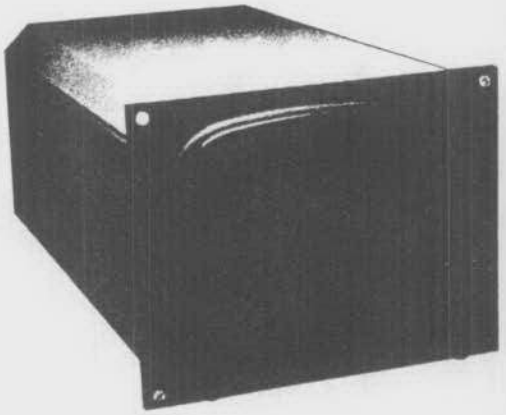

BRIGHT DISPLAY

FIGURE 23 **Total system weight—220 pounds including display**

AN/APS-128 SERIES INSTALLATIONS

Agency	Aircraft
Brazilian Air Force	Embraer EMB-111
Chilean Navy	Embraer EMB-111
Japanese Maritime Safety Agency	Beech 200T
Gabon Air Force	Embraer EMB-111
Royal Malaysian Air Force	Lockheed C-130MP
Indonesian Air Force	Lockheed C-130MP
Uruguayan Navy	Beech 200T
Spanish Air Force	CASA C-212
Uruguayan Air Force	CASA C-212
Spanish Air Force	Lockheed C-130 (Retrofit)
NASA	Short Bros. Skyvan
U.S. Customs Service	ILC Aerostat

FIGURE 24

3. EXPERIMENT CONSIDERATIONS

1. If two or more surveillance radars are to be compared, fly them as close in time and space as possible so that conditions are as identical as possible.
2. For a short test, e.g. less than one month, have the radar companies provide the radar operator so that maximum performance from the radar/operator combination can be obtained. Full radar performance is not obtained from a new or inexperienced operator.
3. Artifical but calibrated targets are a "must". A variety of sizes should be used, for example, radar cross-sections of 100, 50, 10, 5, 2, and 1 sqm. Some sort of extended test target should be used, representing the physical size of the ice targets of interest. This more fairly evaluates the longer pulse radars, since the ice targets are not point targets in the same sense as periscopes.
4. It is imperative to know the location at all times of all targets being used for the experiment. One or more surface vessels should maintain this log, aided with photos of their PPI displays. Note that the calibrated targets could be simultaneously used to measure ship's radar performance.
5. The surface vessels should have TV video recording equipment, with time stamp encoded, to document the target dynamics and sea conditions. Even in simple swell, ice targets may oscillate vertically, producing a wake. A visual estimate of the resulting Doppler effects, e.g. on SAR, is of interest.

6. Continuous recordings of the radar displays should be made, together with verbal annotation by the radar operator. The time on the various radars should be synchronized with the surface vessel recorders.
7. The surveillance radars should be flown at several altitudes, and on upwind, downwind, and crosswind passes.
8. The pack ice mapping capability of the surveillance radars should be tested, for example, ability to estimate concentration, as well as their ability to delineate the edge of the pack. Iceberg detection within the pack should be tested.
9. If practical, the surveillance radar should be operated for a period of several months, to permit its evaluation under almost all conditions, and to train an operator. This suggestion was made by Eaton personnel.
10. The airborne surveillance radar should be tested on a surface-based platform, e.g. derrick top, to assess the performance improvement to be gained (vis-a-vis the marine radar) through the better signal processing and display.

4. PERFORMANCE COMPARISON CONSIDERATIONS

1. Based on design considerations only, the TI APS-134 is expected to offer the best detection performance, followed by the Litton APS-504(V)5, and then the Eaton APS-128( ) PC.
2. The TI radar is the most expensive and the heaviest. It requires a larger aircraft, which is more expensive to purchase, maintain and operate.
3. The TI radar can give equivalent performance from higher altitudes, meaning greater coverage area in fewer flights.
4. The reliability and maintainability of the radar seems to vary inversely with the complexity. The Eaton radar is the smallest, lightest, and seemingly easiest to maintain.
5. Delivery after receipt of order is a consideration. TI and Litton indicate 12-18 month delivery. Eaton indicates about 6 months.
6. In terms of responding to custom design changes (e.g. downlinking target coordinates), Eaton seems to be the most responsive company.
7. Care must be taken in choosing the target parameters by which the radars are evaluated. The TI radar is designed for detecting a periscope-size 1 sqm target. Consequently it reduces its range resolution to 3 ns (1.5 feet) to reduce the competing sea clutter. However, a 1 sqm piece of ice may have physical dimensions in terms of feet, such that the 1.5 foot pulse may be overly reduced. The longer pulse radars may perform better than expected on a physically extended 1 sqm target.

5. OTHER RADARS

The authors know of two other radars of this class. One is the Thorn-EMI Searchwater radar from Great Britain. Most of the technical details are apparently classified. Heresay suggests the radar is very large and heavy, and very expensive and difficult to operate. The other radar is the Thompson-CSF Varan radar from France. Again not much technical information is available, but apparently its performance falls between the Litton and the Eaton radars.

6. COMPARISON OF THE VARIOUS RADARS

Figure 25* shows a comparative evaluation of four airborne surveillance radars (the Texas Instruments, Litton, Thomson-CSF, and Eaton radars). In this figure, the probability of detection is plotted versus range. The curves included in this figure are based on the following assumptions (Dyer [8]):

1. The test data were generated by using a propagation model that is representative of a semitropical environment. This model has been validated by comparison with actual sea clutter data.
2. Sea state: 3
3. Aircraft altitude: 1000 - 1500 feet
4. Target: submarine periscope of radar cross-section equal to 1 square meter.

The curves of Figure 25 demonstrate the superiority of the Texas Instruments radar over the other three. Indeed, this radar is the only one to realize a probability of detection close to one for the assumed environmental conditions.

Table 4 summarizes the major parameters of the three radars considered in this study. The parameters listed are those which vary significantly from radar to radar. Those items not listed are similar for each radar, and can be obtained from the individual radar sections.

---

*Figure 25 is included by courtesy of Georgia Tech.

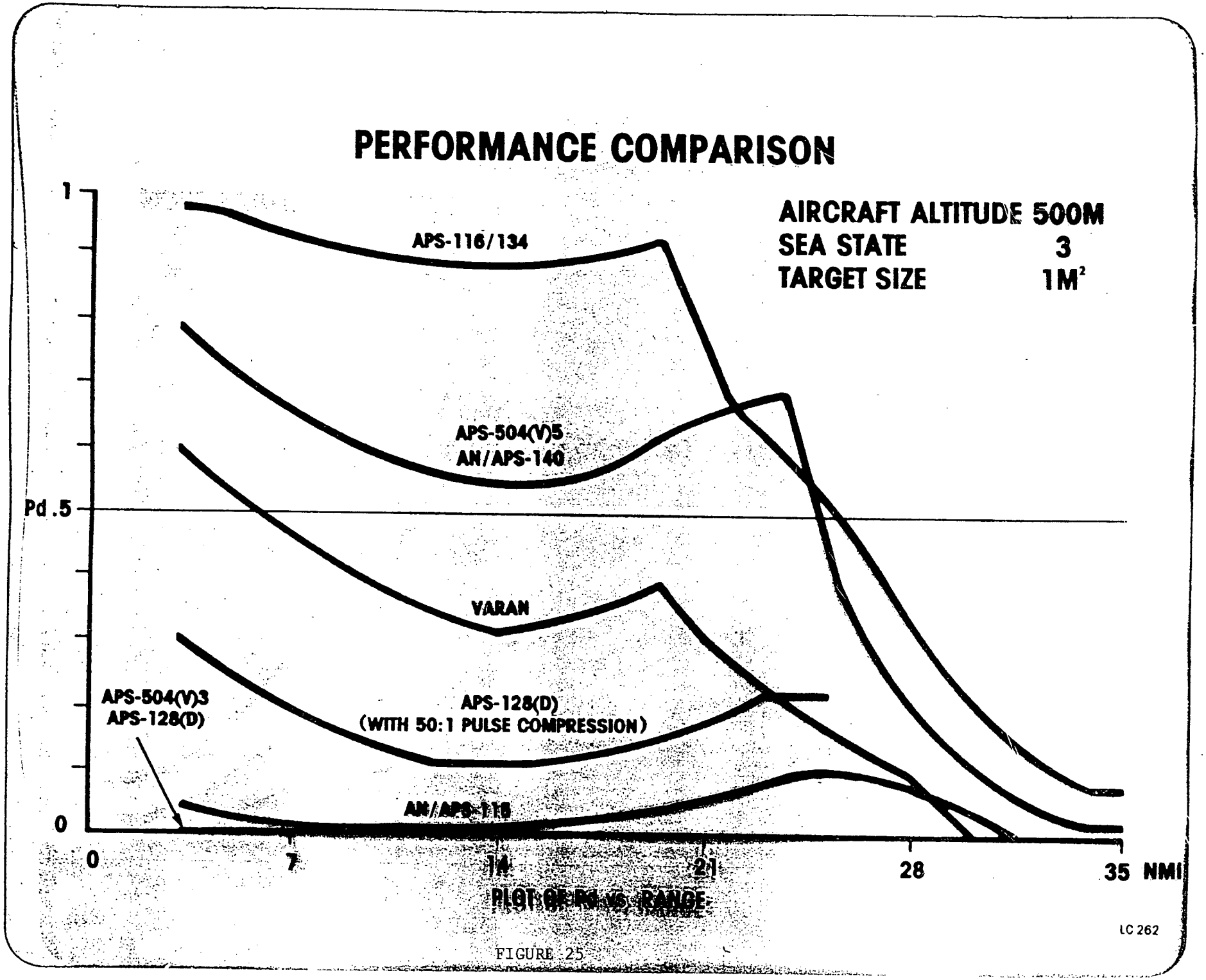
PERFORMANCE COMPARISON
AIRCRAFT ALTITUDE 500M
SEA STATE 3
TARGET SIZE 1M²
APS-116/134
APS-504(V)5
AN/APS-140
VARAN
APS-128(D)
(WITH 50:1 PULSE COMPRESSION)
APS-504(V)3
APS-128(D)
AN/APS-118
1
Pd .5
0
0
7
14
21
28
35 NMI
PLOT OF Pd VS RANGE
LC 262

FIGURE 25

Table 4: Major Parameters of the Three Radars Compared in this Report

	TI APS-134	Litton APS 504(V)5	Eaton APS 128( )PC
Transmitted Pulse Length:			
non-compressed (ns)	500	10,000	5000
compressed, weighted (ns)	3	30	100
Transmitted Power (peak)			
Actual (kW)	500	10	10
Effective (kW)	83,333	3,333	500
Antenna:			
Beamwidth			
(vertical) deg.	4.0	7	7.0
(horizontal) deg.	2.4	2.5	2.3
Gain (db)	35	33	32.0
Rotation rate (rpm)	6,40,150	8-120	15,60
Polarization	vertical	horizontal	horizontal
Display			
(number of lines)	525	875	875
(number of bits/pixel)	8	4	3
Weight (kG)	265	164	100
Typical Airframe	Dash 7 or 8	Beech T200	Beech T200
Cost			
US dollars	$1,500,000.*	$769,230.	$515,000.*
CDN dollars (assume $1 US=$1.3 CDN)	$1,950,000.	$1,000,000.*	$669,500.

*quoted price

7. AVAILABILITY OF TEST RADARS FOR SPRING 1986 EXPERIMENT

1. Texas Instruments cannot supply an APS-134; they do not stock any. Possibilities include (1) contacting the Naval Research Laboratory, Washington, and enlisting their help in using their APS-137 (classified upgrade to 134), or (2) arranging use of the Canadian Forces CP-140 containing a TI APS-116, the APS-134's predecessor with similar point target capability but without the multilevel processing.
2. Litton cannot provide an APS-504(V)5. Only possibility is to contact the U.S. Customs, Florida, to enlist their Nomad aircraft containing the V5 prototype.
3. Eaton can supply an APS-128( ) pulse compression radar in February 1986. They do not have an airframe. Another possibility is to contact Beech aircraft to fly their Beech King Air demonstration aircraft in which the Eaton radar (except pulse compression) is already installed.

8. RECOMMENDATIONS

1. The TI radar offers the best operational performance. Accordingly, every attempt should be made to arrange for some tests (even for limited duration) to assess the capability of this radar in an ice-related environment. The results of such a test would represent some measure of "standard of performance" against which one or both of the other two radars (Eaton and Litton) can be assessed.
2. In terms of availability and price, the Eaton radar has an advantage over the other two. Accordingly, the experiments should definitely include the use of this radar.
3. If the Eaton radar's performance is insufficient, but the TI radar is considered "overkill", then the Litton radar should be considered since it offers intermediate performance.

9. REFERENCES

[1] Nathanson, F.E., Radar Design Principles, McGraw Hill, New York, 1969.

[2] Smith, J.M. and Logan, R.H., "AN/APS-116 Periscope-Detecting Radar", IEEE Transactions on Aerospace and Electronic Systems, vol. AES-16, no. 1, January 1980.

[3] Smith, J.M., "AN/APS-134(V) Maritime Surveillance Radar", RADAR-82 International Conference, London, England, October 1982.

[4] Smith, J.M., "Fast-scan Processing in Maritime Surveillance Radars," Proceedings of 1984 International Symposium on Noise and Clutter Rejection in Radars and Imaging Sensors, October 1984, Tokyo, Japan.

[5] Ward, K.W., "Microwave Sea State Measurements", in IEE Colloquium on 'Measurement of Wave Height and Direction', March, 1982.

[6] Lind, G. "Measurement of Sea Clutter Correlation With Frequency Agility and Fixed Frequency Radar", Philips Telecommunication Review, vol. 29, no. 1, April 1970.

[7] Trunk, G.V., "Radar Properties of Non-Rayleigh Sea Systems, vol. AES-8, no. 2, March 1972.

[8] Dyer, F., Private Communication.

APPENDIX D

Iceberg Detection by Airborne Radar - Theoretical Prediction of Performance

PROJECT NO. 107-85I

ICEBERG DETECTION BY AIRBORNE RADAR - THEORETICAL PREDICTION OF PERFORMANCE

BYRON R. DAWE

OCTOBER 1985

REPORT PREPARED FOR CANPOLAR
CONSULTANTS LTD.

by

NORDCO Limited
St. John's, Newfoundland

TABLE OF CONTENTS

LIST OF TABLES

LIST OF FIGURES

1. INTRODUCTION

This report provides the results of theoretical modelling of airborne radar detection of icebergs. Side looking airborne radars (SLAR), and surveillance radars were evaluated. Synthetic Aperture Radar (SAR) was also evaluated using conventional modelling. However, it would appear that, because of the complex manner by which an image is formed and the complications introduced in imaging a slow moving point target against a moving ocean background, such a model is probably inaccurate and unrealistic.

The performance of various government owned and commercially available radars were compared. The results are presented in terms of probability of detection versus range. The predicted effect of varying certain system and operational parameters are provided also.

It should be noted that the performance predictions provided are not verified by actual data. Therefore, some caution must be utilized in assessing the radars based on the predictions, even though theoretically the models have been made as accurate as possible within reason.

2. MODEL DESCRIPTION

2.1 THE RADAR EQUATION

The fundamental basis for the radar modelling is the pulsed radar equation formulated to determine the power received, P_r, and given by:

$$P_r = \frac{P_t^2(\theta)\lambda^2\sigma F^4}{(4\pi)^3 R^4 L} \qquad (1)$$

where,

P_t is the peak transmitter power,
$G(\theta)$ is the antenna power gain, which is a function of the depression angle, θ,
λ is the wavelength of the carrier frequency,
σ is the radar cross section,
F is the pattern propagation factor,
R is the slant range to the target,
L is the sum of the system and atmospheric losses,
τ_u is the uncompressed pulse length, and,
τ_c is the compressed pulse length.

The terms, P_t, λ, and R, τ_u, and τ_c are fairly straight forward, but the others require further explanation.

The antenna power gain, $G(\theta)$, is normally adjusted to counteract the $1/R^4$ spherical loss that is shown in

Equation (1). Therefore $G(\theta)$ must be proportional to R^4. This results in using a so-called "Cosecant-squared" gain pattern. This pattern is mathematically described here by the equation:

$$G(\theta) = \frac{G_p \csc^2\theta \cos^{1/2}\theta}{\csc^2\theta_{min} \cos^{1/2}\theta_{min}} \qquad (2)$$

where, G_p is the peak antenna gain, and,
θ_{min} is the minimum depression angle defined directly, or, indirectly, by the maximum slant range.

Certain systems do not incorporate this gain pattern and use a "Gaussian" gain pattern given by:

$$G(\theta) = G_p e^{-(2.772/\theta^2_b)\,(\theta-\theta_p)} \qquad (3)$$

where, θ_b is the vertical half-power beamwidth, and,

θ_p is the depression angle corresponding to peak gain.

For the Gaussian gain pattern $G(\theta)$ is set at G_p for depression angels less than θ_p.

The radar cross section model used for the iceberg target is that developed by Dawe (1985) and, for horizontal polarization (h) at X-band frequencies, is given by:

$$\sigma_h = 10 \log \frac{(L \times H)}{2} - 18.5 \quad (4)$$

or,

$$\sigma_h = 10 \log \frac{(L \times H)}{2} - 11db \quad (5)$$

for tabular and blocky icebergs. For vertical polarization (v):

$$\sigma_v = 10 \log \frac{(L \times H)}{2} - 14.7\ db \quad (6)$$

The equation for σ_v for blocky and tabular icebergs is the same as (5).

To determine σ for the ocean surface a modified version of a sea clutter backscatter coefficient (σ^o) model developed Chan and Fung (1977) is used (Soofi, 1978). This σ^o value is multiplied by the projected area of the resolution cell normal to the radar to obtain σ.

The curved earth form of the pattern propogation factor, F, as described by Blake (1980), is utilized taking into account the complex electromagnetic form of the surface reflection coefficient for a perfectly flat surface, modified by the rough surface coefficient as

derived by Brown and Miller (1974). The divergence factor, which accounts for the earth's curvature, is included. F is calculated for the interference, intermediate, and diffraction zones at incremental heights on the target and is then averaged over the entire height of the target.

The system losses accounted for are those due to wave guide and duplexer losses between the antenna and the transmitter and receiver. The atmospheric losses for each radar type were calculated by obtaining the standard atmospheric loss in decibels per kilometre at sea level and at the normal operating altitude of the particular radar (SLAR - 3000 metres (m), SAR - 10,000 m, surveillance radar 500 m) and taking the average of the two. The individual absorption rates were obtained from Blake (1980).

2.2 PROBABILITY OF DETECTION

For the purpose of determining the probability of detection the iceberg is assumed to be a Swerling Type I target. Also, except in Section 2.3, where the effect of varying it is demonstrated, the probability of false alarm is set at 10^{-6}. The calculation of the instantaneous probability of detection was undertaken using the numerical computation method provided by Rohan (1983) which includes the effect of pulse integration and false alarm probability, P_{fa} (system threshold level). The calculation of, k, the number of pulses integrated depends on the radar system and the operational situation.

In a noise (system noise) limiting situation the ratio of the peak received signal to the system minimum

detectable signal (MDS) is used to obtain the instantaneous signal-to-noise ratio (S/N). In a SLAR system, unless otherwise specified, the number of pulses effectively integrated in one azimuth beamwidth in a noise limited situation is given by:

$$k = \frac{r_a \ (PRF)}{v} \tag{7}$$

where v is the aircraft speed,
r_a is the azimuth resolution, and,
PRF is the pulse repetition frequency.

For SAR, k is given by:

$$k = \frac{(PRF)\ R\ \lambda}{2\ v\ r_a\ D} \tag{8}$$

where, R is the slant range,
λ is the wavelength, and,
D is a processing degradation factor.

The other factors are defined in Equation (7).

In the case of SAR, because it is a fully coherent system, the S/N is multiplied by k to obtain an effective S/N ratio. The number of incoherent looks is used as the number of pulses integrated along with the S/N ratio in the calculation of the probability of detection. The processing degradation factor, D, is

used to account for imperfect coherent integration and processing.

For surveillance radars, when pulse-to-pulse integration is undertaken, k, in a S/N situation, is determined from the equation:

$$k = \frac{\theta\ (PRF)}{(RPM)\ 6} \qquad (9)$$

where,

θ is the half power azimuth beamwidth in degrees,
PRF is the pulse repetition frequency, and,
RPM is the antenna scan rate in revolutions per minute.

When the return from the sea clutter exceeds the MDS the signal-to-clutter ratio (S/C) determines the detection probability. Recent studies have shown that sea clutter decorrelates within about 5 milliseconds (ms) on the average (Shoji and Shimizu, 1978). This is much longer than the time between pulses as dictated by the PRF. Therefore, only pulses spaced 5 ms apart will contribute to and improve the S/C ratio. Hence, to determine k in a clutter limiting situation the PRF in Equations (7), (8), and (9) are replaced by an effective PRF which is equal to the reciprocal of the decorrelation time, or 200 Hz.

Surveillance radars make use of scan-to-scan integration to reduce the effects of second order sea

clutter on "sea spikes", which have a decorrelation time in the order of seconds. The improvement in the detection probability through scan-to-scan integration (Rohan, 1983), or the cumulative probability of detection (P_c), is given by:

$$P_c = 1 - \prod_{i=1}^{n}(1 - P_i) \qquad (10)$$

where n is the number of scans integrated, and,

P_i is the instantaneous probability of detection in the ith scan.

In the model only one P_i value, or P, is calculated (using pulse-to-pulse integration where applicable). Equation (10) then reduces to:

$$P_c = 1 - (1 - P)^n \qquad (11)$$

Two of the surveillance radars have pulse-to-pulse frequency agility in the modes used for point target detection. The change in frequency on a pulse-to-pulse basis is greater than the system bandwidth, which is a requirement to significantly decorrelate the sea clutter. A check on the expected improvement in the S/C ratio using frequency agility indicates an improvement ranging anywhere from 4 (radar manufacturer) to 14 db (Currie and Haykin, 1985) may be possible. This presents some difficulty in simulating the effect of frequency agility. In order to simulate the actual improvement in the S/C ratio it was decided not to reduce the number of pulses integrated in clutter when frequency agility is used. That is,

Equation 9 is used to calculate k in this case. An examination of the improvement obtained by doing this shows that it gives a 5 db increase (approximately) in the S/C ratio. Thus, this method is felt to give a reasonably conservative estimation of the improvement to be expected by using frequency agility.

2.3 MODEL VERIFICATION - AN ATTEMPT

There is only one small data set which the model might be verified against and even this set is not really adequate. The data was collected during BERGSEARCH '84 (Rossiter et al, 1985). The data consists of the percentage of bergy bits detected by the operators of the Atmospheric Environment Service (AES) AN/APS-94E SLAR and the International Ice Patrol (IIP) APS-135 SLAR during a number of passes over the open ocean.

Figures 1 to 4 show the model prediction and gives the actual measured results. The attempt at comparison highlights a number of important points:

1) Because no information is provided on the location of the targets within the ground swath, and the probability of detection is a function of this location, it is rather difficult to compare the results directly.

2) The sizes of the actual targets are not provided, therefore accurate estimates of the iceberg cross sections cannot be utilized in the comparison.

3) The settings on the radar system are not known. One major impact of this is to provide

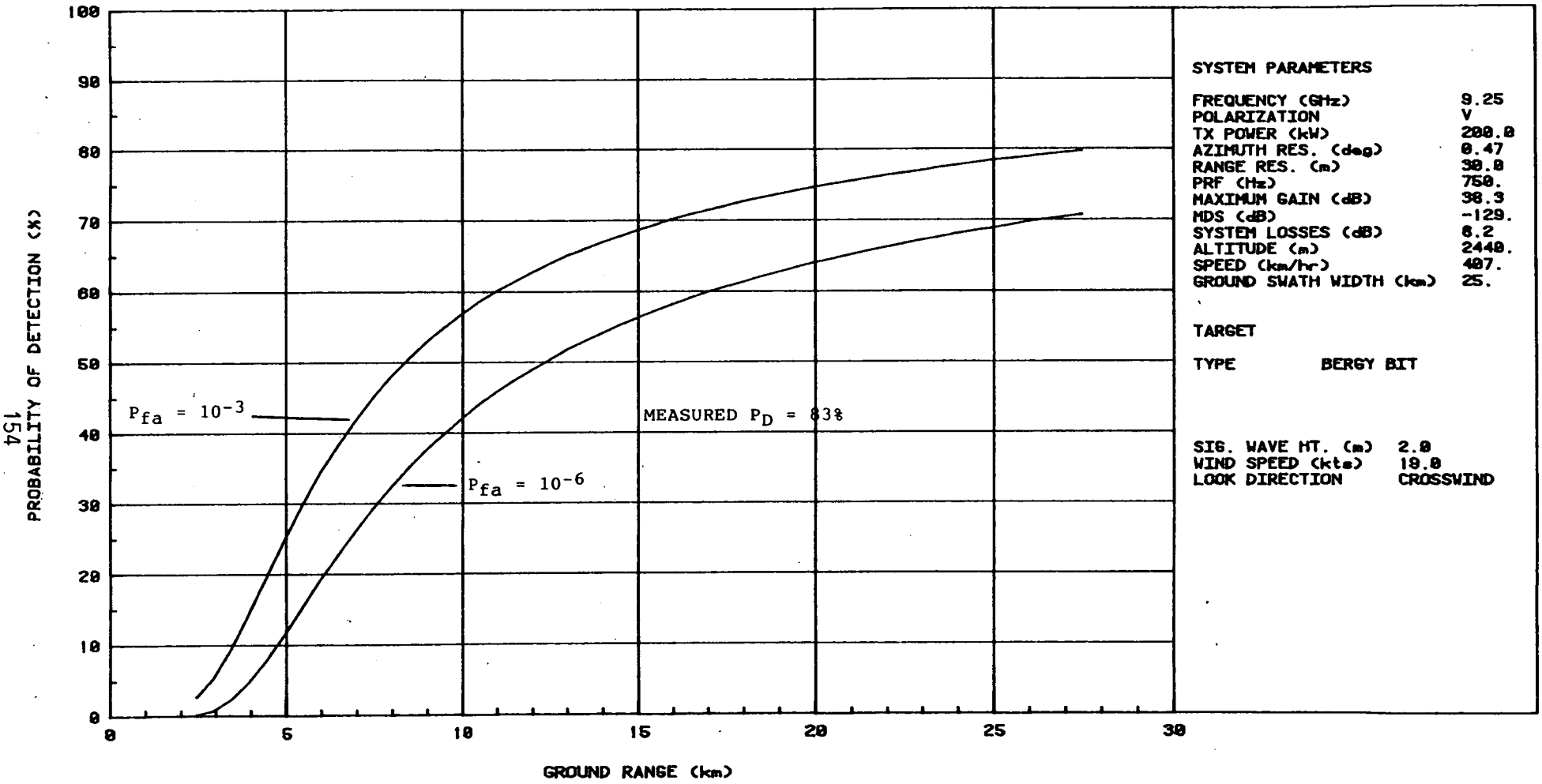

FIGURE 1 - PREDICTED PERFORMANCE OF IIP SLAR ON APRIL 5, 1984 DURING BERGSEARCH '84

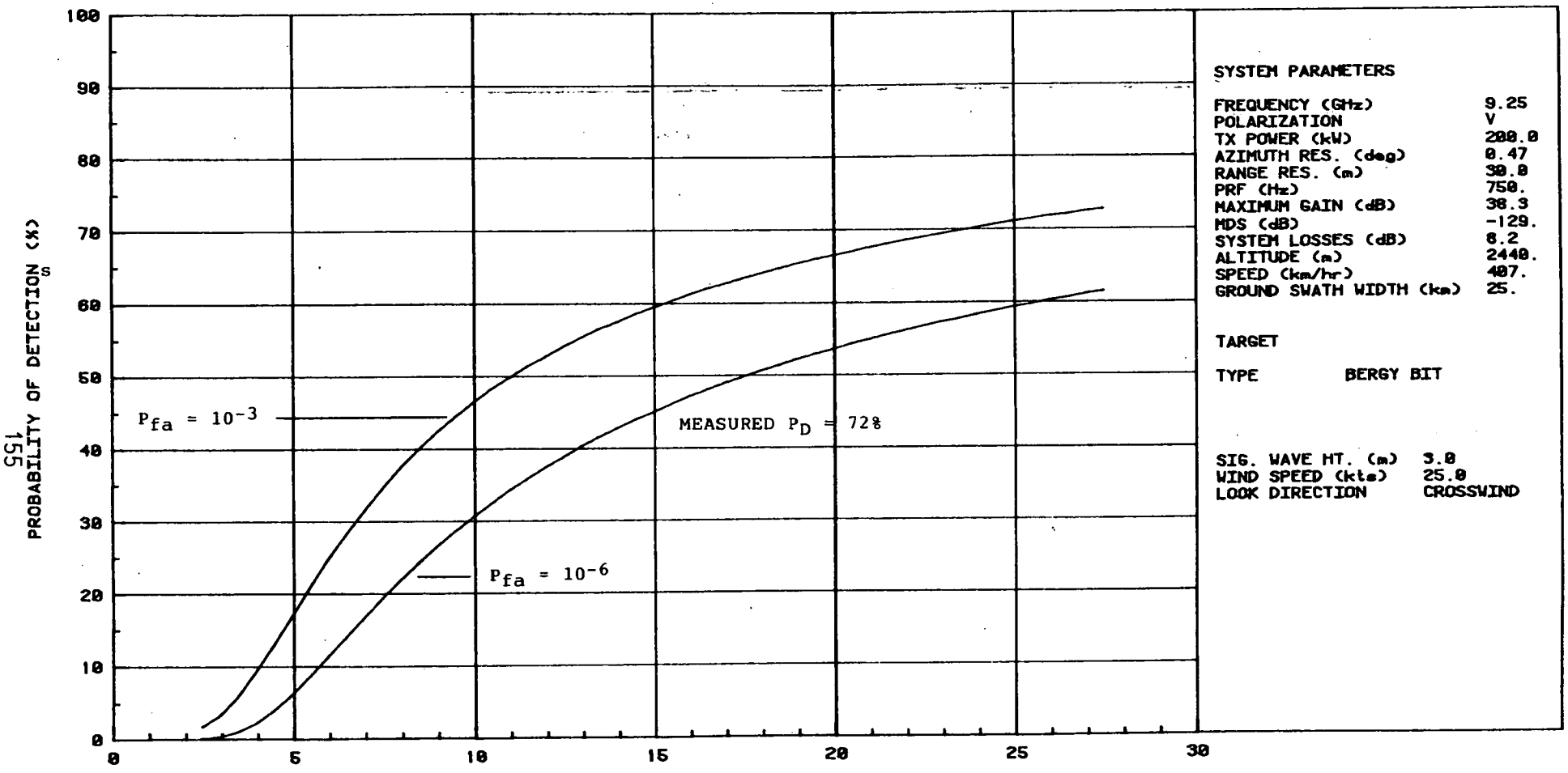

FIGURE 2 - PREDICTED PERFORMANCE OF IIP SLAR ON APRIL 7, 1984 DURING BERGSEARCH '84

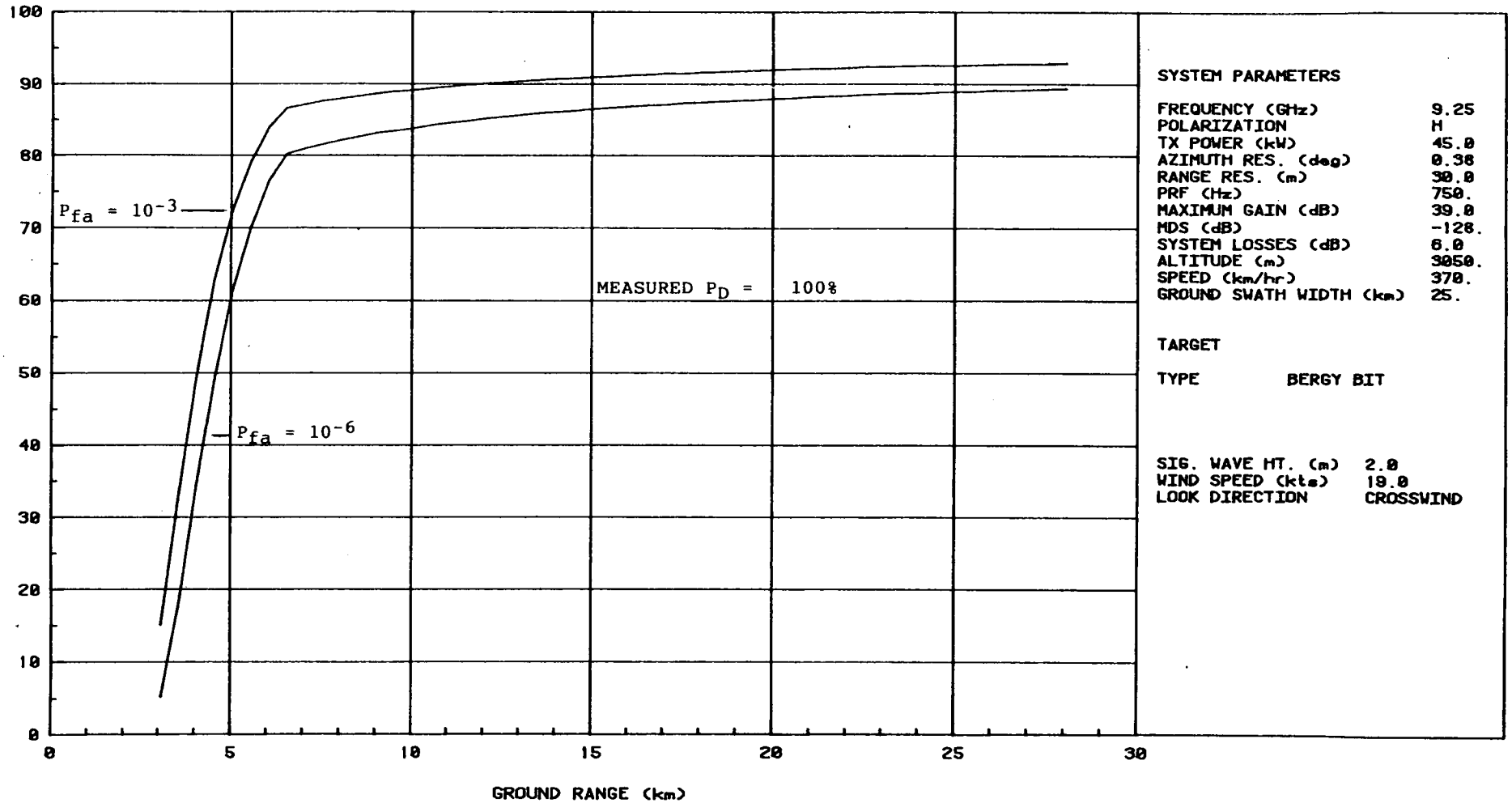

FIGURE 3 - PREDICTED PERFORMANCE OF AES SLAR ON APRIL 5, 1984 DURING BERGSEARCH '84

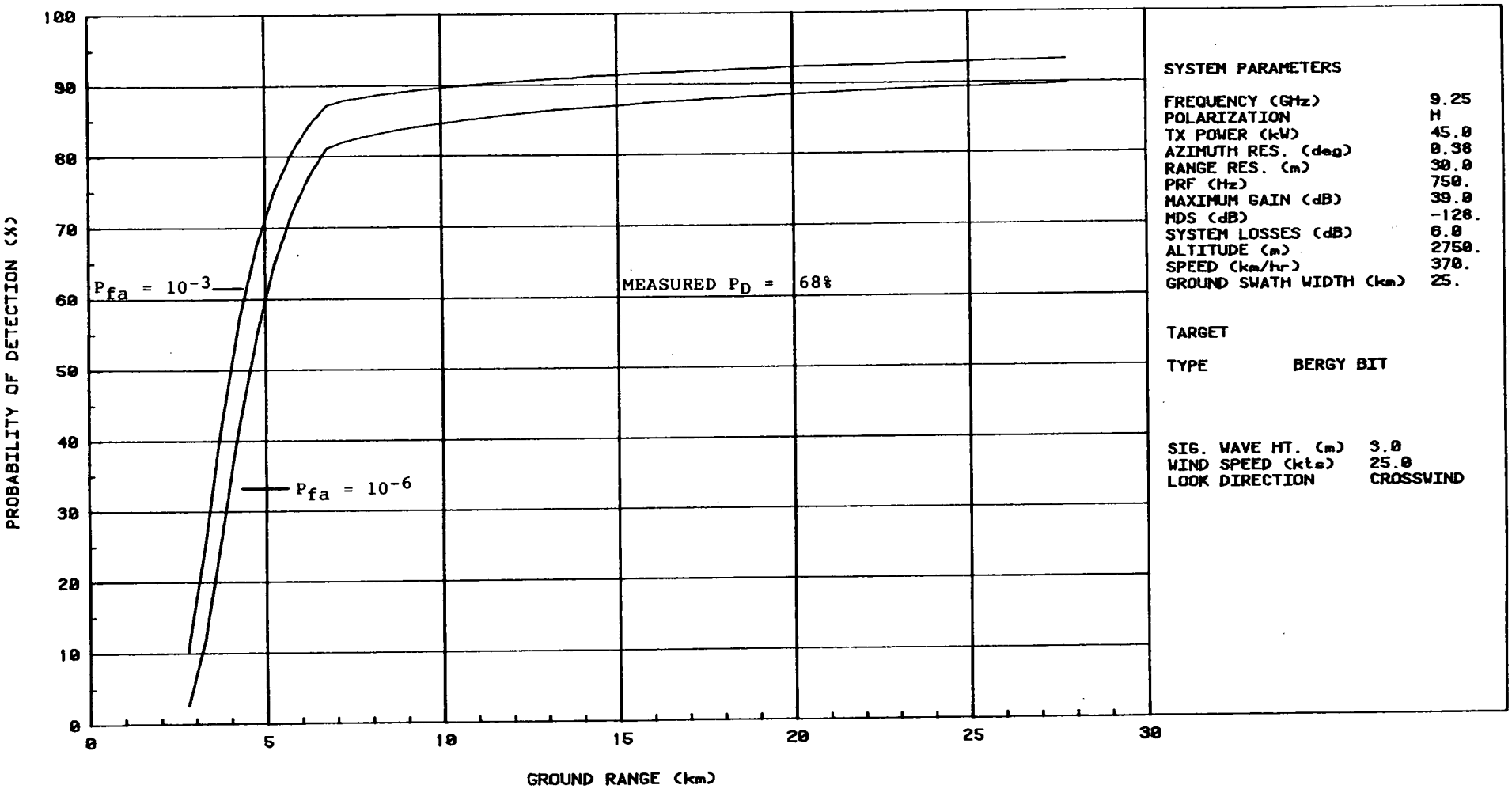

FIGURE 4 - PREDICTED PERFORMANCE OF AES SLAR ON APRIL 7, 1984 DURING BERGSEARCH '84

uncertainty as to the probability of false alarm (P_{fa}).

4) The environmental data consists of wind direction, the variation of the surface windspeed, with the upper limit being almost double the lower limit in one case and fifty percent higher in the other, and the range of the significant wave height, again with the upper limit double the lower limit in one case and over fifty percent higher in the other. It would be possible no doubt to select the appropriate combination of values within these ranges to ensure a proper fit to the data.

The probability of detection curves shown in Figures 1 to 4 are plotted using the average wind and sea state conditions. As can be seen the detection probability changes across the swath and the goodness of agreement depends on where the targets are located in range.

There is one other date during BERGSEARCH '84 for which SLAR detection measurements were available. However, on this date (April 5, 1984) an anomalous sea condition occured in which the winds were virtually calm but large swells were present. As there is no way of properly predicting the sea clutter levels in this condition from the models available, it would be useless to try to compare the results with the model.

2.4 DISCUSSION

A comprehensive model has been described which can be used to predict the performance of radars against

icebergs in the open ocean. There is, however, one general shortcoming and this is with regard to the inability to predict the effects of second order sea clutter or "sea spikes". There is no model apparently available in the published literature to predict this. SLAR's have no mechanism for overcoming this problem as the time period in which they image an area on the ocean is very small compared to the decorrelation time (seconds) for this type of clutter. As noted earlier surveillance radars make use of high speed scanning to overcome this problem. The model results in the case of SLAR's will then produce erroneously high detection results in the higher sea states.

3. RADARS EVALUATED

Table 1 lists the radars evaluated. The Appendix provides the specifications of each of the radars. In a number of instances not all the parameters were available and values were either assumed or calculated. In the predictive modelling, the antenna gain pattern for each system is optimized for the particular altitude and ground swath width (or maximum range setting in the case of the surveillance radars) tested.

The surveillance radar scan rates given are those which would be normally used in the detection of very small targets in the ocean. Smith (1984) suggests that the maximum scan integration time employed these types of radars would be 10 seconds. This determines the number of scans that would be integrated by each radar and this value is given in the specifications.

For all the SLAR's except the SLAR-100 system, it is assumed that the hard copy recording device provides incoherent integration of all the pulses possible within the azimuth beamwidth. The number of pulses integrated is calculated at each range increment. For the SLAR-100 system this number is fixed at 64 by the manufacturer.

The MARS Limited Motorola AN/APS-94D SLAR is not included in this evaluation. It is virtually the same SLAR as the AES system with the exception that the peak transmitter power is somewhat higher. Therefore, its performance should parallel that of the AES system with a slight increase in detection probability in a S/N situation.

TABLE 1 - RADARS EVALUATED

SLAR'S:

Motorola Inc. AN/APS-94E (used by Atmospheric Environment Service)

Motorola Inc. AN/APS-135 (used by International Ice Patrol)

Intera Technologies Limited MAPR

Canadian Astronautics Limited SLAR-100 (built for Atmospheric Environment Service)

SAR'S:

Canada Centre for Remote Sensing SAR-580

Intera Technologies Limited STAR-1

Surveillance Radars:

Eaton Corporation AN/APS-128

Litton Systems (Canada) Limited APS-504(V)5

Texas Instruments Inc. AN/APS-134(V)

4 MODELLING RESULTS

4.1 INTRODUCTION

This chapter provides the results of the modelling work undertaken. Only surveillance radar and SLAR results are presented. Because SAR is fully coherent, its K value is very high, and its resolution is extremely fine the model predicts effectively 100 percent detection probability for all targets and sea conditions. Based on experimental results this is obviously erroneous, and as pointed out in Chapter 1, is probably due to the inability of the model to take into account the complex mechanisms which come into play in the formation of an image.

4.2 GENERAL COMPARISONS AMONG RADARS OF THE SAME TYPE

Figure 5 shows a comparison between the 4 SLAR's selected for evaluation. Also, included is the radar now being built for the (AES) by Canadian Astronautics Limited. The aircraft speed (400 km/hr) and altitude (3,000 m) is set the same for all the SLAR'S. Sea state 3 is utilized as it approximates the average sea condition on the Grand Banks.

It can be seen that overall the AES AN/APS-94D SLAR out-performs the rest according to the model. The poor performance of the IIP radar is attributed to its vertical polarization and the resulting high sea clutter levels. The MAPR SLAR gives better performance in the near range, but because it does not use a cosecant-squared antenna gain pattern its performance rapidly falls off. The SLAR-100 system performance is close to that of the AN/APS-94D but the fixed 64 pulse

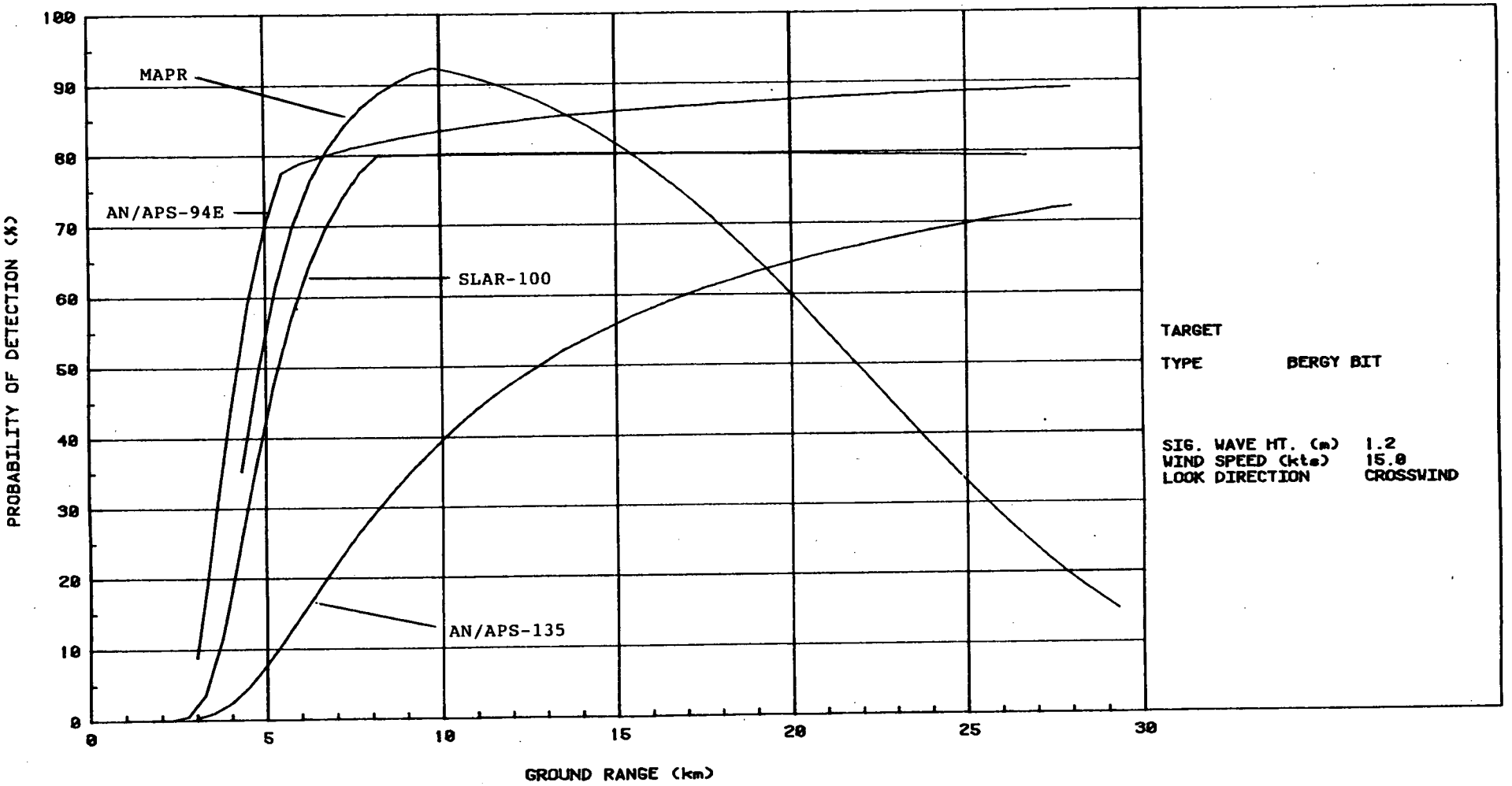

FIGURE 5 - SLAR PERFORMANCE COMPARISON

integration limits it somewhat. Because of their closeness and uncertainties in the modelling, it is impossible to say with confidence which of the MAPR, AN/APS-94E, and SLAR-100 radars would perform the best in reality. The model predicts that growlers will not be detected on any of the systems.

The surveillance radars are compared in Figure 6. It is obvious here that the AN/APS-134 (V) greatly outperforms the others, obviously due to a number of system parameters (transmitter power, resolution, pulse compression ratio, and scan rate (scan-to-scan integration)). It is noted that because of the very short pulse lengths and low altitude, noise rather than sea clutter is the limiting factor even in high sea states. Also the model predicts that neither of the systems will reliably detect a growler.

4.3 COMPARISON BETWEEN TYPES

It is apparent from a comparison between Figures 5 and 6 that the AN/APS-134(V) outperforms all the SLAR's. However, it is also apparent that caution must be used in selecting a surveillance radar as the other two are indicated to give a very poor performance.

4.4 PERFORMANCE AS A FUNCTION OF SEA STATE/LOOK DIRECTION

Modelling results for the AN/APS-134(V) radar show that the probability of detection as a function of sea state and look direction remains at 100 percent. Figure 7 shows the predicted performance of the AN/APS-94E SLAR at three sea states looking crosswind. Figure 8 is the same as Figure 7 with the exception that the radar is looking upwind. Figure 7 shows that

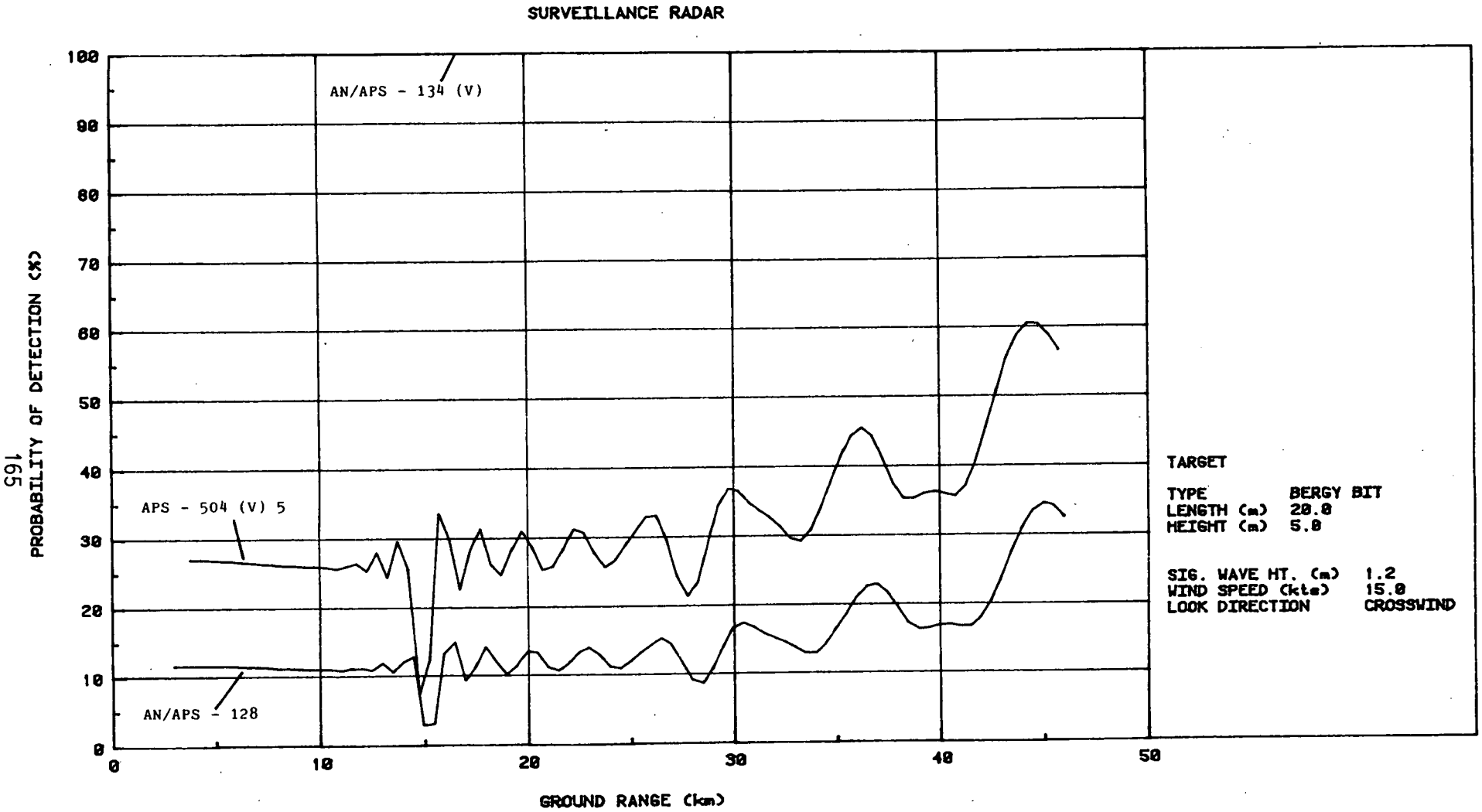

FIGURE 6 - SURVEILLANCE RADAR PERFORMANCE COMPARISONS

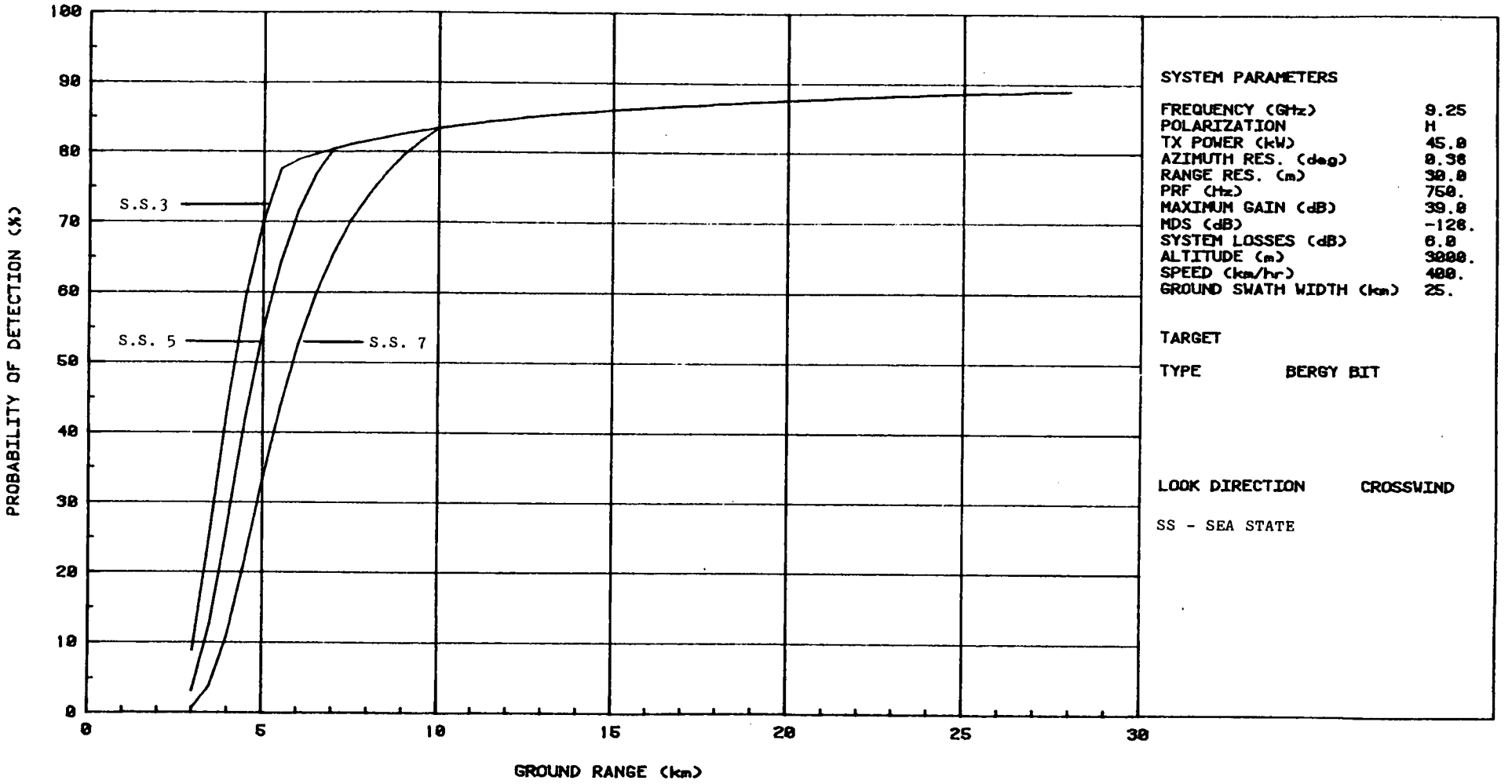

FIGURE 7 - EFFECT OF SEA STATE ON AN/APS-94E PERFORMANCE WHEN LOOKING CROSS WIND

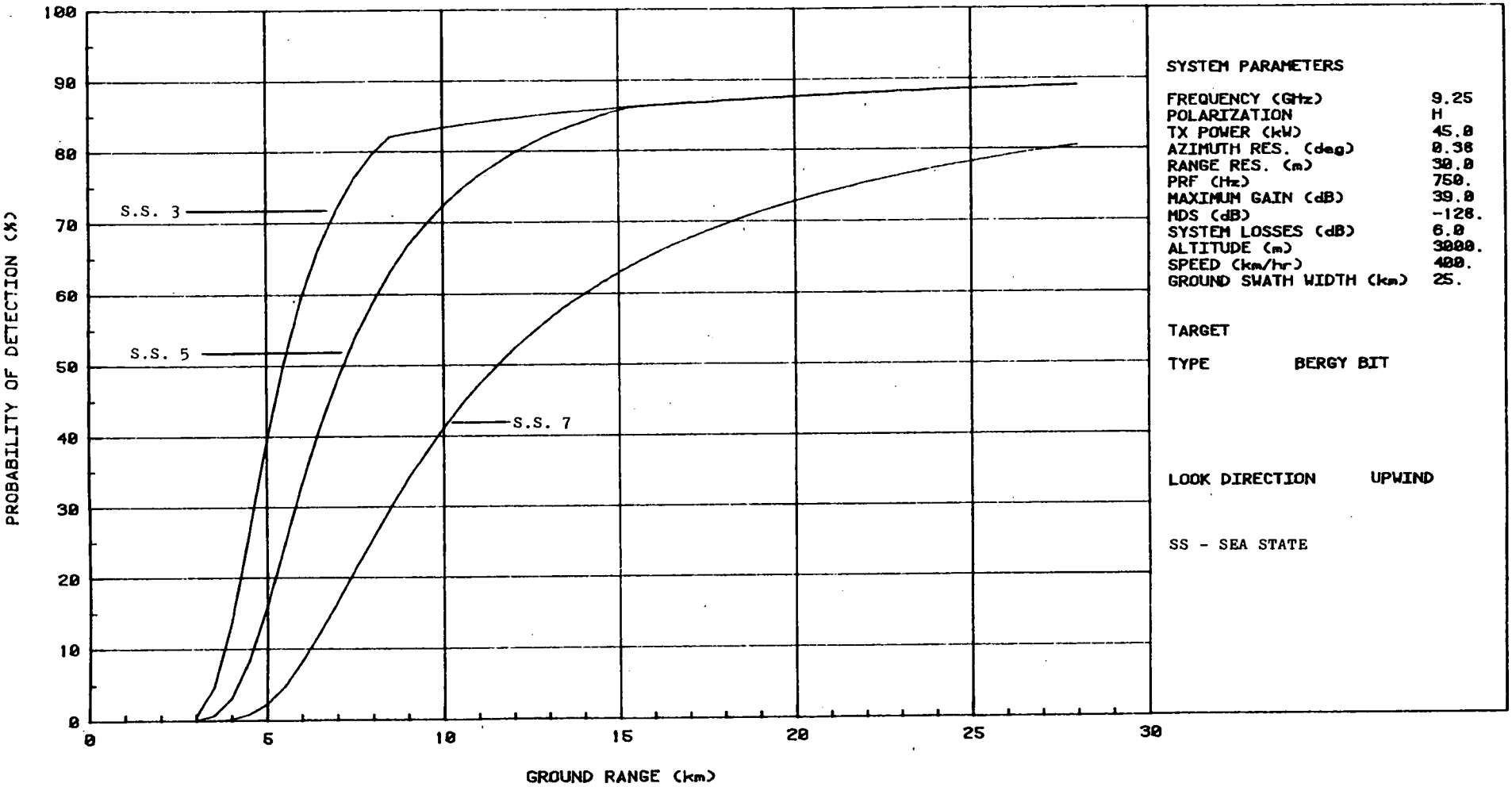

FIGURE 8 - EFFECT OF SEA STATE ON AN/APS-94E PERFORMANCE WHEN LOOKING UPWIND

looking crosswind and considering only first order sea clutter the primary effect of sea state is minimal and that the net result is a reduction in performance in the near range portion of the swath.

The predicted upwind performance given in Figure 8 shows that at the higher sea states there is a significant performance reduction. The overall preformance is reduced over that looking crosswind as well. In the higher sea states (say, 5 and 7) the second order sea clutter will probably be the major problem and the results given here probably largely overestimate the actual performance.

4.5 METHODS FOR IMPROVING PERFORMANCE

Figure 9 shows the improvement in performance to be expected by changing the polarization on the AN/APS-135 to horizontal. The improvement is dramatic and with this change it outperforms the AN/APS-94E because of the much higher transmitter power. In a clutter limiting situation the higher power advantage will disappear. It is noted that the reason for utilizing vertical polarization on this radar was to detect oil slicks, not icebergs.

Figure 10 shows the improvement to be expected by incorporating pulse compression into the AN/APS-94E. The compressed pulse length is set at 2.5 nanoseconds (ns), with a compression ratio of 400 and minimum detectable signal is adjusted to -120 db. The improvement is significant and, for the example given, results in almost 100 percent detection performance across the swath. Figure 11 shows the effect of adding the same pulse compression to the AN/APS-135. Again

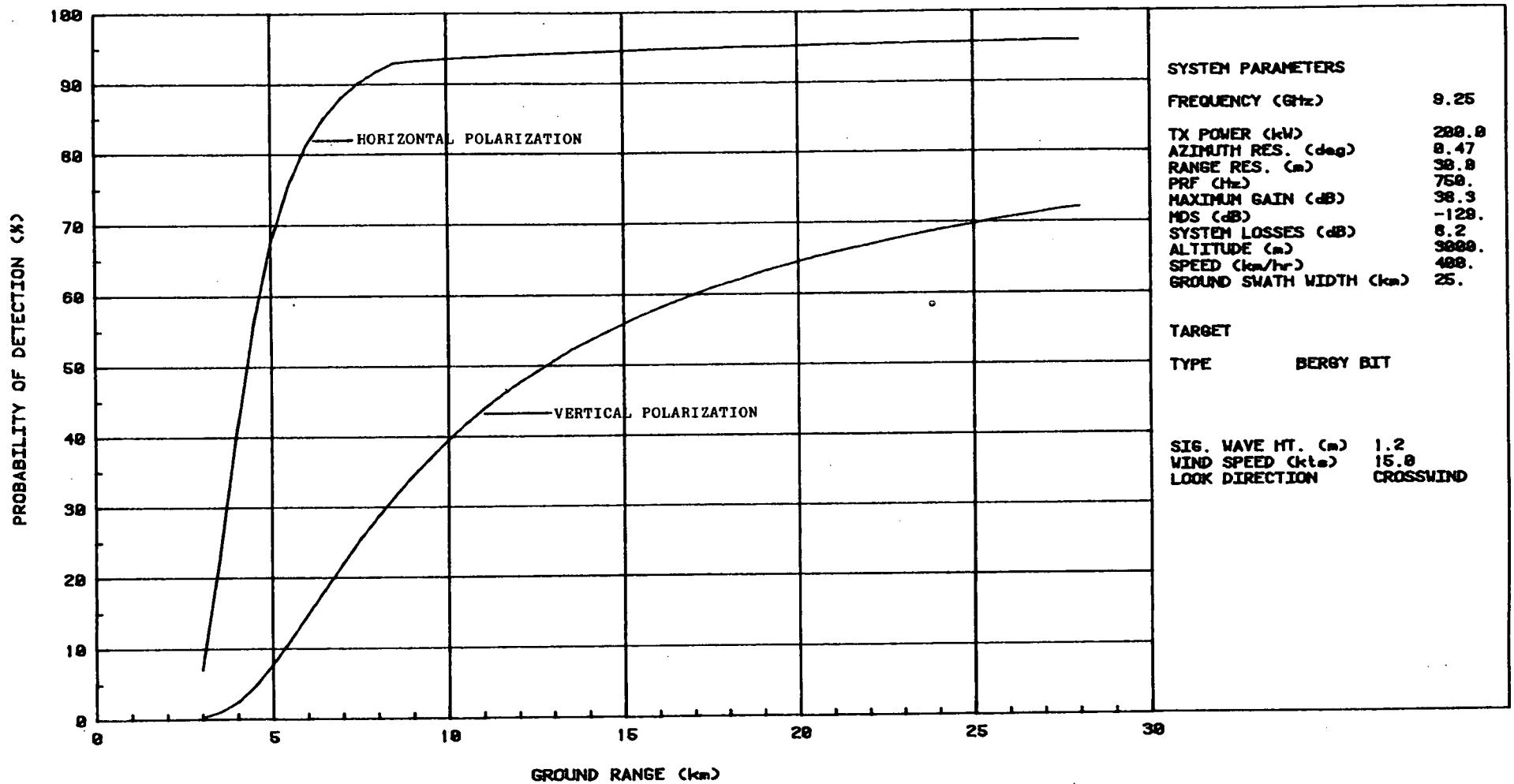

FIGURE 9 - EFFECT OF CHANGING POLARIZATION OF AN/APS-135 FROM VERTICAL TO HORIZONTAL

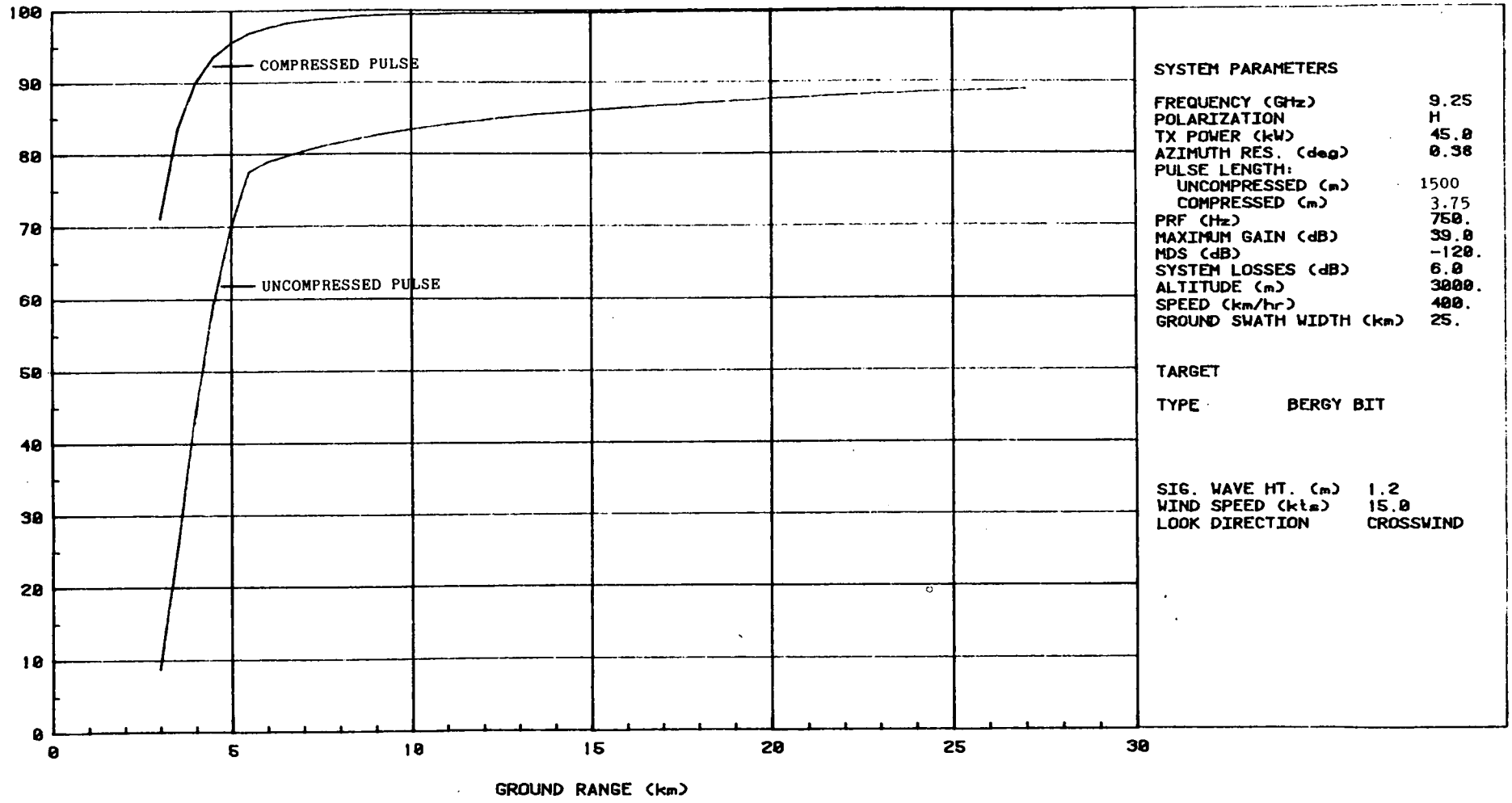

FIGURE 10 - EFFECT OF PULSE COMPRESSION ON AN/APS-94E PERFORMANCE

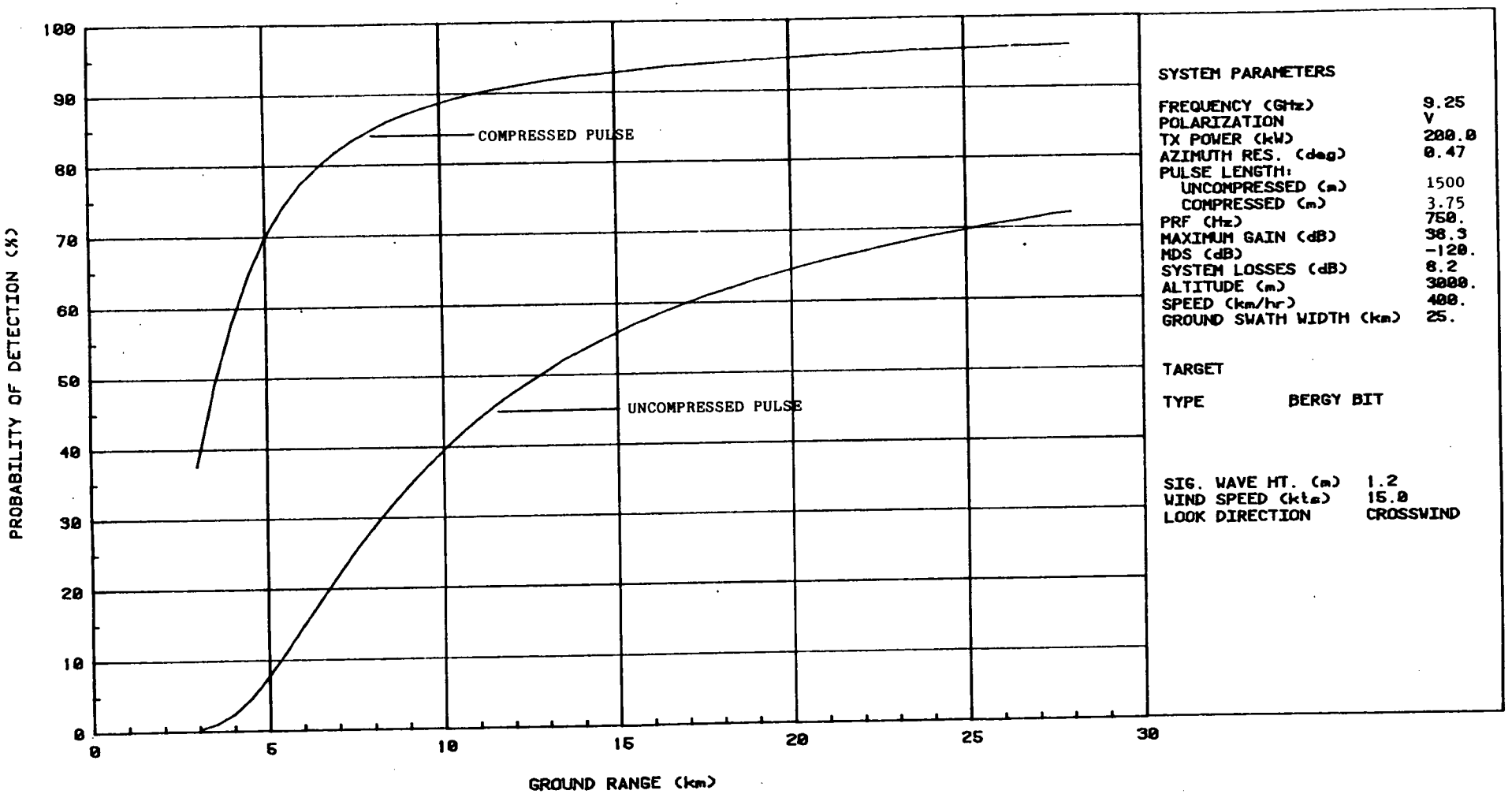

FIGURE 11 - EFFECT OF PULSE COMPRESSION ON AN/APS - 135 PERFORMANCE

there is significant improvement and with a coincident change to horizontal polarization would, no doubt, have resulted in 100 percent detection performance across the swath.

Figure 12 shows the improvement to be expected by flying at an altitude of 1,500 m instead of 3,000 m using the AN/APS-94E. In this case the improvement is only marginal. Figure 13 shows the improvement to be expected by flying the AN/APS-135 at the lower altitude, and in this case it is significant.

With certain system changes the performance of the AN/APS-128 and the APS-504(V)5 surveillance radars could also be significantly improved. The result of increasing the peak transmitter power by a factor of 3 in a noise limiting situation is shown in Figure 14. This effect is dramatic and results in their performance being on a par with that of the AN/APS-134(V) and the SLAR's. The sharp drop in the P_D at 15 km on both systems is a direct result of the pattern propagation factor. It is not believed to be significant.

4.6 DISCUSSION

The predictive modelling demonstrates that with the exception of the AN/APS-135 SLAR little difference can be expected in the performances of the SLAR's evaluated. The performance of each will be optimized by ensuring that the radars are looking crosswind. The effect of increasing sea state is minimized when this look direction is utilized. Flying the AN/APS-135 at 1,500 m puts its performance on a par with the others.

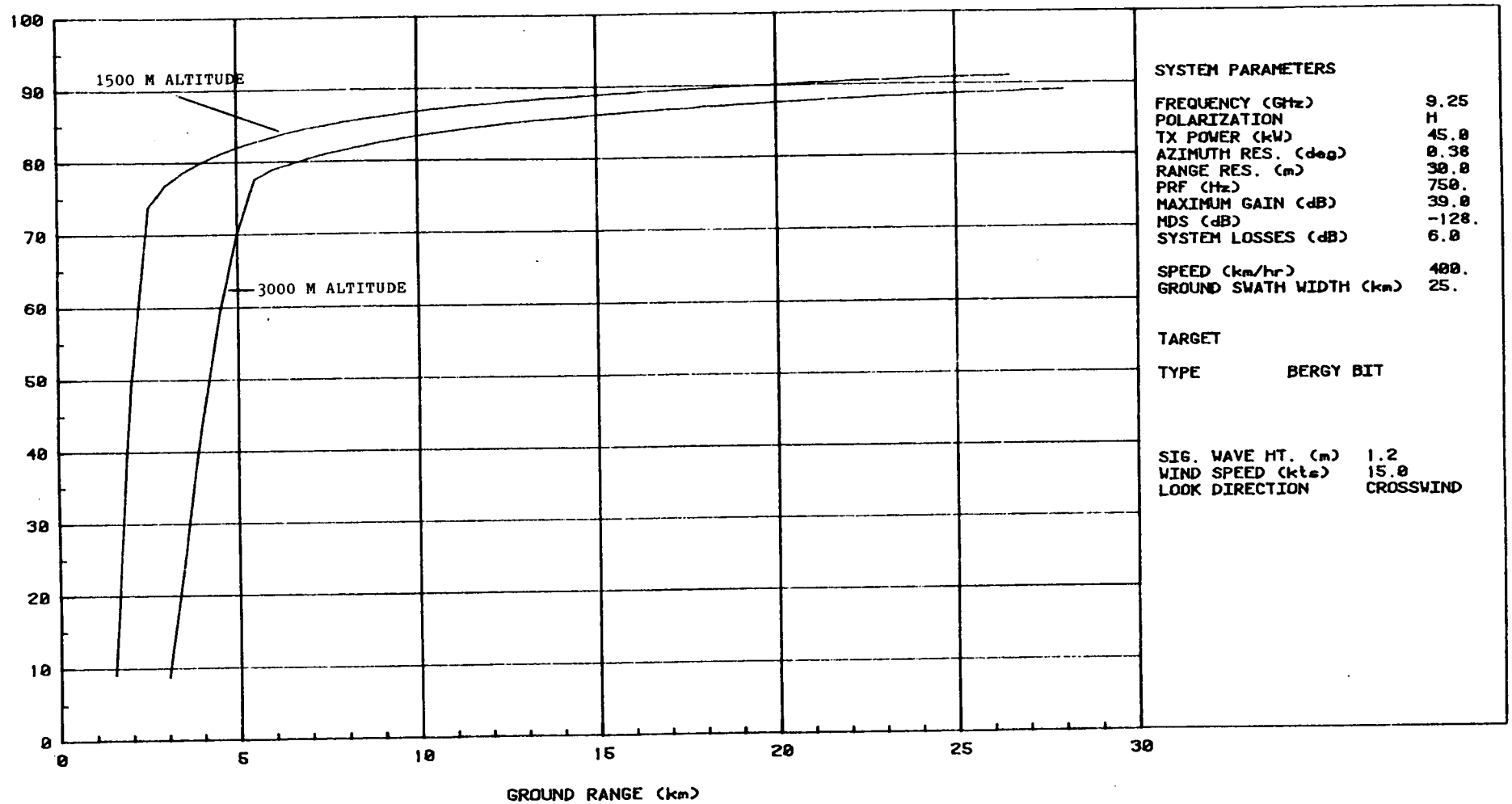

FIGURE 12 - EFFECT OF CHANGING ALTITUDE ON AN/APS-94E

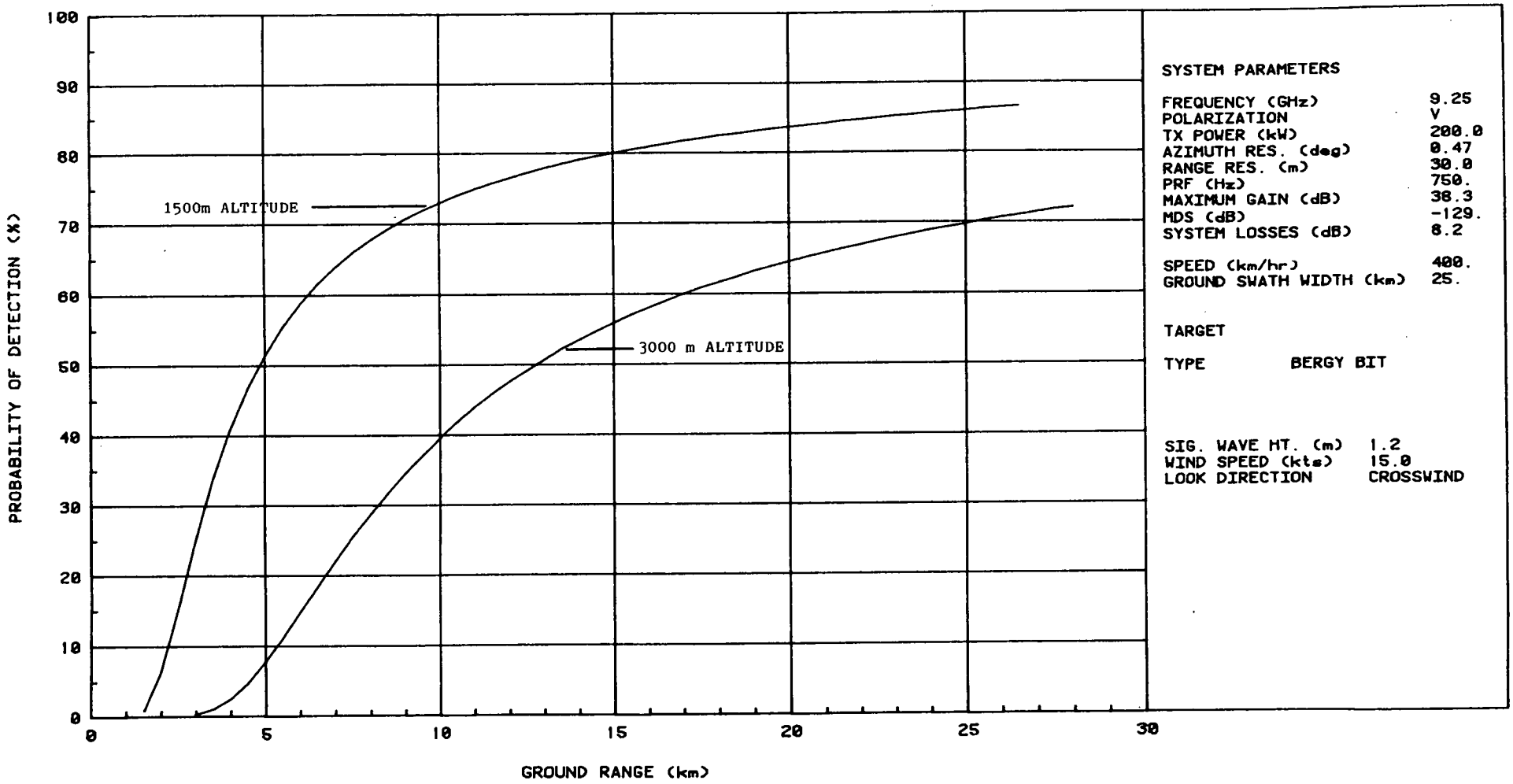

FIGURE 13 - EFFECT OF CHANGING ALTITUDE ON AN/APS-135 PERFORMANCE

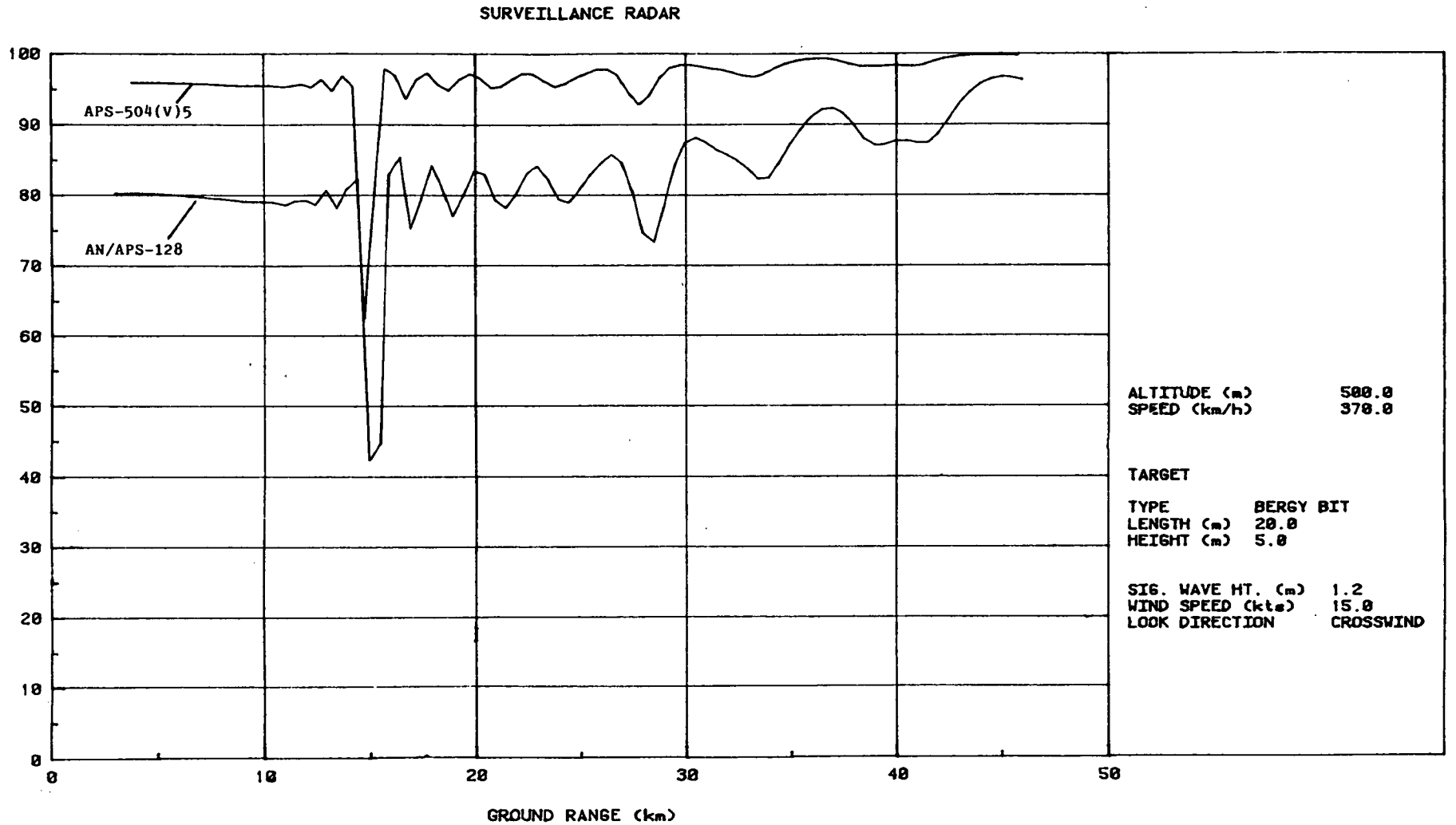

FIGURE 14 - EFFECT OF A 3X INCREASE IN PEAK POWER ON THE PERFORMANCE OF THE AN/APS-128 AND APS-504(V)5 RADARS

The performance of each SLAR can be significantly improved by the addition pulse compression. A change in the polarization of the AN/APS-135 to horizontal results in a predicted performance which is better than all the others. The addition of pulse compression with the polarization change would make this difference considerably greater.

The performance of the AN/APS-134(V) surveillance radar is shown to exceed that of all the SLAR's, while the other two surveillance radars are shown to give the worst performance. Increasing the peak powers on the AN/APS-128 and APS-504(V)5 radars by a factor of three, results in a performance which exceeds the SLAR's and is close to that of the AN/APS-134(V).

The predicted performance of the SLAR's and SAR's in higher sea states is probably signficantly over estimated because of second order clutter, or sea spikes, which will probably be a major problem. The AN/APS-134(V) surveillance radar is designed to suppress this clutter. It will no doubt significantly outperform all these radars in these conditions.

5 CONCLUSIONS AND RECOMMENDATIONS

5.1 CONCLUSIONS

Based on theoretical modelling, it is concluded that at this point a surveillance radar having the characteristics of the AN/APS-134(V) would be the optimum radar currently available for iceberg reconnaissance in the open ocean. This does, however, require verification by a well planned experiment.

Currently available SLAR's cannot be depended on to provide reliable detection of icebergs having maximum height and length dimensions less than 5 m and 20 m, respectively, in moderate to high sea states. The actual performance level needs to be further quantified. A lack of knowledge on the characteristic effects (in numerical terms) of second order sea clutter on the performance of SLAR's. The lack of a suitable model for backscatter (first order) for SAR's and the current inability to adequately model SAR limits the capability to accurately quantify its performance.

5.2 RECOMMENDATIONS

It is recommended that an experimental program be undertaken to verify the performance of a surveillance radar. It is preferable that the AN/APS-134(V) radar be utilized, but either of the other two would be acceptable for model verification. The experiment should be planned such that raw full bandwidth radar data is recorded. Extensive ground truthing is required. The experiment should also be conducted in such a manner that the data collected can be used to

properly compare the results with performance prediction models. An accurate measurement of the radar parameters will also be required. This would avoid the problems encountered in trying to work with the BERGSEARCH '84 data. During the experimental program sea clutter data should be collected using a calibrated radar (scatterometer) operating at the same frequency.

The level of effort dictated by this project did not allow an extensive investigation of the theoretical modelling and its accuracy. Confidence in the modellng work is also limited by certain unknown radar characteristics (e.g., exact MDS, actual system losses, actual pulse-to-pulse integration processes, etc.). It is, therefore, recommended that further refinement of the predictive models be investigated and more detailed and more accurate information be gathered on the individual radars so as to maximize the accuracy of the models. This work should involve, if possible, the development of a proper model for SAR and second order sea clutter models for SLAR.

REFERENCES

Blake, L.V. (1980), Radar Range - Performance Analysis, D.C. Heath & Co., Lexington, Mass.

Brown, R.M. and Miller, A.R. (1974), "Geometric - Optics Theory for Coherent Scattering of Microwaves from the Ocean Surface", Naval Research Labratory Report No. 7705, Washington: GPO.

Chan, H.L. and Fung, A.K. (1977), "A Theory of Sea Scatter at Large Incidence Angles", Journal of Geophysical Research, v. 82, pp 3429-3444.

Currie, B.W., and Haykin, S. (1985), "Airborne Surveillance Radars (Draft Report)" McMaster University, Communications Research Laboratory, report no. CRL-146, Hamilton, Ontario.

Dawe, B.R., (1985), "A Radar Cross Section Model for Icebergs", IEEE 1985 International Radar Conference, pp. 259 - 264.

Rohan, P. (1983), Surveillance Radar Performance Prediction, Peter Peregrinus Ltd. London, U.K.

Rossiter, J.R., Arsenault, L.D., Guy, V.G., Lapp, D.J., and Wedler, E. (1985), "BERGSEARCH '84, Assessment of Airborne Imaging Radars for the Detection of Icebergs, Summary Report - Results, Conclusions and Recommendations," Environmental Studies Revolving Funds Project no. 099-19-03.

Soofi, K. (1978), "Clutter Model for Land, Forest, Snow, Sea Ice, and Ocean", University of Kansas RSL TR 2923-2.

Shoji, K. and Shimizu, T. (1978), "Statistical Properties and the Suppression of Radar Sea Clutter", Japan Institute of Navigation.

Smith, J.M. (1984), "Fast Scan Processing in Maritime Surveillance Radars," Proceedings of the 1984 International Symposium on Noise and Clutter Rejection in Radars and Imaging Sensors, Tokyo, Japan, pp. 506-511.

APPENDIX

SPECIFICATIONS OF RADAR SYSTEMS EVALUATED

SIDE LOOKING AIRBORNE RADARS

ATMOSPHERIC ENVIRONMENT SERVICES

AN/APS--94E SLAR

Frequency:	9.25 GHz
Polarization:	Horizontal
Azimuth Beamwidth:	0.38^{o}
Vertical Beam Pattern:	$CSC^{2}\theta$
Peak Antenna Gain:	39 dB
Peak Transmitter Power:	45 kW
Pulse Length:	0.2 us
Pulse Repetition Frequency:	750 Hz
2-way System Loss:	6 dB
Minimum Detectable Signal:	-128 dB

ATMOSPHERIC ENVIRONMENT SERVICES

SLAR-100

Frequency:	9.25 GHz
Polarization:	Horizontal
Azimuth Beamwidth:	0.39^{o}
Vertical Beam Pattern:	$CSC^{2}\theta$
Peak Antenna Gain:	37 db
Peak Transmitter Power:	250 kW
Pulse Length:	0.23 us
Pulse Repetition Frequency:	800 Hz
2-way System Losses:	7.5 dB
Minimum Detectable Signal:	-131 dB
Digital Integration:	64 pulses incoherently averaged

INTERA TECHNOLOGIES LTD

MAPR SLAR

Frequency:	9.25 GHz
Polarization:	Horizontal
Azimuth Beamwidth:	0.6°
Vertical Beam Pattern:	Gaussian
Peak Antenna Gain:	32.5 dB
Peak Transmitter Power:	20 kW
Pulse Length:	0.27 us
Pulse Repetition Frequency:	1536 @560 km/h
2-way System Loss:	5 dB
Minimum Detectable Signal:	-130 dB

INTERNATIONAL ICE PATROL

APS-135 SLAR

Frequency:	9.25 GHz
Polarization:	Vertical
Azimuth Beamwidth:	0.47^{o}
Vertical Beam Pattern:	$CSC^{2}\theta$
Peak Antenna Gain:	38.3 dB
Peak Transmitter Power:	200 kW
Pulse Length:	0.2 us
Pulse Repetition Frequency:	750 Hz
2-way System Loss:	8.2 dB
Minimum Detectable Signal:	-129 dB

SYNTHETIC APERTURE RADARS

INTERA TECHNOLOGIES LTD.

STAR-1 SAR

Frequency:	9.25 GHz
Polarization:	Horizontal
Azimuth Beamwidth:	2.3^{o}
Vertical Beam Pattern:	$CSC^{2}\theta$
Peak Antenna Gain:	30.5 dB
Peak Transmitter Power:	2 kW
Uncompressed Pulse Length:	30 us
Compressed Pulse Length:	0.04 us/0.08 us
Pulse Repetition Frequency:	2000 Hz @ 650 km/h
Azimuth Resolution:	6 m
2-way System Loss:	3.4 dB
Minimum Detectable Signal:	-124 dB
Number of Looks (noncoherent):	7/3
Processing Degradation Factor:	2 dB

CANADA CENTRE FOR REMOTE SENSING

CV-580 SAR

Frequency:	X, C, & L
Polarization:	HH, HV, VV, HH
Azimuth Beamwidth:	X 1.2°
	C 3°
	L 8°
Vertical Beam Pattern:	Gaussian
Peak Antenna Gain:	X 32 dB
	C 27 dB
	L 17 dB
Peak Transmitter Power:	X 1.5 kW
	C 1.0 kW
	L 5.0 kW
Uncompressed Pulse Length:	X 2.7 us
	C 2.7 us
	L 1.7 us
Compressed Pulse Length:	0.02 us
Pulse Repetition Frequency:	2000 Hz @ 650 km/h
Azimuth Resolution:	3 m
2-way System Loss:	4 dB
Minimum Detectable Signal:	-130 dB
Number of Looks:	1
Processing Degradation Factor:	7 dB

SURVEILLANCE RADARS

EATON CORPORATION

AN/APS-128

(WITH PULSE COMPRESSION)

Frequency:	9.2-9.5 GHz
Polarization:	Horizontal
Azimuth Beamwidth:	2.3^{o}
Vertical Beamwidth:	9^{o}
Vertical Gain Pattern:	$CSC^{2}\theta$
Peak Antenna Gain:	32 dB
Peak Transmitter Power:	10 kW
Uncompressed Pulse Length:	5 us
Compressed Pulse Length:	0.1 us
Pulse Repetition Frequency:	2000 Hz
2-way System Loss:	3 dB
Minimum Detectable Signal:	-129 dB
Antenna Rotation Rate:	60 rpm
Frequency Agility:	Yes
Number of Scans Integrated:	11
Maximum Range:	46 km

TEXAS INSTRUMENTS, INC.

AN/APS-134(V)

Frequency:	9.75 GHz
Polarization:	Vertical
Azimuth Beamwidth:	2.4^{o}
Vertical Beamwidth:	4.0^{o}
Vertical Gain Pattern:	$CSC^{2}\theta$
Peak Antenna Gain:	35 dB
Peak Transmitter Power:	500 kW
Uncompressed Pulse Length:	0.5 us
Compressed Pulse Length:	3.0 ns
Pulse Repetition Frequency:	2000 Hz
2-way System Loss:	3 dB
Minimum Detectable Signal:	-114 dB
Antenna Rotation Rate:	150 rpm
Frequency Agility:	No
Number of Scans Integrated:	25
Maximum Range:	59 km

LITTON SYSTEMS (CANADA) LTD.

APS-504(V)5

Frequency:	8.9-9.4 GHz
Polarization:	Horizontal
Azimuth Beamwidth:	2.5^{o}
Vertical Beamwidth:	7.0^{o}
Vertical Gain Pattern:	$CSC^{2}\theta$
Peak Antenna Gain:	32 dB
Peak Transmitter Power:	8 kW
Uncompressed Pulse Length:	10 us
Compressed Pulse Length:	30 ns
Pulse Repetition Frequency:	2000 Hz
2-way System Loss:	3 dB
Minimum Detectable Signal:	-123 dB
Antenna Rotation Rate:	120 rpm
Frequency Agility:	Yes
Number of Scans Integrated:	20
Maximum Range:	46 km

APPENDIX E

Feasibility of Discriminating Ships from Icebergs using Electronic Support Measures (ESM)

FEASIBILITY OF DISCRIMINATING SHIPS FROM ICEBERGS USING ELECTRONIC SUPPORT MEASURES (ESM) TECHNOLOGY

Provided for
Canpolar Consultants Ltd
Toronto, Ontario

Provided by
INTERA Technologies Ltd.
Calgary, Alberta

October 1985
R85-181

TABLE OF CONTENTS

1. INTRODUCTION

1.1 THE PROBLEM

The ability to discriminate ships from icebergs on the radar imagery is highly desirable in an operational rig support program for the East Coast. A vessel or group of vessels incorrectly identified as iceberg targets may cause unnecessary deployment of supply vessels for confirmation or action, thus tying up resources and causing extra expenditures. On the other hand, incorrectly identifying an iceberg as a vessel may result in a lack of action, thus negating the purpose of the rig's ice management system. In either case, there is a cost associated with mis-identification of or uncertainty of discrimination between berg and vessel.

Experience gained during Bergsearch '84 suggested that iceberg/ship discrimination could not be accomplished without some ambiguity on either SLAR or SAR imagery. The radar cross-section of bergs and vessels is highly variable and overlaps, so that target brightness alone is not adequate as a discriminator. In the case of SLAR or search radar, resolution is generally inadequate to permit vessel shape to be used as the determinant. The resolution of STAR-1 (high resolution mode 6 m x 6 m) is sufficient for identification of ships the size of standard supply vessels or larger, provided there are no motion effects to smear the target image. Unfortunately, motion of the target in open water conditions produces the phenomenon known as, 'azimuthal smear', which is described elsewhere in this report. The resulting SAR target smear makes unambiguous identification of vessels vs bergs very difficult in open water.

If the vessels are in transit, they can be identified by their motion between one pass and the next. Fishing vessels may be drifting no faster than bergs, however, and in some cases they may be located among the bergs.

In summary, it appears that the present capability for discriminating ships from icebergs on the basis of their appearance on imagery is unsatisfactory for all the airborne radar systems. There is obvious merit in meeting the need with a different approach.

1.2 THE APPROACH

Ships are active emitters of radio and radar radiation signals, while icebergs, of course, are passive. In principle, therefore, it is possible to provide a listening system aboard the surveillance aircraft that will allow it to locate the emitting target(s) during an imaging pass, and co-locate it on the imagery with one of the observed targets.

Because radio transmissions from vessels occur sporadically, the probability of radio signal interception during the time the aircraft is in the area will be too low to be of value.

On the other hand, all vessels in the area can be expected to carry standard navigational radar, which should be emitting pulses at all times, provided they are turned on and operational.

In order to check this assumption, Newfoundland fishing colleges and major fishing vessels were polled. The following information was obtained:

- All large fishing vessels and 90% of the smaller vessels have radars;
- All of these vessels carry at least X-band radar. Some of the larger vessels also have S-band;
- While the larger vessels have radar turned on permanently, it is possible that those with S- and X-band may have only one of them turned on; and
- The smaller vessels may turn their radar off in clear weather conditions.

From this information, it appears there is a high probability that the vessels of concern will be emitting X-band or possibly S-band radar pulses, particularly in poor weather.

In this document, we will examine the possibilities of obtaining a cost-effective airborne radar listening device for locating vessels operating marine-type radars. The first three questions to be addressed are: (1) What are the cost limitations? That is, what is the user willing to pay for the information? (2) What are the operational requirements? That is, what information do we need? (3) What are the characteristics of the marine radars that affect the design of our listening devices?

The technology of interest to us appears to have been developed almost exclusively for the EW (Electronic Warfare) interests of the military. The approach is, therefore, at least in the first instance to seek the solution through suppliers of ESM (Electronic Support Measures) equipment. The results of this approach are described below. Some of the major design considerations are also presented as it becomes clear that trade-off studies will be necessary before arriving at an optimum solution.

2. PROBLEM INPUT DATA

2.1 COST LIMITATIONS

In discussions with the suppliers of ESM equipment to the military, it rapidly became clear that depending upon the desired specifications, system costs could range from $100 K to $1.5 M and higher ($U.S.). Where, in this range (if in the range at all), does our application fit?

Two representatives of the East Coast Users (J. Benoit - Mobil; G. Worbansky - Bow Valley/Husky) were polled with respect to the incremental cost that they thought the industry would be prepared to pay for the additional ship/iceberg discrimination capability. The answers translated into a capital cost of $100 K - $200 K ($Cdn.).

2.2 SYSTEM REQUIREMENTS

Ideally the listening system should be able to locate the vessel with sufficient precision to ensure co-location with the appropriate target on the radar imagery. The system should be able to detect X- or S-band and should be able to handle several vessels simultaneously. The range should correspond to the maximum imaging range (e.g. 100 km). The time required to 'acquire' or 'intercept' the emitted radar signal should be brief enough to enable several fixes to be made during the flypast. At prop-jet speed (say 120 m/s), this implies that the mean-time between intercepts should be less than about 2 minutes.

The most difficult of these specifications to achieve is high location accuracy. Location is usually obtained through a triangulation technique based upon direction of arrival of the emitted pulse, and the baseline flown by the aircraft between successive 'fixes'. Accuracy is limited by direction finding (DF) accuracy, which is in turn related to cost. The ability to specify emitter locations within 1 km, for example, is possible with existing

ESM systems but well outside the specified cost ceiling. The requirement with respect to location accuracy is therefore somewhat ill-defined for this report, but for working purposes, we are considering ± 3 km as desirable. This in turn suggests DF accuracy of 1° - 3° as being appropriate.

These requirements are summarized in table 1.

Direction Finding Accuracy	1° - 3°
Location Accuracy	± 3 km
Frequency Bands	X- and S-band
Number of Emitters	10
Target Acquisition Time	< 2 minutes
Maximum Range	100 km

Table 1. Functional requirements of airborne listening system with respect to radar emitters described in table 2.

2.3 VESSEL RADAR CHARACTERISTICS

The important characteristics of X-band vessel radar(s) from the point of view of the listening system are listed in table 2. The designer would normally use the most unfavourable parameters.

	X-BAND
Frequency Range(1)	9380 - 9440 MHz
Peak Power Transmitted	3 KW - 25 KW
Antenna Gain	23 - 30 db
Beam Width (3 db)	2° - 0.7°
Sidelobe Gain	≃ 0 db
PRF	∝ 800, 1600, 3200 Hz
Pulse Width	≃ 1 μs, 0.25 μs, 50 ns
Rotation Period	2 - 3 sec

Table 2. Vessel radar characteristics.

(1) The RF band spanned by X-band marine type radar magnetrons is 9380 - 9440 MHz which is only part of the spectrum 8000 - 12000 MHz designated as X-band.

3. E. S. M. SUPPLIERS

A partial survey of the suppliers of ESM (Electronic Support Measures) equipments to military users was made on the assumption that:

(i) off-the-shelf systems capable of meeting the present requirements would be available; and

(ii) purchase of an existing military system would be cheaper than designing and fabricating a custom system.

3.1 NATURE OF THE INDUSTRY

To help place our own application and cost ceiling into perspective, it is worth noting that the U.S. military alone was projected to spend $5.8 billion in 1985 for EW (Electronic Warfare) R & D and procurement, of which ESM systems form a significant component. The top 50 suppliers had 1983 sales ranging from $400 million to $30 million. Company brochures typically describe the many military aircraft types that are supplied by their particular RWR (Radar Warning Receiver) or ESM system, suggesting production quantities of hundreds.

Some of the companies contacted by telephone were more helpful than others. Some apparently want to deal only with military customers. Others saw the opportunity for selling existing systems, while two of the companies were interested in creating a quasi-custom or hybrid system for our application. These are described in Section 5.

The radar warning systems and full ESM systems tended in many cases to be highly over-specified for the iceberg/ship discrimination requirements. This is because their functions are quite different. The major factors contributing to this over-specification are:

1. Very broad band coverage: In response to frequency-agile enemy radar, the receivers

provide broad-band coverage of many GHz - in some cases from 1-18 GHz, compared to our requirement (in X-band) of 60 MHz. This has implications for receiver noise bandwidth and ultimate sensitivity and introduces considerably more cost.

2. Threat Identification: The received signals are examined in real-time for characteristic features and compared (in real-time) to a library of such characteristics in order to identify the nature of the emitter (friend or foe, guidance or search radar, etc). This is usually associated with a process for separating signals from multiple emitters (often 30-100) so that the processing becomes quite complex and contributes strongly to cost.

3.2 DISCUSSIONS WITH SUPPLIERS

During the telephone poll of suppliers, the approach taken was to describe the application and requirements, then to ask them to suggest a solution. The first response was, invariably: How many copies? How much were we willing to pay per copy? What delivery schedule? Considering the limited, low-end portion of the market this application represents, it is not surprising that not all suppliers were overly enthusiastic. It was learned that the budgetary ceiling ($200 K) for the iceberg/ship application is close to the bottom-end of their off-the-shelf radar warning system price range. For this price, however, it appears that the requirement would probably not be met. Typically, this price would buy a 15° directional accuracy and system sensitivity of approximately -35 dbm, which will be shown in Section 4.2 to be inadequate.

To achieve the level of capability summarized in Table 1 would cost $300 K - $400 K for an off-the-shelf system. ESM systems providing direction-finding accuracy of a fraction of a degree and locational accuracies of 300 m cost approximately $1.5 M (U.S.).

One of the manufacturers suggested that an early version Radar Warning Receiver (designated APR-39) might be developed to meet the requirement. The follow-on contacts in this case were not successfully pursued. The order of magnitude cost estimate to achieve this was about $100 K.

One of the suppliers proposed a development concept that is described in Section 5 with a target cost of $100 K (Cdn). Proposals from two other suppliers are described in Section 5 for comparison.

4. DESIGN CONSIDERATIONS

4.1 INTRODUCTION

The requirements of a system capable of detecting and locating a ship-based marine radar are relatively straightforward, compared to those for military systems. The major considerations relate to: (1) system sensitivity, which is itself related to receiver sensitivity and antenna gain, (2) probability of interception, (3) direction finding and location, and (4) aircraft installation. These considerations will be addressed in the following sections. Additionally, there is a data processing and display consideration which will not be addressed.

4.2 SYSTEM SENSITIVITY

The one-way radar equation is given by

$$P_r = P_t \left(\frac{G_t G_r}{R^2} \right) \left(\frac{\lambda}{4\pi} \right)^2 \frac{1}{L}$$

where

P_r = received power
P_t = peak transmitted power
G_t = antenna gain of emitter
G_r = antenna gain of receiver
λ = wavelength
R = range
L = combined losses of both systems

Letting $S_{min} = P_r$ be the minimum required receiver sensitivity for detection of a given radar at maximum range we get

$$\left(\frac{S_{min}}{G_r} \right) = \frac{P_t G_t}{R_{max}^2} \left(\frac{\lambda}{4\pi} \right)^2 \frac{1}{L}$$

Using Table 2, and taking P_t =3KW → 65 dbm, G_t = 25 db, Rmax = 100 km → 50 db, L = 10 db, we obtain :

$$\left(\frac{S_{min}}{G_r} \right) = -72 \text{ dbm.}$$

The requirements of the receiver depend on the type of antenna chosen - that is, on G_r . Some of these choices are discussed in Section 4.4. The implications for Smin are shown in Table 3.

ANTENNA TYPE	G_r	Smin
Isotropic	0 db	-72 dbm
Cavity Backed Spiral	≃ 5 db	-67 dbm
Small Rotating Antenna	≃ 15 db	-57 dbm
SAR Antenna	30 db	-42 dbm

Table 3. Smin vs G_r.

When operated in the noise-limited mode, the major factor influencing receiver sensitivity is the noise bandwidth B_n . The expression for receiver sensitivity (often referred to as Tangential Signal Sensitivity) is :

$$S = (kT) F B_n \quad ,$$

where

kT = 4.14×10^{-21} J → -174 dbm
F = noise factor ≃ 10 db ± 5 db
B_n = noise bandwidth

The noise bandwidth is dependent on the type of receiver being used and the conditions of use. A reasonable expectation would be for B_n = (100-1000) MHz → (80 db to 90 db). Thus a receiver with sensitivity in the range S ≃ -70 dbm to -85 dbm should be achievable for a system covering the limited X-band of interest in this application.

Comparing this range of sensitivity to the requirements of Table 3 suggests that there is an option to consider both low gain and higher gain antenna systems.

Two types of receivers are likely candidates for this performance:

1. Crystal Video Receivers have the advantage of relatively low cost, simplicity and availability. Their performance is limited to about -70 dbm and in many standard wideband applications is considerably poorer (e.g. -35 to -50 dbm). Because they have broadband capability they should be able to cover the required band without tuning. This reduces the 'probability of intercept' problem described in Section 4.3. On the other hand, broader RF bandwidth leads to increased noise bandwidth and reduced sensitivity performance.
2. Superhetorodyne Receivers are more expensive but have improved sensitivity. Typically, the sensitivity is achieved by use of a narrow IF bandwidth which is tuned across the broader RF band of interest. It appears that wideband superhets are also available that would cover the required band without tuning and provide sensitivity better than -80 dbm.

In both cases, the dynamic range may be limited to 50 db or so. On the other hand, saturation is probably not a problem for this application.

Because the onboard surveillance radar will be transmitting at an adjacent frequency, the receiver will have to be switched out of circuit during the transmit pulse.

4.3 PROBABILITY OF INTERCEPT

In order to detect and locate the ship's radar, the receiving system must have an acceptable probability of intercepting that emitter's signal over a time period appropriate to the input requirements. For example, if the airplane is flying a straight line path at 150 m/s and it requires two sitings of a target along a 50 km baseline in order to achieve the desired locational accuracy, the two samples would have to be acquired with near 100% probability in about 5 minutes.

If the receiving system is tuned to the frequency of the emitter and has sufficient sensitivity to detect the main beam of the radar as it sweeps past every 2 seconds, for instance, and, moreover, if it is directed toward the radar continuously, then it will have near 100% intercept probability with a mean-time between intercepts of 2 seconds. There are, however, two situations which change this significantly however:

1. The receiver antenna may be changing its viewing direction, as in the case of a rotating or scanning antenna;
2. The receiver may be a narrow band receiver, scanning through the 60 MHz marine radar band.

In the former case, the main beams of the radar and receiver antennas overlap only briefly as they are both relatively narrow with respect to 360° [Figure (1a)].

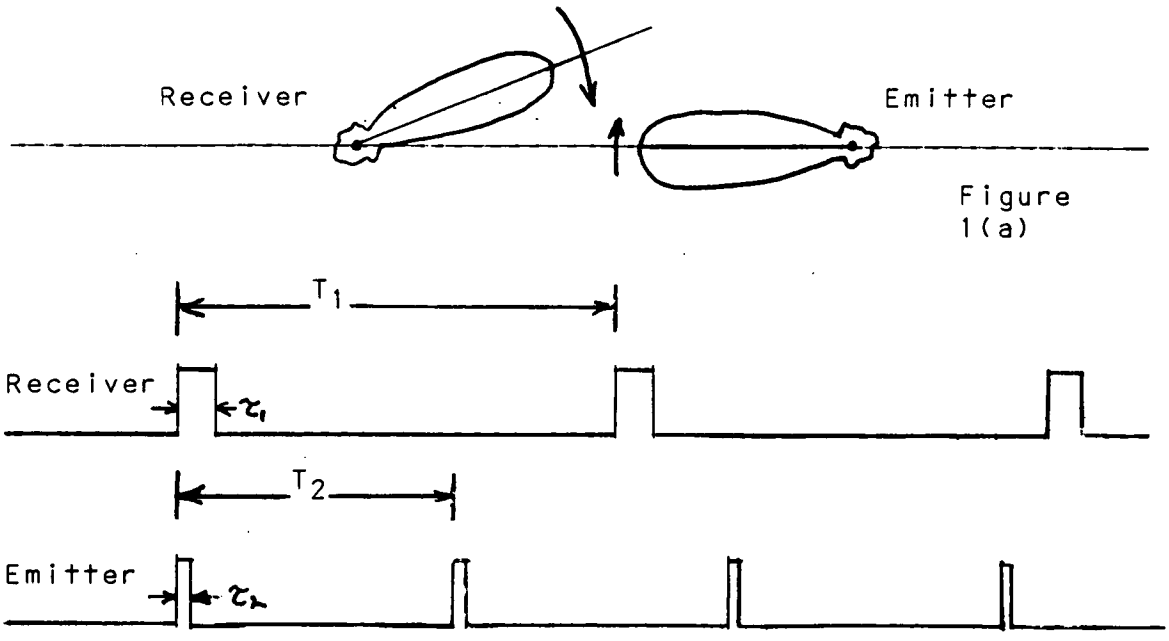

Figure 1(a)

Figure 1(b)

The rotating beam patterns can be more easily treated as overlapping windows in time as shown in Figure 1(b). τ represents the main beam while T is the rotation period. Normally, the beams have an arbitrary phase relationship. The question that interests the designer is: What is the mean-time between overlaps (i.e. intercepts) as a function of the variables open to him (T_1 and, to a lesser extent, τ_1)?

Fortunately, the problem has been solved in an analytical fashion. The relevant expression for the mean-time, T_0, between coincidences for two window functions is (Wiley):

$$T_0 = \frac{T_1 T_2}{(\tau_1 + \tau_2)}$$

For a given probability of intercept, P(t), the time taken, t, will be $(t/T_0) = -\ln[1-P(t)] + \ln[1-f]$, where $f = \left(\frac{\tau_1 \tau_2}{T_1 T_2}\right)$.

For example let $T_2 \simeq 2$ sec,

$\tau_2 \simeq (2/360) \times T_2 \simeq 0.01$ sec,

$\tau_1 \simeq (4/360) \times T_1 \simeq 0.01\, T_1$ sec.

Should the receiver rotation rate be very much slower or faster than the emitter?

$$T_0 = \frac{2T_1}{0.01(1+T_1)} = 200\left(\frac{T_1}{1+T_1}\right) \text{ sec}.$$

For $T_1 \ll 1$ sec, $T_0 \rightarrow 200\, T_1$ sec $\ll 200$ sec

$T_1 \gg 1$ sec, $T_0 \rightarrow 200$ sec.

Thus the receiver rotation rate should be much faster than that of the emitter, all other factors being equal.

For example if $T_1 \simeq 0.5$ sec as is practical according to one of the proposals described below,

$T_0 = 0.33 \times 200$ sec $\simeq 1$ minute.

Since $f = 5 \cdot 10^{-5}$, $(t/T_0) \simeq -\ln[1-P(t)]$.

Therefore a 90% interception probability would require $(t/T_0) \simeq 2.3$, , or $t_{90\%} \simeq 2.3$ minutes. This would be acceptable. On the other hand, a very slow receiver scanning antenna would increase this time by a factor of three, which is only marginally acceptable.

If the receiver was also scanning in frequency the revised expression for T_0 becomes (Wiley):

$$T_0 = \frac{T_1 T_2 T_3}{(\tau_1\tau_2 + \tau_1\tau_3 + \tau_2\tau_3)}.$$

Suppose the receiver was scanning 10 sub-bands of 10 MHz width at a repetition period T_3 so that $\tau_3 = 0.1\, T_3$. With similar antenna parameters to those previously used,

$$T_0 = \frac{666\, T_3}{(0.033 + T_3)} \text{ sec}.$$

τ_3 must be greater than the pulse repetition interval of the emitter ($\simeq 10^{-3}$ sec.), so we might expect $T_3 \geq 0.1$ sec. In this example, To $\simeq$ 8 minutes!

This is probably not acceptable as the airplane would have moved too far to allow several sitings at a high probability level.

From the foregoing discussions and examples, it is clear that a very thorough trade-off analysis must be performed before fixing design.

4.4 DIRECTION FINDING TECHNIQUES

The problem faced by an airborne DF (direction finding) system is that of simultaneously covering the complete field of view (360° for example) at suitably small angular resolution. At suffcient cost this can be achieved for levels of resolution of fractions of 1°. In the following discussion, we will limit our attention to two methods which appear to be in the lower end of the cost spectrum. These two methods use rotating antennae and fixed multi-lobe antennae respectively.

4.4.1 Rotating Antenna

Broadband airborne systems have been developed with practical rotation rates up to 200 RPM. Some of the advantages and disadvantages of this type of system are listed in Table 4.

ADVANTAGES	DISADVANTAGES
High Gain ($\simeq$ 15 db) Narrow Beamwidth ($\lesssim$ 5°) Low Capital Cost	Low probability of intercept Size and mechanical effects High installation cost

Table 4. Advantages and disadvantages of rotating antenna.

The direction finding accuracy is better than the beamwidth. As the main lobe sweeps past the emitter, the beam pattern can be traced out and the DOA (direction of arrival) will correspond to the maximum of the antenna pattern. Depending upon the signal to noise available, DF accuracy of 1° - 2° should be possible. This, of course, applies to a single emitter. If more than one emitter appears within the beam width, and if there are no other means to discriminate between them (such as frequency), the emitters will be lumped together within the beamwidth.

An advantage of this system, relating ultimately to cost, is that only one receiver is required.

Several types of antenna might be usable in this system, including: (1) linear marine radar-type antennas, and (2) cylindrical systems with a parabolic reflector on one side of the cylinder and feed-horn on the other.

The size of the antenna is related to the usual diffraction limit $\theta \simeq \frac{\lambda}{D}$ where θ is the beam width (3 db) and D is the aperture dimension. A 5° beamwidth corresponds to $D \simeq 0.6\ m \simeq 2\ ft.$ One of the penalties, therefore, is horizontal size. In the vertical plane, a 30° - 45° beamwidth is desirable to overlap the airborne radar swath. A thickness of 10 cm is typical of this requirement

4.4.2 Multi-lobe Systems

This concept is illustrated in Figure 2(a). In this example, each of the four antennas is a broad-beam, fixed unit placed in quadrature with the others to cover 360° horizontally. Each has its own receiver. The beam pattern of each overlaps that of its neighbour so that as an emitter is detected simultaneously in two adjacent antennas, the respective signal amplitudes can be ratioed to provide a unique direction with respect to this antenna pair. The concept will work with any number of antenna, although both cost and angular resolution performance increase with number of channels.

The antenna and receivers have to be carefully matched and well-calibrated to minimize errors. Particular attention is required with respect to stray reflections from the aircraft, which are not accounted for in the beam pattern.

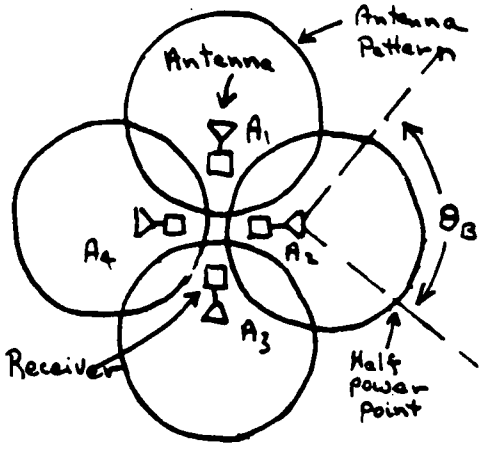

Figure 2(a)

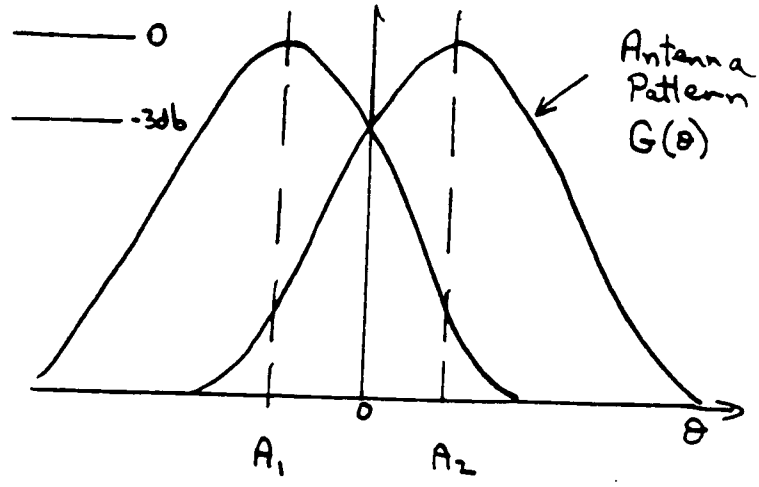

Figure 2(b)

The angular sensitivity for a well-calibrated antenna pair is dependent on the signal-to-noise ratio, which itself varies with angle of arrival. This has been analysed by Wiley, who shows that the RMS angular noise width $\sigma_{\theta=\theta_1}$ is given by

$$\sigma_{\theta=\theta_1} = 0.7 \left(\frac{\theta_B}{\sqrt{(SNR)_0}} \right) \text{ degrees},$$

where

$\sigma_{\theta=\theta_1}$ = RMS uncertainty at $\theta = \theta_1$,

θ_1 = cross-over angle of the adjacent beam patterns

= $\theta_B / 2$,

θ_B = beam width (3db) of the Gaussian antenna patterns ,

$(SNR)_0$ = signal-to-noise ratio (SNR) at peak of pattern $(\theta = 0°)$.

Letting $\theta_B = 90°$ and $(SNR)_0 = 14$ db we find $\sigma_{\theta=\theta_1} = 13°$. By doubling the number of antennas and receivers to eight we reduce $\sigma_{\theta=\theta_1}$ to $\approx 6°$, which approaches the performance of the angular rotating antenna.

Such a system has two advantages over the rotating antenna:

1. The probability of intercept is 100% and the time between 'updates' is just the pulse repetition interval of the emitter - that is, $\simeq$2 seconds;
2. The size of the antennae are small (few inches) and they are hard-mounted to the aircraft.

On the other hand, the disadvantages are:

1. reduced gain ($\simeq$5 db depending on size);
2. increased cost because of multiplicity of receivers.

The antennas often used in these applications are cavity backed spirals.

4.4.3 Other Methods

Improved performance can be obtained by use of interferometric or hybrid amplitude/phase comparison systems. These lead to greater expense and other design problems and will not be discussed here.

4.5 DETECTION OF BACKLOBES

The discussions in Sections 4.2 and 4.3 were premised on the detection of the main lobe of the emitter antenna as it rotated across the receiving system. This determined the receiver sensitivity requirements on the one hand, and the probability of intercept calculations on the other hand.

The sidelobes of the emitter antenna are typically 25 db - 30 db below the main lobe peak. If the receiving system were sufficiently sensitive, it could detect the emitter from every direction in which it was pointed. It has little impact in the case of multilobe antenna systems. According to Table 3, a rotating antenna system would require receiver sensitivity of -87 dbm to detect the sidelobes of an emitter antenna. This may be feasible with a good superheterodyne receiver, but is much more feasible with a high gain antenna such as that of STAR-1.

The question also arises as to whether there are circumstances under which the back lobe of the receiving antenna would detect the emitter main lobe. This would conceivably cause a loss of directional information for some systems. In the case of fixed multi-lobe detectors, the problem would not exist. However, with a rotating antenna, high sensitivity receiver and a relatively close emitter with high gain antenna, it could occur. In this instance, it would be recognized as being a 'back-lobe entry' because it has a recurrence interval of approximately 2 seconds - the emitter antenna rotation rate. The logic section would discriminate against spurious direction-finding on this basis, and would key on the pulses corresponding to the receiver rotation rate which would be at a higher rate, (typically 1/2 - 1 second).

4.6 LOCATION DERIVATION

Using the angle of arrival information supplied by the DF system and the baseline information supplied by aircraft INS, location is determined, to greater or lesser accuracy, depending upon the number of 'fixes' and the accuracy of the underlying information.

Consider the geometry of Figure 3.

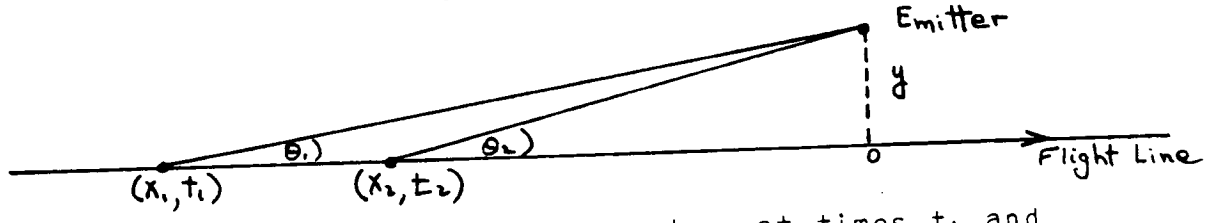

Figure 3. Aircraft location x_1 and x_2 at times t_1 and t_2.

$d = (X_1 - X_2)$ is known from INS. Assume zero error.

θ_1, θ_2 are known from DF

From trigonometry, $$y = \frac{d}{(\cot\theta_1 - \cot\theta_2)}$$

The RMS error in Y can be calculated as

$$\sigma_y = \sigma_\theta \cdot y \cdot \frac{(\csc^4\theta_1 + \csc^4\theta_2)^{1/2}}{(\cot\theta_1 - \cot\theta_2)}$$

where we have assumed the RMS errors in θ_1 and θ_2 are $\sigma_{\theta_1} = \sigma_{\theta_2} = \sigma_\theta$.

To provide a concrete example, consider an emitter located at y=50 km which is first detected at X_1=100 km, and subsequently at fixed intervals of d=20 km. The error in y, assuming $\sigma_\theta = 2°$, is shown for these values of (X_1, X_2) in table 5.

X_1	X_2	θ_1	θ_2	σ_y/y
100 km	80 km	27°	32°	0.59
80 km	60 km	32°	40°	0.37
60 km	40 km	40°	51°	0.27
40 km	20 km	51°	68°	0.18
20 km	0 km	68°	90°	0.13

Table 5. Error estimate example of y as function of x.

4.7 INSTALLATION PROBLEMS

When comparing system costs, installation must also be taken into account. The major impact is caused by equipment which is external to the aircraft. This is related mainly to the antenna or antennae systems.

The rotating antenna installation appears to be significantly more costly than the fixed multilobe system. It would be necessary to cut a hole in the fuselage to mount the pedestal/turning unit assembly. The antenna would protrude through the hole and be protected by a radome. The unit would be pressure sealed and would meet federal aviation authority requirements. The cost of this installation will depend on the aircraft type and, to a lesser extent, on the size of the hole. Larger aircraft are more expensive to modify. It is estimated that installation of an 18" rotating

antenna unit on a small aircraft would cost a minimum of $50,000 U.S., while aboard a larger aircraft it could be 2-4 times as much.

Small cavity backed spiral antennas, on the other hand, would install relatively easily on the belly or wings of the aircraft. It is estimated that this type of installation would cost about $10,000 U.S.

5. THREE PROPOSALS

Three E.S.M. suppliers submitted proposals.

Watkins - Johnson International San Jose, California	Formal Proposal, Firm Cost, Existing W-J equipments specified
M.E.L. Ottawa, Ontario	Draft Proposal, Cost Target, Top Level Design, Equipments unspecified
General Instrument Corp. Government Systems Division Hicksville, New York	Product Literature, Telephone Cost Estimate

Both Watkins-Johnson and M.E.L. recommended rotating antenna systems in order to achieve the desired accuracy in the specified cost range.

M.E.L. recommended a modified small marine radar antenna rotating very slowly. The smallest version could be something like a Ratheon Model 1200. This would be followed by either a crystal video or wide-band superheterodyne receiver. The system would have 2 channels to accommodate X- and S-band. A digital pre-processor, followed by a processor to separate and determine the beam peak, would complete the system.

This design suffers from the probability of intercept problem unless the receiver is given sufficient sensitivity to enable sidelobe detection. Also, the marine X-band antenna would not handle S-band very well, so the design is inadequate for S-band. Extensive modifications and tests would be required to ensure that the pedestal and antenna

assembly were airworthy.

Cost: $100,000 (Cdn) target cost
Delivery: Unspecified - possibly 6 months

Watkins-Johnson manufacture a number of sub-system modules that can be interfaced to form the system of choice. They proposed a rapid-rotating antenna that they have manufactured for airborne applications. The rotating system consists of their L6-24 antenna and EP30-1 pedestal. The antenna would cover X- and S-band with ± 2° DF accuracy. The antenna consists of a lightweight parabolic reflector with a circularly polarized hornfeed. It can rotate, sector scan or dwell on an operator-set bearing. The RF is passed through an RF pre-processor into a manually tunable X-band superhet receiver. The tuner bandwidth is 26 MHz, thus eliminating the need for extensive tuning over the band. A similar S-band receiver/tuner is offered as an option. A polar display shows amplitude vs. angle information. The operator can lay a cursor onto the maximum and output these readings on an RS-232 line (optional).

Cost: 1 off $270,000 (U.S.)
5 off $187,000 (U.S.) each
RS-232 option $ 25,000 (U.S.) (includes other items)
S-Band Option $ 55,000 (U.S.)
Delivery: 9 months

General Instrument Corp proposed their ALR-606(V), which is a 4-antenna multilobe system designed for maritime helicopter use. The DF accuracy is between 10° and 15°, which doesn't meet requirement. The crystal video receivers have a sensitivity of only -35 dbm, which is inadequate for this application according to Table 3.

Cost: Approximately $100,000 (U.S.)
Delivery: Unspecified

It should be noted that this system was proposed to meet the price limitation. For $300,000 - $400,000 (U.S.) a 2° version with sensitivity -65 dbm is produced.

The salient features of the three proposals are summarized in Table 6.

Table 6. Summary of ESM Proposals.

Supplier	Watkins-Johnson	M.E.L.	General Instruments
Antenna Type Receiver Type	Rotating Wideband tunable Superheterodyne	Rotating Unspecified	Multi-lobe (4) fixed Crystal Video
Meets Requirement?			
Angular Accuracy	Yes	Yes	No
Sensitivity	Yes	Yes	No
Time Between Intercepts	Yes	No	Yes
S-band	Yes (optional)	No	No
Cost (Purchase)	1 ea 270 K (U.S.) 5 ea 187 K (U.S.)	$100 K (Cdn) target	$100 K (U.S.) Approximate
Cost (Installation)	$ 50 K (US) to $200 K (US)	$ 50 K(US)to $200 K(US)	$ 10 K to $ 20 K (US)
Delivery	9 months	6 months	unspecified

6. AN ALTERNATIVE APPROACH

The previous discussions have assumed a DF system independent of the airborne radar. An alternative approach is to consider the use of the SAR or SLAR antenna to pinpoint direction. The general problem with this approach is that the antenna is narrow and sidelooking. Thus the antenna beam sweeps across the emitter very quickly, apparently lowering the probability of intercept substantially. The other inadequacy is that range cannot be readily obtained because the baseline is so short.

Consider a sidelooking antenna of beamwidth θ_B. If the aircraft is travelling at velocity V m/s the main lobe will sweep across an emitter at range R in a time

$$\tau = \left(\frac{R\,\theta_B}{V}\right) \text{ sec.}$$

Consider two speeds corresponding to prop-jet and jet aircraft, and two ranges, corresponding to inner and outer swaths, as well as 2 beam widths corresponding to STAR-1 and typical SLAR. τ is shown as a function of these parameters in Table 7.

	$\theta_B \simeq 1.7°$ (STAR-1)		$\theta_B \simeq 0.6°$ (SLAR)	
	R_1=20 km	R_2=80 km	R_1=20 km	R_2=80 km
V = 140 m/s (Prop-jet)	4.2 sec	17 sec	1.4 sec	5.6 sec
V = 250 m/s (Jet)	2.3 sec	9.4 sec	0.8 sec	3.1 sec

Table 7. τ as a function of R, θ_B, V.

We see from this that STAR-1 should be able to capture at least two main lobe sweeps of an emitter over the whole of the swath. On the other hand, a SLAR antenna, having a narrower beam, may not intercept the main beam at all, depending on the location of the emitter in the swath.

Both STAR-1 and SLAR antennae have high gain, as shown in Table 3, and with sensitive receivers (S -70 dbm) should be able to detect the side and back lobes of the emitter.

The approach would be to tap a small portion (-10 to -20 db) of the RF energy off the front end of the radar receiver and couple it into a 'listening' receiver. The receiver would need an additional 10-20 db sensitivity to detect this fractional power tap if the emitter sidelobes are to be detected.

The cost would be mainly in the receiver. The modifications to the SAR or SLAR would be minimal. Installation costs would also be minimal.

If a receiver with this sensitivity was prohibitively expensive, the technique would still be acceptable for detection of the emitter main lobe in the case of STAR-1, but would be marginal for SLAR because of the reduced probability of intercept.

7. CONCLUSIONS AND RECOMMENDATIONS

In conclusion, a radar direction finding system is a feasible means of detecting vessels and providing the information required to discriminate them from icebergs. While military systems exist, the cost of systems which meet the present requirement are beyond the 'allowable' cost ceiling ($200 k Cdn). On the other hand, it appears that a design trade-off study of a 'custom' system will reveal a cost-acceptable, technically suitable solution. An alternative approach, which could meet much of the desired requirements at a considerably reduced cost, is also proposed. This approach takes advantage of the existing SAR/SLAR antenna system aboard the aircraft, tapping power off to an independent receiver.

In particular, we recommend the following:

1. Do not purchase an off-the-shelf ESM system;
2. Perform a design trade-off study for a custom built D.F. system using commercial and/or military components. In particular, examine:
   - o rotating antenna vs. multilobe antennae of comparable DF accuracy;
   - o receiver sensitivity vs. cost;
   - o minimum processing requirements.
3. Perform a design and cost analysis for the STAR-1/SLAR add-on approach (Section 6).
4. Add such a system to STAR-1 for a field test;
5. Based upon experience with the STAR-1 add-on, determine whether a stand-alone DF system is required.

8. REFERENCES

The International Countermeasures Handbook (8th Edition, 1982-83; 10th Edition, 1985), EW Communications, Inc., Palo Alto, CA.

Wiley, Richard G., Electronic Intelligence: The Interception of Radar Signals, Artech House, Inc., Dedham MA, 1985.

Watkins-Johnson International, Proposal Document of August 8, 1985, San Jose, CA.

M.E.L. Defense Systems Ltd, Proposal Document of August 16, 1985, Stittsville, Ontario.

General Instrument Corporation, Technical Description of the ALR-606(V)1 RWR/ESM System, Hicksville, NY, 1983.

APPENDIX F

A Comparison of the Capabilities and Costs of Aircraft for an Iceberg Radar Surveillance Role

APPENDIX F

A COMPARISON OF THE CAPABILITIES AND COSTS OF AIRCRAFT FOR AN ICEBERG RADAR SURVEILLANCE ROLE

Provided by
INTERA Technologies Ltd.
Calgary, Alberta

Provided for
Canpolar Consultants Ltd.
Toronto, Ontario

October 1985

R85-181

1. COMPARISON OF AIRCRAFT FOR RADAR SURVEILLANCE ROLE

There currently exist a number of aircraft that have been or could be configured for airborne iceberg surveillance missions. These aircraft represent a fairly wide range of performance capabilities that may or may not be totally suitable for an operational iceberg surveillance platform. The purpose of this review of selected aircraft is to provide a summary of operating cost and performance factors, in order to evaluate their suitability for an operational program. Because of the many factors related to purchase price, the capital cost factors have not been included in this review.

The performance characteristics are presented in Table 1 while Table 2 provides a comparison of operating costs. When examining these tables, one needs to consider several key factors, as described briefly below.

1.1 AIRCRAFT PERFORMANCE TO OPTIMIZE RADAR APPLICATION EFFECTIVENESS

The altitude at which optimum radar effectiveness occurs depends on the radar type. SAR geometry is most effective at look angles corresponding to high altitude (approximately 30,000 ft or greater). SLAR appears to more effective at lesser altitudes for iceberg detection, although it is not yet clear what the optimum altitude should be. Search radar apparently requires a low operating altitude of a few thousand feet.

Aircraft performance is a strong function of altitude. In all cases range, speed and cost performance deteriates at lower altitudes. In some cases the aircraft do not have an adequate ceiling for the application.

Range and speed are important factors to consider for application effectiveness. A minimum range of 1,500 n.mi. is desirable for most large scale surveillance missions. Speed is important as it relates to the responsiveness of the system.

1.2 PAYLOAD

An 1,100 lb equipment payload is desirable for aircraft carrying SAR. Two of the aircraft do not meet this requirement at full fuel load. On the other hand, both could meet the requirement if some range performance is sacrificed. This is acceptable for the Citation SII but is less so for the Beech K-200.

Payload requirements for SAR and search radar are less than for SAR. It should be noted that those aircraft with substantial payloads (over 9,000 lbs for instance) are over-sized for these applications. The penalty paid is increased capital and operating costs.

1.3 SPEED

Speed is relevant in terms of response time and mission duration. Long duration missions induce crew fatigue. A 250 knot cruising speed or better is desirable.

1.4 COST EFFECTIVENESS

Cost effectiveness is presented with respect to fuel consumption by the parameter known as Specific Range. This indicates the range obtained per unit of fuel consumed. Together with engine maintenance and fuel costs this leads to the operating costs presented in table 2.

1.5 CONCLUSION

Most of the aircraft presented in tables 1 and 2 can 'do the job'. A smaller number can do the job more effectively. In terms of capability and operating cost per nautical mile, the Cessna Conquest and Cessna Citation appear to be optimum platforms.

Table 1. Aircraft performance characteristics.

AIRCRAFT	MAX GROSS WEIGHT (LBS)	MAX PAYLOAD (LBS)	PAYLOAD[2] WITH MAX FUEL (LBS)	MAX[3] CEILING (FT)	MAX[4] CRUISE (KTS)	MAX[4] RANGE (N.Mi.)	MAX[4] ENDURANCE (HRS)	MAX RANGE @ 5,000 FT ALTITUDE (N.Mi)	TAKE-OFF DISTANCE @ SEA LEVEL(FT)
Turbo-prop									
Cessna 441 Conquest (1)	10,800	2,450	1,500	35,000	287	2,100	7.3	866	2,465
Beech K-200 (1)	12,500	2,800	1,110	35,000	280	1,650	5.9	821	3,300
Twin Otter	12,500	7,593	2,332	10,000	182	718	3.9	500	2,280
Embraer Brasilia	24,000	6,750	2,721	32,000	302	2,166	7.8	950	4,230
Dash 8 100	33,200	9.010	5,950	25,000	259	1,637	6.3	623	3,700
Dash 8 300	39,000	11,800	9,122	25,000	266	2,500	9.4	1,273	3,700
Gulfstream G-1	35,100	4,270	1,660	33,000	302	2,600	7.3	1,100 est	4,300
De Havilland Dash 7	44,000	16,600	6,400	21,000	230	1,400	8.0	700 est	2,260
Convair 580	55,000	15,800	-	23,000	261	1,070	4.1	1,185	4,400
Lockheed Electra	116,000	26,500	19,500	28,000	352	3,500	8.0	1,600	5,500
Lockeed C-130	155,000	50,760	33,000	23,000	327	3,300	12.0	1,664	6,000
Jet									
Cessna Citation SII (1)	14,700	2,630	710	43,000	397	2,300	5.8	1,070	3,240
Canadair Challenger 600	41,100	7,830	5,375	41,000	443	3,040	6.8	1,490	5,750

Notes:
1. Single-pilot, one operator. All others assume two pilots, one operator.
2. Payload refers to the equipment payload available plus three or two man crew as required.
3. Maximum ceiling is close to the optimum performance ceiling except for the Jets which have approximately 39,000 ft ceiling for optimum preformance.
4. Refered to optimum altitude. Will be slower at lower altitude.
5. Assumes maximum fuel load at takeoff, VFR conditions. Reserve not included.

Table 2. Aircraft cost comparisons.

AIRCRAFT	SPECIFIC RANGE (NM/LB FUEL)	OPERATING COST @ OPTIMUM ALTITUDE $/HR	$/NM	OPERATING COST @ 5000 FT ALTITUDE $/HR	$/NM	COMMENTS
Turbo-prop						
Cessna 441 Conquest	0.67	335	1.17	505	1.91	-
Beech K-200	0.56	425	1.52	659	2.35	Marginally acceptable payload for SAR.
Twin Otter	0.28	250	1.37	300	1.65	Range unacceptable for most missions. Ceiling Limitations.
Embraer Brasilia	0.41	390(est)	1.40	650(est)	2.71	-
Dash 8 100	0.29	475	1.79	736	2.79	-
Dash 8 300	0.44	475	1.79	736	2.79	-
Gulfstream G-1	0.21	820	2.70	1270	4.21	-
De Havilland Dash 7	0.21	625	2.72	968	4.21	-
Convair 580	0.15	1100	4.21	1705	6.53	Range limited.
Lockheed Electra	0.09	approx 2600	7.38	4030	11.45	-
Lockheed C-130	0.08	approx 3000	9.17	4650	14.22	-
Jet						
Cessna Citation SII	0.40	500	1.29	775	2.87	Range penalty if SAR payload flown. Approximately 300 n.mi.
Canadair Challenger 600	0.18	1150	2.60	1783	4.02	-

1 Operating costs include fuel and engine maintenance but does not include crew costs.

2 Derived by assuming 100% fuel flow increase at 5000 ft. from optimum cruise. Manufacturers do not provide full performance curves vs. altitude.

APPENDIX G

Draft Field Plan Distribution List

CANPOLAR Consultants Ltd.

MEMO TO: Distribution

FROM: J. Rossiter

DATE: September 30, 1985

RE: ESRF PROJECT: ICEBERG DETECTION BY AIRBORNE RADAR REVIEW, EVALUATION AND FIELD PROGRAM DESIGN

As you are probably aware, CANPOLAR Consultants Ltd. has been contracted by the ESRF to design an experiment to extend our iceberg detection capability using airborne radar. To this end the project team met on September 3rd and 4th to design an experimental field program. We are hopeful that an experiment will be funded by the ESRF during Spring 1986.

A brief experiment plan is attached for your review. We would be pleased to receive any comments you might have on this plan. However, in order to submit our report for timely consideration by the ESRF, we need your comments by October 18, 1985. Feel free to contact either myself or Jeff Proctor at the number below.

J. Rossiter 1026

JRR:es

4711 Eglinton Ave West, Suite 4, Toronto, Ontario, Canada M5N 1A4 • Phone (416) 487-1581 • Telex: 06-218813

DRAFT FIELD PLAN DISTRIBUTION

LYN ARSENAULT, CCRS
JACQUES BENOIT, MOBIL
DON CHAMP, AES
BRIAN CURRIE, CRL
BYRON DAWE, NORDCO
SUE DIGBY, BERCHA/RADARSAT
NORM EDWARDS, USCG-IIP
ROGER GRAVES, CAL
LAURENCE GRAY, CCRS
EUGENE GUY, C-CORE
SIMON HAYKIN, CRL
DAVID LAPP, NORLAND SCIENCE & ENG.
ED LEWIS, CCIW
CHUCK LIVINGSTONE, CCRS
RAY LOWRY, INTERA
LYN MCNUTT, RADARSAT
HUGH MCRUER, AES
BRYAN MERCER, INTERA
DAVE PEARSON, PETRO CAN
HERB RIPLEY, ATLANTIC AIRWAYS
VAL SHAW, BERCHA
DEREK STRONG, COGLA
ED WEDLER, N.S. LAND SURVEY INST.
PETER WOOD, ESRF
GREG WARBANSKI, HUSKY BOW-VALLEY

September 30, 1985